Investigating the role of myeloperoxidase as a key mediator of renal damage in crescentic glomerulonephritis and reno-cardiac disease

Marilina Antonelou

UCL

Thesis submitted for the degree of Doctor of Philosophy

Declaration of originality

I, Marilina Antonelou confirm that the work presented in this thesis is my own. Where information has been derived from other sources, I confirm that this has been indicated in the thesis.

Abstract

Crescentic glomerulonephritis (CGN) describes a severe form of glomerular inflammation, which results from various systemic or renal specific diseases, including anti-neutrophil cytoplasm antibody (ANCA) associated vasculitis (AAV) characterised by glomerular neutrophil and monocyte activation and neutrophil extracellular trap deposition. Diseases associated with CGN are frequently associated with increased cardiovascular disease, which represents a significant cause of premature mortality. Myeloperoxidase (MPO), a heme containing peroxidase stored in neutrophils and monocytes, is a key component of innate immune defence, generating hydrochlorous acid and free radicles that can also lead to host tissue damage. Additionally, MPO has been shown to contribute to vascular inflammation and atherosclerosis through oxidation of lipoproteins and catabolism of nitrous oxide leading to endothelial damage. In humans, MPO deficiency does not appear to lead to an immunodeficient phenotype. In this thesis, the role of selective MPO inhibition using AZM198, as a therapeutic target in CGN and associated reno-cardiac disease is explored.

Our data demonstrate that free MPO levels are elevated in patients with active AAN and reduced when disease reaches remission. Renal biopsies of patients with diverse forms of CGN had extracellular glomerular MPO deposition that correlated significantly with clinical and histological disease severity. In vitro, AZM198 led to a significant reduction in neutrophil extracellular trap (NET) formation, reactive oxygen species (ROS) production and neutrophil degranulation and attenuated neutrophil-mediated endothelial cell damage. In vivo, delayed AZM198 treatment at two different doses reduced glomerular inflammation.

Combining a murine model of chronic glomerular inflammation and atheroma formation showed that the presence of nephritis enhances atheroma formation. This model will be used in future work to compare treatment with AZM198 with corticosteroid therapy, currently used to treat most conditions associated with CGN.

Impact statement

The impact of this research project is both academic and clinical. On the academic side, the data presented in this thesis increase the understanding of the basic mechanisms mediating glomerular inflammation and crescentic glomerulonephritis, with specific emphasis on systemic vasculitis, and the role played by myeloperoxidase. Data on the influence of myeloperoxidase and on neutrophil extracellular trap formation might be of considerable interest to a wide variety of medical specialities including nephrology, immunology and rheumatology.

Furthermore, these data may have significant clinical impact, helping to define a novel therapeutic target, myeloperoxidase, in the various diseases that are characterised by aberrant NET formation or neutrophil activation. Critically, some forms of crescentic glomerulonephritis have no current successful treatments, meaning there are still significant unmet clinical needs that this project could impact on.

Crescentic glomerulonephritis is not common, but frequently leads to end-stage renal failure if not treated adequately and renal replacement therapy consumes a very significant proportion of the healthcare budget. Moreover, while individual (speciality specific) immune-mediated diseases that are characterised by neutrophil degranulation or NET formation are also uncommon, overall the burden of diseases is substantial, necessitating uptake of many health care resources. There are further economic costs incurred in managing the considerable disability resulting from prolonged immunosuppression therapy which is required for many of these neutrophil/NET dependent diseases. The ability to define novel therapies, such as myeloperoxidase inhibition, may allow for synergy with current treatments and allow lower doses of current immunosuppressants to be used, with reduced side effect profiles.

Table of contents

3   MYELOPEROXIDASE AS A MARKER OF DISEASE SEVERITY IN CRESCENTIC GLOMERULONEPHRITIS 61

4 THE EFFECT OF MYELOPEROXIDASE INHIBITION ON NEUTROPHIL DEGRANULATION, ROS PRODUCTION, NET FORMATION AND NEUTROPHIL-INDUCED ENDOTHELIAL CELL DEATH *IN VITRO* 81

5 INVESTIGATION OF MYELOPEROXIDASE INHIBITION IN A PRE-CLINICAL MODEL OF CRESCENTIC GLOMERULONEPHRITIS 107

6 INVESTIGATION OF THE ROLE OF NEPHRITIS ON ATHEROMA FORMATION AND FUTURE WORK 129

7   DISCUSSION   143

REFERENCES   151

Acknowledgements

List of Publications

Neutrophils are key mediators in crescentic glomerulonephritis and targets for new therapeutic approaches, **Antonelou M**, Evans RDR, Henderson SR, Salama AD. Invited review by NDT, submitted December 2019

Therapeutic myeloperoxidase inhibition attenuates neutrophil activation, ANCA-mediated endothelial damage and crescentic glomerulonephritis, **Antonelou M**, Michaëlsson E, Evans RDR, Wang CJ, Henderson SR, Walker LSK, Unwin R, Salama AD, J Am Soc Nephrol. 2019 Dec. 31 (2), 350-364

Anti-myeloperoxidase antibody positivity in patients without primary systemic vasculitis., **Antonelou M**, Perea Ortega L, Harvey J, Salama AD. Clin Exp Rheumatol. 2019 Apr 37 Suppl 117 (2), 86-89

High Incidence of Arterial and Venous Thrombosis in Antineutrophil Cytoplasmic Antibody-associated Vasculitis. Kang A, **Antonelou M,** Wong NL, Tanna A, Arulkumaran N, Tam FWK, Pusey CD. J Rheumatol. 2019 Mar;46(3):285-293.

Binding Truths: Atypical Anti-Glomerular Basement Membrane Disease Mediated by IgA Anti-Glomerular Basement Membrane Antibodies Targeting the α1 Chain of Type IV Collagen. **Antonelou M**, Henderson SR, Bhangal G, Heptinstall L, Oliveira B, Hamour S, Harber M, Salama AD. Kidney Int Rep. 2018 Aug 22;4(1):163-167.

Emerging evidence of an effect of salt on innate and adaptive immunity. Evans RDR, **Antonelou M,** Henderson S, Walsh SB, Salama AD. Nephrol Dial Transplant. 2018 Dec; 34 (12), 2007-2014

Increased Prevalence of Thyroid Disease in Patients with Antineutrophil Cytoplasmic Antibodies-associated Vasculitis. Prendecki M, Martin L, Tanna A, **Antonelou M,** Pusey CD.J Rheumatol. 2018 May;45(5):686-689

List of figures

List of tables

Abbreviations

AAV	ANCA-associated vasculitis
ANCA	Anti-neutrophil cytoplasmic antibody
APC	Antigen presenting cell
BrdU	Bromodeoxyuridine / 5-bromo-2'-deoxyuridine
C-ANCA	Cytoplasmic ANCA
CatC	Cathepsin C
CGD	Chronic granulomatous disease
CGN	Crescentic glomerulonephritis
CKD	Chronic kidney disease
DHR 123	Dihydrorhodamine 123
EC	Endothelial cell
eGFR	Estimated glomerular filtration rate
ERK	extracellular signal-regulated kinase
G-CSF	Granulocyte colony–stimulating factor
GBM	Glomerular basement membrane
H_2O_2	Hydrogen peroxide
HFD	High fat diet
HNP	Human neutrophil peptide
HOBr	Hypobromous acid
HOCl	Hypochlorous acid
ICAM-1	Intracellular adhesion molecule 1
IFTA	Intestitial fibrosis and tubular atrophy
IL	Interleukin
INF	Inteferon
JAM	Junctional adhesion molecule
LDG	Low density granulocyte
LDL	Low-density lipoprotein
LPS	Lipopolysaccharide
MAPK	Mitogen-activated protein kinase
MEK	Mitogen-activated protein kinase/ extracellular signal-regulated kinase

MPO	Myeloperoxidase
NADPH	Nicotinamide adenine dinucleotide phosphate
NE	Neutrophil elastase
NET	Neutrophil extracellular trap
NO	Nitric oxide
NSP	Neutrophil serine protease
NTN	Nephrotoxic nephritis
P-ANCA	Perinuclear-ANCA
PAD4	Protein-arginine deiminase type 4
PAMPs	Pathogen associated molecular patterns
PAS	Periodic acid Schiff (PAS)
PECAM	Platelet endothelial cell adhesion molecule
PI3K	Phosphoinositide 3-kinase
PMA	Phosphol myristrate acetate
PMN	Polymorhonuclear cell
PR3	Proteinase 3
RA	Rheumatoid arthritis
RAVE	Rituximab for ANCA-Associated Vasculitis
RIPK1	Receptor-interacting serine/threonine-protein kinase 1
RIPK1/3	Receptor-interacting serine/threonine-protein kinase 1/ 3
ROS	Reactive oxygen species
SyK	Spleen tyrosine kinase
TLR	Toll like receptor
TNFα	Tumour necrosis factor α
VCAM-1	Vascular cell adhesion molecule-1
VE cadherin	Vascular endothelial cadherin
vWF	Von Willebrand Factor

1 Introduction

1.1 Neutrophil biology

1.1.1 Neutrophil production in the bone marrow

Neutrophils account for 50% to 70% of all circulating leukocytes in humans, and they are the first line of host defence against a wide range of infectious pathogens (Mayadas, Cullere and Lowell, 2014). The production of neutrophils is largely regulated by the rate of apoptosis of neutrophils in tissues.

They are formed within the bone marrow during hematopoiesis in response to several cytokines, principally granulocyte colony–stimulating factor (G-CSF), a factor which is also important for granulopoiesis (Borregaard, 2010). The presence of granules is the hallmark of granulocytes (eosinophils, basophils, and neutrophils). In fact, neutrophil maturation is defined by the sequential formation of three different granules and secretory vesicles as well as nuclear segmentation. Granulopoiesis begins with the development of azulophilic granules in myeloblasts/promyelocytes and concludes after the creation of secretory vesicles in mature segmented neutrophils. Neutrophil granules are classified into three distinct subsets based on the presence of characteristic granule proteins: primary (azurophil) granules (myeloperoxidase (MPO)), secondary (specific) granules (lactoferrin), and tertiary (gelatinase granules) (gelatinase). Secretory vesicles are the first to be mobilised after minimal neutrophil stimulation and contain membrane- associated receptors that are key for migration through the vascular endothelium (Lawrence, Corriden and Nizet, 2017). Figure 1-1 shows the different stages of granulopoeisis and neutrophil maturation.

Neutrophils that leave the bone marrow are terminally differentiated and short lived, with an average life span of 8-12 hours in the circulation and up to 1-2 days in tissues.
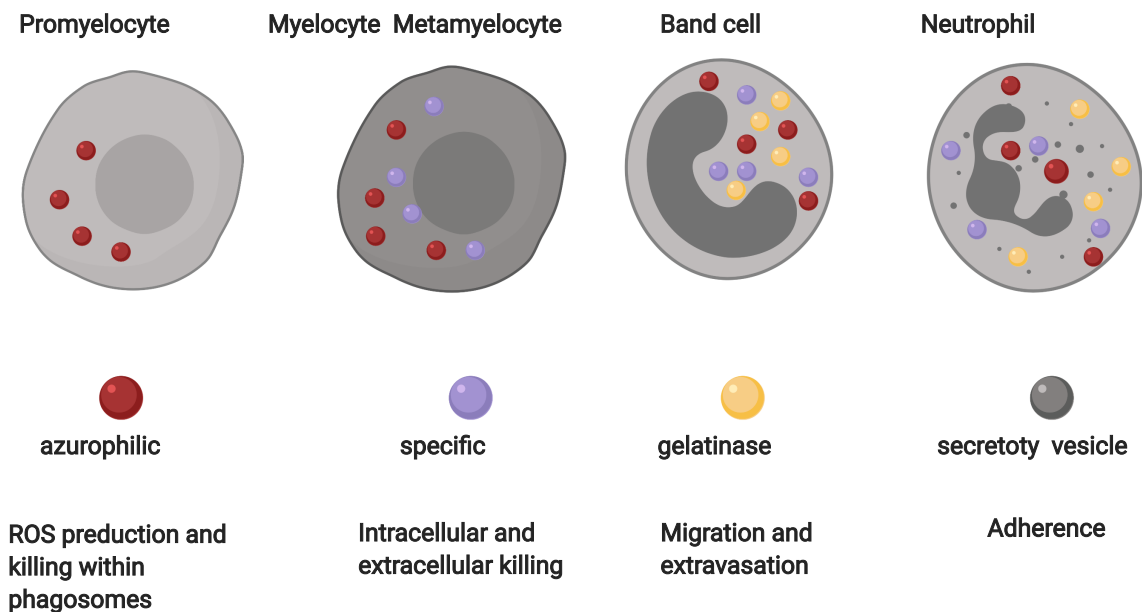
Figure 1-1 Neutrophil granulopoeisis.

Neutrophil maturation is defined by the formation of three different granules (azulophilic, specific and gelatinase) as well as secretory vesicles and nuclear segmentation.

1.1.2   Neutrophil recruitment

The exit of neutrophils from the blood, primarily via postcapillary venules, follows an ordered process referred to as neutrophil recruitment. Neutrophil recruitment to sites of tissue inflammation is mediated by the sequential interaction of receptors present on neutrophils with ligands induced on the surface of the inflamed endothelium (Mayadas, Cullere and Lowell, 2014). The classical multistep adhesion cascade is outlined in Figure 1-2. It consists of the following steps: (*a*) initial attachment of the neutrophil to the endothelium supported by the transient interaction of P-, E- and L-selectins, (*b*) rolling of the neutrophil along the endothelium causing upregulation of β2 and β1 surface integrins on the neutrophil allowing them to interact with ligands, primarily intracellular adhesion molecule (ICAM-1), expressed on the inflamed endothelium, (*c*) firm arrest of the neutrophil after engagement with integrins

with accompanying cell spreading, (*d*) crawling of the neutrophil along the endothelium, and (*e*) transmigration of the neutrophil into the tissue (Mayadas, Cullere and Lowell, 2014).

Transmigration of neutrophils occurs predominantly via endothelial cell-cell junctions (paracellular transmigration) and in some cases through the endothelium (transcellular transmigration) and is facilitated by adhesion molecules including junctional adhesion molecule (JAM), platelet endothelial cell adhesion molecule (PECAM) and CD99 expressed on endothelial cell junctions and leukocytes (Sullivan and Muller, 2014). Neutrophil transmigration into tissues results in full neutrophil activation and subsequent phagocytosis and pathogen killing via generation of ROS and neutrophil extracellular trap (NET) formation.
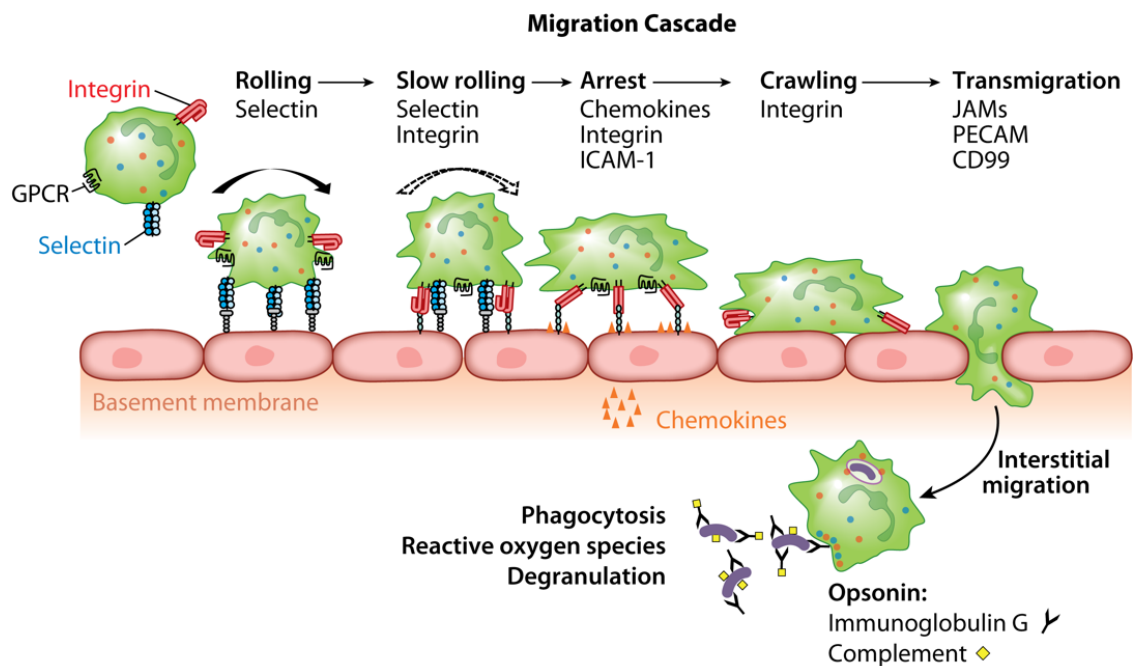
Figure 1-2 Multiple step adhesion cascade of neutrophil recruitment in the inflamed endothelium (Mayadas, Cullere and Lowell, 2014)

1.1.3 Neutrophil activation: degranulation, ROS production and NETosis

When neutrophils encounter pathogenic bacteria, they trap them within intracellular vacuoles called phagosomes, into which they discharge their granule-derived anti-microbial peptides such as MPO, neutrophil elastase (NE) cathepsin G and defensins. Simultaneously phagocyte NADPH oxidase reduces dioxygen to superoxide that dismutates and delivers hydrogen peroxide, a reaction known as the respiratory burst. In the presence of hydrogen peroxide and a low molecular-weight intermediate, MPO catalyses the formation of powerful reactive intermediates including hypochlorous and hypobromous acid as well as other reactive oxygen species (ROS) (Bardoel *et al.*, 2014).

Neutrophils can also trap, immobilise and kill microorganisms through the extracellular release of NETs (Brinkmann *et al.*, 2004). NETosis, is a process of cell death distinct from apoptosis or necrosis, that can be triggered by both infectious as well as 'sterile' stimuli such as cytokines (Keshari *et al.*, 2012), cholesterol crystals (Warnatsch *et al.*, 2015), autoantibodies (Söderberg and Segelmark, 2016) and immune complexes (Behnen *et al.*, 2014). Numerous granule-derived peptides have been detected on NETs including MPO, proteinase 3 (PR3), NE, cathepsin G, calprotectin, defensins and actin (Papayannopoulos, 2018). Subsequent studies have extended this list, suggesting that the composition of NETs varies depending on the stimulus and the environment in which they develop. For example, mucoid and non-mucoid Pseudomonas aeruginosa strains induce the formation of NETs containing a conserved set of proteins across the two strains but also up to 50 variable proteins (Dwyer *et al.*, 2014). In addition, the size of the invading pathogen may also selectively tailor their antimicrobial response. When neutrophils encounter yeast spores they tend to phagocytose, whereas when they encounter large pathogens such as hyphae neutrophils tend to release NETs (Branzk *et al.*, 2014).

1.1.4 The role of neutrophils in shaping the adaptive immune system

In addition to their vital role in innate immunity neutrophils and NETs have a very important regulatory role of the adaptive immune system. They can both activate or downregulate T cells responses. Neutrophils function as antigen presenting cells (APCs) or influence the capacity to present antigens by professional APCs. In particular, they can cross-prime CD8^{+} T-cells in an MHC-I-dependent manner (Beauvillain *et al.*, 2007). In addition, dendritic cells have been shown to take up antigens acquired from phagocytosed apoptotic neutrophils (Schuster, Hurrell and Tacchini-Cottier, 2013). Conversely, serine proteases such as PR3, elastase and cathepsin G can suppress T cell proliferation while ROS can also directly suppress inflammation through intracellular signalling (Han *et al.*, 2013; Fazio *et al.*, 2014). Neutrophils also synthesize cytokines crucial for B-cell development and they can act as B-cell helpers in a T-cell independent manner in the spleen (Gupta and Kaplan, 2016). NETs can independently activate Toll like receptors (TLR) and prime T cells (Warnatsch *et al.*, 2015). In addition, granule derived peptides presented on NETs can lead to autoantibody generation against these peptides and the development of autoimmune conditions such as AAV and Systemic Lupus Erythematosous (SLE) (Sangaletti *et al.*, 2012). For example, P-ANCA and C-ANCA containing sera from patients with AAV selectively target MPO and PR3 on NETotic neutrophils (Panda *et al.*, 2017). Furthermore, NET-associated vasculitis in cocaine users derives from levamisole-triggered NETosis and is characterized by the development of ANCA predominantly specific for NE and to a lesser extent MPO and PR3 (Wiesner *et al.*, 2004).

1.2 Myeloperoxidase biology

1.2.1 Biosynthesis, cellular storage and release

MPO is a highly cationic, heme-containing, glycosylated peroxidase which is found mainly in primary (azurophilic) granules of neutrophils, making up approximately 5% of the total dry cell weight (Klebanoff, 1999). It was first described in the early 1940s by Agner who initially named MPO

verdoperoxidase due to its intense green colour (Agner, 1941). Human neutrophils contain about 5–10-fold higher levels of MPO than murine neutrophils (Rausch and Moore, 1975). MPO synthesis is initiated in the promyelocyte stage of neutrophil development and terminates at the beginning of the myelocyte stage, at which time the MPO containing azurophilic granules intermingle with the newly formed peroxidase negative, specific (secondary) granules.

MPO is also found, to a lesser extent, in monocytes where it constitutes about 1% of total cell protein (Bos, Wever and Roos, 1978) and a peroxidase has also been identified in the cytoplasmic granules of eosinophils (Bainton and Farquhar, 1970).

MPO is the product of a single gene located in the long arm of chromosome 17 (Inazawa *et al.*, 1989). Its initial translation product is an 80-kD protein which undergoes glycosylation with the incorporation of mannose-rich side-chains (Strömberg, Persson and Olsson, 1986) to generate enzymatically inactive apoproMPO. With the insertion of a heme and further proteolytic cleavage apoproMPO is converted to proMPO and eventually the enzymatically active MPO (Grishkovskaya *et al.*, 2017). Figure 1-3 shows the structure of the mature MPO dimer (Fiedler, Davey and Fenna, 2000). Mature MPO has a molecular mass of 150 kD and consists of a pair of heavy-light protomers whose heavy subunits are linked by a disulfide bond along their long axis. The mannose-rich carbohydrate and the two hemes are covalently bound to the heavy subunit (Olsen and Little, 1984)
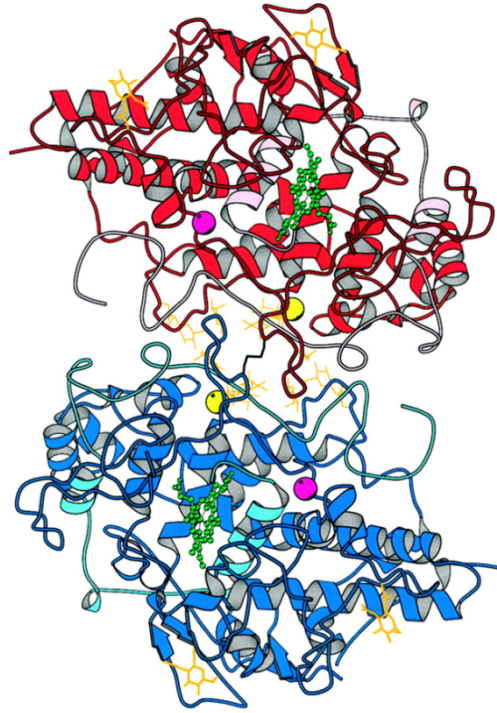
Figure 1-3 Entire MPO dimer, viewed along the molecular dyad axis.
The large polypeptides of the two halves are coloured *red* and *blue*, whereas
the small polypeptides are in *lighter shades* of the same colours. Other colour
coded features include: hemes (*green*), carbohydrate (*orange*), calcium
(*purple*), and chloride (*yellow*). The disulfide linking the two halves is at the
centre of the molecule (Taken from Fiedler et al. J. Biol. Chem. 2000)

1.2.2   The MPO-H_2O_2-halide system

When neutrophils encounter pathogenic bacteria, they trap them within
intracellular vacuoles called phagosomes, into which they discharge their
granule contents. Simultaneously phagocyte NADPH oxidase reduces
dioxygen to superoxide that dismutates and delivers hydrogen peroxide, a
reaction known as the respiratory burst (Klebanoff, 1999; van der Veen, de
Winther and Heeringa, 2009). In the presence of hydrogen peroxide and a low
molecular-weight intermediate (halide: chloride, bromide, thiocyanate, tyrosine
or nitrite) MPO catalyses the formation of powerful reactive intermediates
including hypochlorous (HOCl), and hypobromous (HOBr) acid as well as other
reactive oxygen species (ROS) (Klebanoff, 2005) (Figure 1-4). Klebanoff was
the first to describe that MPO, H_2O_2, and iodide, bromide, chloride, or

thiocyanate ions formed a powerful antimicrobial system in neutrophils (Klebanoff, 1968).
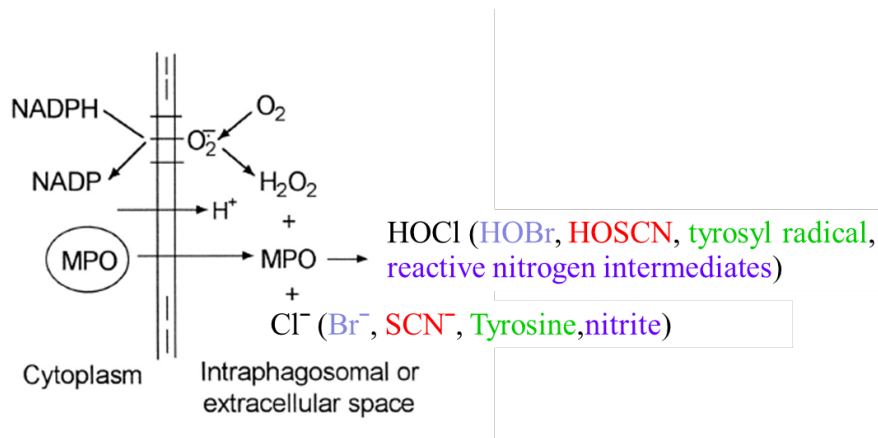
Figure 1-4 MPO-H_2O_2-halide system.

NADPH; reduced nicotinamide adenine dinucleotide phosphate, $O_2^{\cdot-}$ superoxide anion, HOCl; hypochlorous acid, HOBr; hypobromous acid, HOSCN; hypothiocyanous acid, SNC^-; thiocyanate (adapted from Klebanoff, 2005)

The contribution of the MPO-H_2O_2-halide system to the microbicidal activity of phagocytes is further illustrated by experiments in which one of the components of the system is inhibited or lacking. Patients with chronic granulomatous disease (CGD), a group of inherited disorders caused by single gene mutations, leads to complete or, less frequently, partial loss of NADPH oxidase activity, predisposing sufferers to recurrent, often life-threatening bacterial and fungal infections, as their neutrophils are unable to mount a respiratory burst and are therefore impaired in their microbicidal activity (Dinauer, 2014). Interestingly, this defect can be restored *in vitro* by adding H_2O_2 extracellularly (Johnston and Baehner, 1970).

What sets MPO apart from other mammalian heme proteins is its exceptional ability to oxidise chloride present at high concentrations in biologic fluids to hypochlorous acid (HOCl) a very potent oxidant that kills bacteria and is toxic to human cells (Winterbourn, 2002). Several lines of evidence have demonstrated

that the MPO/HOCl system plays an important role in optimal intracellular killing of bacteria with MPO-deficient mice showing reduced cytotoxicity to fungi (e.g Candida albicans) (Aratani *et al.*, 1999) and certain bacteria (e.g Pseudomonas aeruginosa) (Aratani *et al.*, 2000) . It should be noted, though, that the clearance of several pathogens including Staphylococcus aureus and Candida glabrata is not affected by the absence of MPO (Aratani *et al.*, 2000; van der Veen, de Winther and Heeringa, 2009).

1.2.3   The formation of Neutrophil extracellular traps

Myeloperoxidase may also kill bacteria outside of neutrophils. In 2004, Zychlinsky and colleagues described a process of neutrophils forming extracellular traps (NETs), since referred to as NETosis, by which neutrophils extrude a meshwork of chromatin fibres decorated with granule-derived antimicrobial peptides and enzymes such as neutrophil elastase and MPO. They suggested that NET formation was a novel form of extracellular bacterial killing (Brinkmann *et al.*, 2004).

NETting neutrophils are distinguished from apoptotic cells by the lack of 'eat me' signals on the cell surface. As a result, NETting neutrophils are not cleared by other phagocytes, and instead, the residual chromatin is disassembled mainly by nucleases (Fuchs *et al.*, 2007). NETosis is stimulated by a variety of inflammatory mediators (e.g., TNFα, IL-8, immune complexes) and pathogen associated molecular patterns (PAMPs) from a wide range of microbes (bacteria, fungi, and protozoa) (Brinkmann *et al.*, 2004; Keshari *et al.*, 2012).

NETs provide antimicrobial function both by localizing and trapping pathogens within a sticky meshwork of chromatin and by exposing pathogens to highly concentrated antimicrobial peptides and enzymes trapped within the chromatin (Figure 1-5). Besides MPO and neutrophil elastase, NETs are a concentrated source of LL-37, calprotectin (S100A8/9), and lactoferrin-chelating proteins. Recent data have shown that MPO is necessary for the formation of NETs (H. Björnsdottir *et al.*, 2015). Neutrophils from donors who are completely deficient

in MPO fail to form NETs in response to Candida infection. In contrast, neutrophils from partially MPO-deficient donors make NETs, while pharmacological inhibition of MPO delays and reduces NET formation (Metzler *et al.*, 2011). In addition, the induction of NETs in neutrophils from healthy subjects mediated by TNFα requires enzymatically active MPO (Keshari *et al.*, 2012).

The mechanism underlying this dependence on MPO has recently become clearer. MPO, together with elastase, have been demonstrated to associate with nuclear DNA/histones (Parker *et al.*, 2011; Papayannopoulos *et al.*, 2010; Metzler *et al.*, 2011). Upon activation by ROS that is generated in an MPO-H_2O_2 dependent manner, neutrophil elastase escapes from azurophilic granules and translocates to the nucleus (Metzler *et al.*, 2014). In the nucleus it partially degrades specific histones, promoting chromatin decondensation. Subsequently, MPO synergizes with neutrophil elastase in driving further chromatin decondensation (Papayannopoulos *et al.*, 2010), which is an essential step in the initiation of NET formation.

1.2.4 Myeloperoxidase deficiency

Since the MPO-H_2O_2-halide system has such a crucial role in innate immune defence, one would expect MPO deficiency in humans to have severe consequences, but this does not appear to be the case. In fact, MPO deficiency does not lead to a clinical phenotype and it only became apparent when peroxidase activity-based systems to differentiate leukocytes became routine practice in clinical laboratories. Partial or full MPO deficiency is not rare in the normal population with a reported prevalence of hereditary MPO deficiencies ranging from 1:1,000 to 1:4,000 in Europe and the United States (Cramer *et al.*, 1982; Kitahara *et al.*, 1981; Bos *et al.*, 1982; Dinauer, 2014) while it appears less common in Japan, with one study reporting prevalence of complete deficiency of 1:57,135 (Nunoi *et al.*, 2003; Kameoka, Persad and Suzuki, 2004).

Mutations in the MPO gene are frequently point mutations that cause defective posttranslational processing of the MPO precursor protein. Deficiency in myeloperoxidase inhibits formation of hypochlorous acid from chloride and hydrogen peroxide. (Hansson, Olsson and Nauseef, 2006; Dinauer, 2014).

In the absence of an overt infection-prone phenotype, the direct clinical consequences of MPO deficiency have not been studied extensively, but Kutter et al. compared a group of 100 totally or sub-totally MPO-deficient individuals to a reference population of 118 controls with normal MPO levels and found a protective effect of the deficiency for cardiovascular damage but a higher occurrence of severe infections and chronic inflammatory processes (Kutter *et al.*, 2000). However, in the majority of cases there was a remarkable lack of clinical symptoms in most individuals with MPO deficiency, despite in vitro defects in the ability to kill C. albicans and Aspergillus fumigatus hyphae and slower than normal bacterial killing (Aratani *et al.*, 1999, 2000). Nevertheless, patients with MPO deficiency rarely develop symptoms unless they also suffer from diabetes mellitus, which can lead to disseminated candidiasis and other fungal infections.

This contrasts with the severe infections observed in CGD patients that lack functional NADPH oxidase suggesting that in presence of MPO-deficiency, MPO-independent microbicidal mechanisms may increase their activity to compensate for the lack of MPO. Evidence to support this argument comes from Klebanoff's observation that the bactericidal activity of MPO-deficient neutrophils is greater than that of neutrophils treated with azide, a peroxidase inhibitor (Klebanoff, 1970).

1.3 The role of neutrophils and MPO in crescentic GN

1.3.1   Crescentic glomerulonephritis

Crescentic glomerulonephritis (CGN) describes a severe form of glomerular inflammation, which results from various systemic or renal specific diseases, and is characterised by glomerular neutrophil and monocyte activation. The

term 'proliferative' is classically used in the histopathological description of CGN and refers to glomerular hypercellularity often resulting from an increase in leukocyte accumulation. A crescent is characterised by disruption of the glomerular capillary wall resulting in a cellular infiltration into Bowman's space (Tarzi and Pusey, 2014).

Diseases leading to CGN can be broadly categorized into three groups based on the underlying pathological pattern. These include proliferative CGN owing to a) the deposition of circulating immune complexes, as seen in systemic lupus erythematosous (SLE) and IgA nephropathy, b) the generation of immune complexes in situ such as autoantibodies against the glomerular basement membrane (GBM) leading to Goodpasture's /anti-GBM disease and finally c) a pauci-immune pattern, often associated with anti-neutrophil cytoplasmic antibodies (ANCA) leading to ANCA associated vasculitis (AAV). ANCA are autoantibodies directed against cytoplasmic constituents of neutrophils and monocytes, the two main specificities being for PR3 and MPO.

Anti-GBM disease and ANCA associated CGN, are the most aggressive and destructive forms of CGN demonstrating more widespread neutrophil infiltration into the glomerular capillaries, crescent formation and areas of necrosis. Patients with a CGN present with proteinuria, haematuria, renal impairment and if untreated, they may progress to end-stage renal failure in weeks to months.

1.3.2   Signalling pathways in neutrophils in CGN

A number of ROS-inducing receptors and kinases are involved in neutrophil degranulation and NETosis in CGN following ligation of neutrophil receptors (Figure 1-5).

In AAV, ANCAs directed against MPO and PR3 can activate neutrophils through engagement of the Fc receptor (FcR), promoting degranulation, serine proteinase release, ROS production (Falk *et al.*, 1990) and NET formation (Kessenbrock *et al.*, 2009). Priming of neutrophils via different proinflammatory

stimuli such as TNFα (Falk *et al.*, 1990), bacterial lipopolysaccharide (LPS) (Huugen *et al.*, 2005) or the complement anaphylatoxin C5a (Schreiber *et al.*, 2009) can also lead to the release of serine proteases at the cell surface and into the microenvironment that can then interact with ANCAs.

Following FcR ligation, phosphorylation of p38 mitogen-activated protein kinase (p38 MAPK) and the extracellular signal-regulated kinase (ERK) induce ROS whereas blockade of MAPK prevents this neutrophil priming and activation (Kettritz *et al.*, 2001). The induction of ROS via MEK (MAPK/ERK kinase) signalling has been shown to trigger a MPO pathway which leads to NETosis. In this pathway, MPO triggers the activation and translocation of NE from azulophilic granules to the nucleus. In the nucleus, NE proteolytically processes histones to disrupt chromatin packaging. Subsequently, MPO binds chromatin and synergizes with neutrophil elastase in chromatin decondensation and NET formation. Chromatin decondensation is also promoted by MPO and the activation of protein-arginine deiminase type 4 (PAD4), which citrullinates histones (Metzler *et al.*, 2014). Pharmacological inhibition of Dek, a nuclear chromatin-binding protein, as well as genetic Dek deficiency impairs NETosis, which can be rescued by the addition of exogenous recombinant Dek (Mor-Vaknin *et al.*, 2017). Similarly, NET formation is abrogated in PAD4 deficient mice, and pharmacological PAD4 inhibition reduces the formation of glomerular NETs and subsequent deposition of the autoantigen MPO in experimental MPO-ANCA GN (O'Sullivan *et al.*, 2019) and anti-GBM disease (Kumar *et al.*, 2015).

ROS produced by NADPH oxidase during the respiratory burst is not the only source of ROS generation following neutrophil activation. Recent work showed that NETosis triggered by ribonucleoprotein-containing immune complexes, prevalent in SLE, depends on mitochondrial ROS. Mitochondrial ROS oxidize NET DNA to increase its ability to activate type I interferons in myeloid cells through activation of the STING (stimulator of interferon genes) pathway (Lood *et al.*, 2016). Compared with reduced DNA, oxidized DNA is more resilient to nuclease degradation (Gehrke *et al.*, 2013) and NETs from patients with SLE

are more oxidized and more immunogenic than NETs from healthy neutrophils. Furthermore, Mitochondrial ROS inhibition with PAD4 inhibitors *in vivo* reduces disease severity and type I IFN responses in a mouse model of lupus.

Spleen tyrosine kinase (SyK) is a cytoplasmic tyrosine kinase that is phosphorylated following neutrophil FcR engagement (Ibarrola *et al.*, 1997). Increased expression and phosphorylation of Syk is detected in renal biopsies of patients with IgA nephropathy (McAdoo and Tam, 2018) and AAV whereas Syk inhibition reduces IL-8 production in MPO-ANCA induced ROS production by neutrophils (McAdoo *et al.*, 2020). These data raise hope that targeting these molecules could have therapeutic effects in patients with CGN.
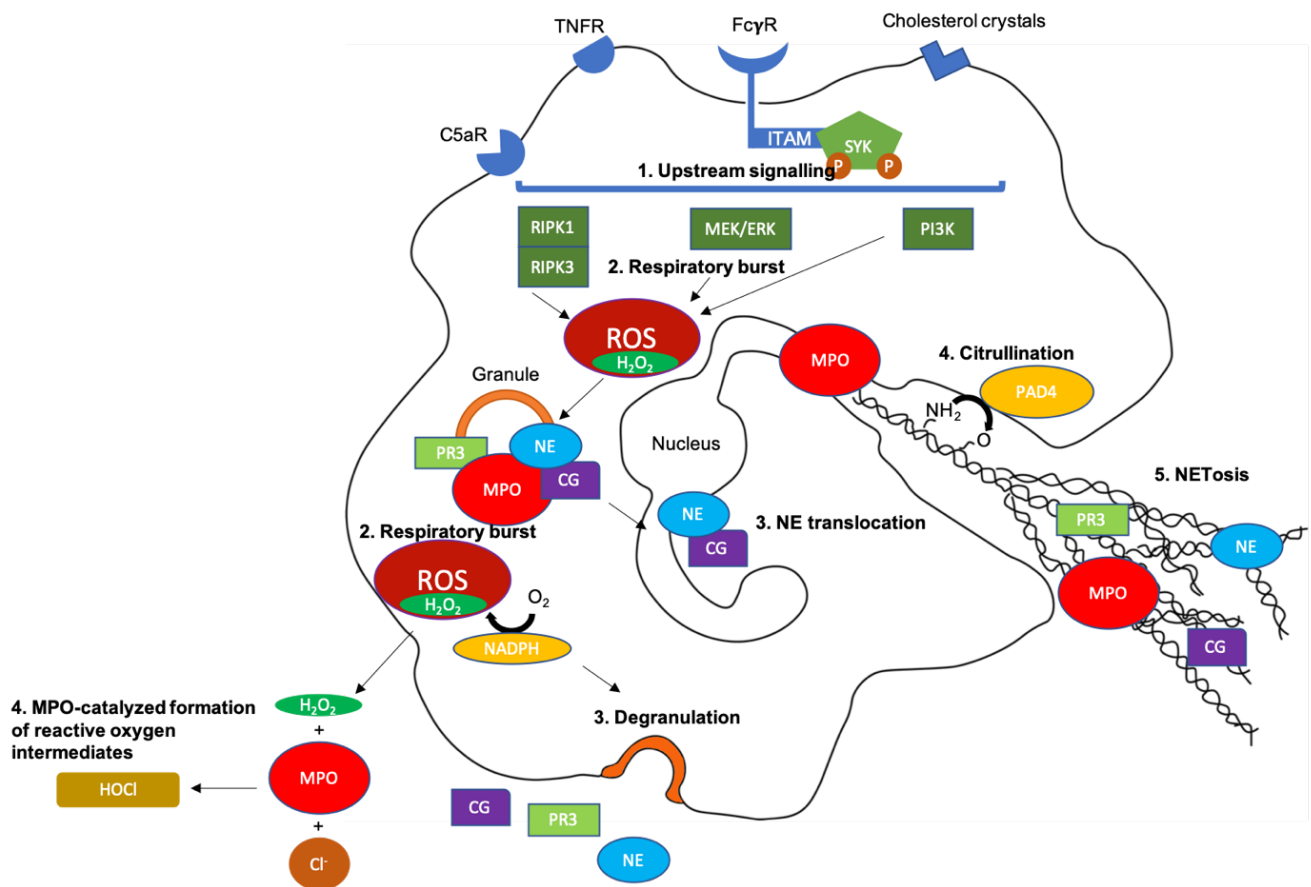
Figure 1-5. Pathways of neutrophil degranulation and NETosis in crescentic glomerulonephritis.

Engagement of neutrophil receptors via complement, cytokines, immune complexes and autoantibodies or cholesterols crystals triggers various signalling pathways resulting in the induction of ROS. These pathways involve the RIPK1/3/MLKL-dependent necroptosis signalling pathway, the MEK/ERK pathway and SyK phosphorylation leading the activation of downstream targets such as PI3K. The induction of ROS via MEK/ERK triggers the MPO-mediated oxidative activation of NE which subsequently translocates to the nucleus where it cleaves histones. Chromatin decondensation is also promoted by MPO binding and the activation of PAD4, which citrullinates arginine by converting amine groups to ketones. Finally, the nuclear membrane is degraded, and a mixture of chromatin and granular proteins is extruded from the cell. The secreted expulsion of nuclear chromatin is accompanied by the release of granule proteins through degranulation. In the presence of H_2O_2 and a low-

molecular weight intermediate such as chloride MPO catalyses the formation of powerful reactive intermediates including hypochlorous (HOCl) which can have profound effects on cellular function by modifying proteins, lipids, and/or DNA. The H_2O_2 required for MPO function comes mainly from the phagocyte NADPH oxidase during the respiratory burst.

CG, cathepsin G; MEK, MAPK/ERK kinase; PI3K, phosphoinositide 3-kinase; RIPK1/3, receptor-interacting serine/threonine-protein kinase 1 and 3, PAD4; protein-arginine deiminase type 4

1.3.3 NET formation in crescentic glomerulonephritis

Although neutrophils are short-lived and not present in sites of chronic inflammation, products of neutrophil degranulation and NETosis may amplify the inflammatory response beyond their short lifespan in tissues.

NETs and products of the respiratory burst are detected in renal biopsies of patients with diverse forms of CGN including ANCA positive and negative pauci-immune GN, lupus nephritis and crescentic IgA nephropathy (Villanueva *et al.*, 2011; O'Sullivan *et al.*, 2015) as well as in necrotizing lesions in preclinical anti-GBM disease. In this model NET-derived histones induced endothelial, podocyte and parietal cell injury whereas inhibition of NETosis reduced crescent formation (Kumar *et al.*, 2015).

In addition, NETs have been found in the circulation of patients with AAV and SLE (Kessenbrock *et al.*, 2009; Yu and Su, 2013; Söderberg *et al.*, 2015). Impairment of DNase1 function and failure to degrade NETs has been observed in SLE and correlated with kidney involvement (Hakkim *et al.*, 2010a). In MPO-ANCA CGN a reduced degradation of NETs has also been observed, implicating NETs as a means of breaking tolerance to ANCA autoantigens (Nakazawa *et al.*, 2014). The latter was corroborated in animal studies where presentation of extracellular DNA derived from NETotic neutrophils to myeloid dendritic cells led to MPO-ANCA and PR3-ANCA production, with subsequent vasculitis-like renal lesions in C57BL/6 mice (Sangaletti *et al.*, 2012). In

addition, augmented NET formation following infection in dectin-/- mice leads to a vasculitic phenotype, which can be attenuated by inhibiting NET generation. Similarly, in a rat model of MPO-AAV, immunization with NETs induced by PMA in combination with propylthiouracil, produced MPO-ANCA and induced pulmonary capillaritis (Nakazawa *et al.*, 2012). In SLE, NETs can further trigger an autoimmune response by exposing cathelicidin–DNA complexes, which, through activation of endosomal TLRs, promote the synthesis of type I interferons by plasmacytoid dendritic cells.

Low-density granulocytes are a distinct granulocyte population found in the peripheral blood mononuclear cell fraction following density separation of whole blood. Patients with SLE display LDGs that have an enhanced capacity to undergo spontaneous NETosis and induce endothelial cell damage. NETs from LDGs contain higher levels of autoantigens and immunostimulatory molecules than are NETs generated by healthy control neutrophils which suggests they might be a pathogenic force in autoimmunity (Carmona-Rivera *et al.*, 2015). NETs expressing PR3 and MPO were also spontaneously released from LDGs of AAV patients (Frangou *et al.*, 2019). However a recent report showed that although LDGs are expanded in patients with acute AAV, they are hyporesponsive to MPO-antibodies compared to neutrophils (Ui Mhaonaigh *et al.*, 2019).

NETs containing granule-derived proteins can present them to APCs leading to autoimmunity against these proteins. In addition, NETs can further trigger an autoimmune response by triggering the synthesis of type I interferons by plasmacytoid dendritic cells. Finally, neutrophils release inflammatory cytokines that activate T and B cells leading to autoantibody production in conditions associated with crescentic GN.

Figure 1-6 illustrates the different mechanisms NETs can cause pathology in CGN.

NETotic neutrophil in CGN

| Macrophages | Endothelial cells | Platelets | pDCS | T cell | B cell |

Atherosclerosis, IL-1, IL-18 release

Atherosclerosis, Necrotizing GN

Thrombosis, Fibrinoid necrosis

IFNα release in SLE

APCs for serine proteases and dsDNA

Activation and cytokine release

Autoimmunity
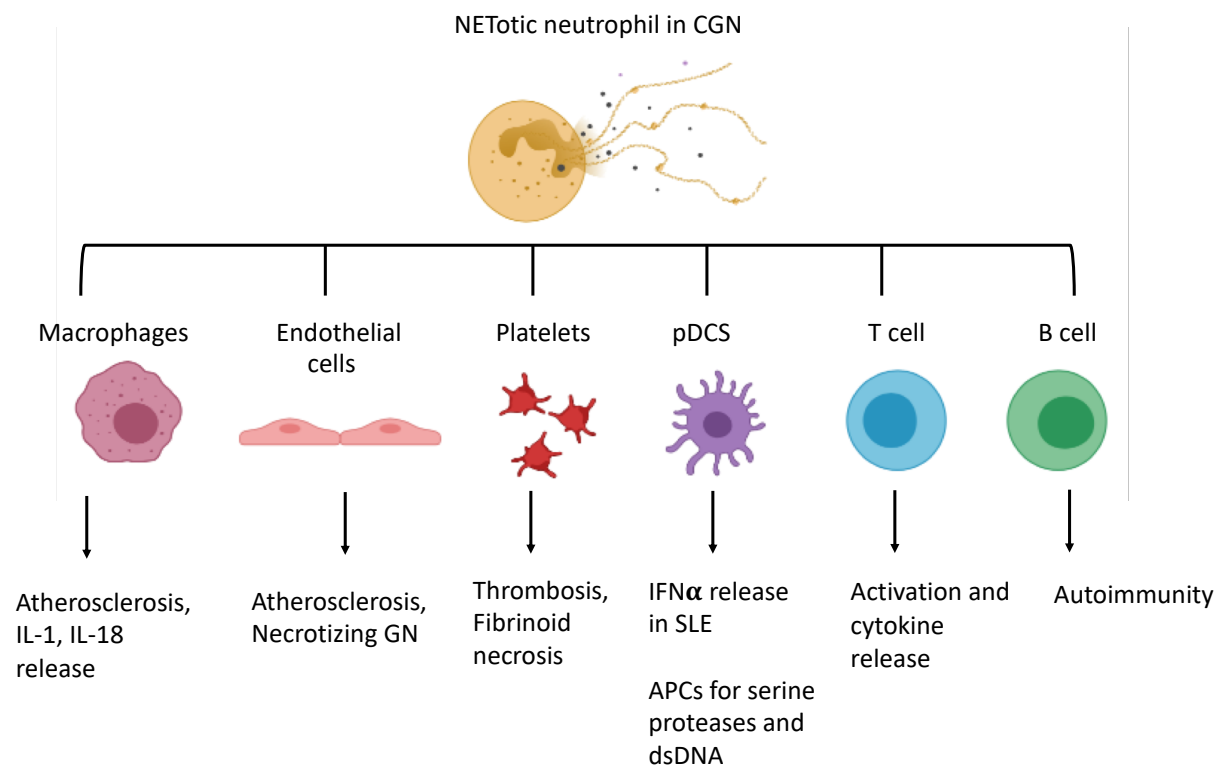
Figure 1-6 Mechanisms of NET mediated pathology in crescentic GN.
Upon release, NETs can cause pathology in crescentic GN through several mechanisms. NET peptides stimulate macrophages to release IL-1 and IL-18 promoting further neutrophil degranulation and NET formation. Secretion of IL-1β by macrophages is a major driver of pathogenesis in atherosclerosis. NET peptides and histones have been shown to induce EC damage and NET peptides such as MPO are also associated with EC dysfunction, a premature sign of atheroma formation. NETs can also promote the expression of tissue factor which activates platelets and coagulation factors promotes thrombosis.

1.3.4   Neutrophil serine proteases (NSPs) in CGN

Endogenous neutrophil serine proteases (NSPs) such as MPO, NE, PR3 and cathepsin G, released during neutrophil degranulation and NETosis, have been implicated in the development of glomerular injury in CGN. Leukocyte-associated and extracellular serine proteinase deposition is observed in renal biopsies of patients with various forms of CGN and correlates with degree of

renal impairment (Hooke, Gee and Atkins, 1987; Brouwer *et al.*, 1994; O'Sullivan *et al.*, 2015).

Cathepsin C (CatC) proteolytically activates pro-NSPs in the bone marrow producing mature neutrophil elastase, cathepsin G, and PR3. Loss-of-function mutations of the CatC gene as well as preclinical pharmacological CatC inhibition reduced NSP expression and proteolyic activity (Korkmaz *et al.*, 2018; Jerke *et al.*, 2019) In addition, Cathepsin G, NE and PR3 promoted IL-1β generation in preclinical anti-MPO CGN (Schreiber *et al.*, 2012) whereas administration of a neutrophil elastase inhibitor attenuated renal injury in a rat model of anti-GBM nephritis (Suzuki *et al.*, 1998). Similarly, pharmacological MPO inhibition ameliorated disease in murine anti-GBM nephritis (Zheng *et al.*, 2015) without augmentation of adaptive immune responses, unlike MPO deficiency in mice (Odobasic *et al.*, 2007). Furthermore, MPO deficiency in humans is common and is not associated with disease (Dinauer, 2014). Similar to MPO, CatC deficiency is associated with Papillon-Lefèvre syndrome where the main phenotype is prepubertal periodontitis but no immunodeficiency despite the almost total absence of proteolytically active NSPs (Pham *et al.*, 2004). The lack of an immunodeficient phenotype in the absence of serine proteases in humans makes NSPs a promising therapeutic target in CGN. Table 1-1 describes selective inhibitors that modulate neutrophils and NETosis in preclinical CGN and have been proposed as potential therapeutic targets.

Therapeutic target	Selective inhibitors	Preclinical models of CGN	Effect on human neutrophils	Ref
RIPK1	Nec-1s		Reduced NET formation from ANCA stimulated neutrophils and NET induced endothelial cell damage	(Schreiber et al., 2017)
MAPK	NPC 31145	Pre-emptive treatment reduced glomerular inflammation, glomerular neutrophil and platelet accumulation but had no effect on endothelial cell damage in rat anti-GBM disease		(Stambe et al., 2003)
	GS-444217 apoptosis signal-regulating kinase 1 (ASK1) inhibitor	Pre-emptive treatment reduced glomerular inflammation in rat anti-GBM disease		(Amos et al., 2018)
SyK	R406 fostamatinib	Delayed treatment reduced glomerular inflammation in preclinical anti-GBM and MPO-ANCA GN	Reduced IL-8 and ROS production from ANCA stimulated neutrophils	(McAdoo et al., 2014, 2020)
PAD4	GSK484	Delayed treatment reduced glomerular NETs, MPO deposition and leukocyte recruitment in murine MPO-ANCA GN		(O'Sullivan et al., 2019)
MPO	PF-1355	Pre-emptive treatment reduced glomerular inflammation and pulmonary vasculitis in chronic model of murine anti-GBM GN		(Zheng et al., 2015)

Cathepsin C	BI01169740	Reduced proteolytic activity of PR3 in bone marrow cells and NE in neutrophils of C57BL/6 mice	Reduced ROS production and ANCA-neutrophil stimulated induced EC damage	(Jerke *et al.*, 2019)
Elastase	ONO-5046	Reduced haematuria, proteinuria and crescent formation in rat anti-GBM GN		(Suzuki *et al.*, 1998)

Table 1-1 Selective inhibitors that modulate neutrophils and NETosis in crescentic glomerulonephritis.

1.3.5 Endothelial cell-neutrophil interactions in CGN

One of the hallmarks of CGN is endothelial injury and rupture of the glomerular capillary loops due to aberrant neutrophil activation. Cytokine-activated endothelial cells produce IL-8, which has a significant role in promoting neutrophil recruitment and migration. In autoimmune disease, humoral components such as immune complexes and autoantibodies as well as activation of the alternative pathway are involved in neutrophil transmigration through the inflamed endothelium. In particular, neutrophil Fcγ receptors trigger rolling and adhesion in the presence of deposited immune complexes (Tsuboi *et al.*, 2008) as well as complement activation with production of complement component 5a (C5a), a potent neutrophil chemoattractant. Activation of the alternative complement establishes a destructive inflammatory amplification loop that attracts and activates more neutrophils (Karsten and Köhl, 2012). A recent Phase II trial of C5a receptor blockade using the small inhibitory compound Avacopan as a steroid sparing treatment in AAV reported significant benefit compared to standard of care with steroids (Jayne *et al.*, 2017), while unpublished results of a larger phase III study suggest superior outcomes with regards renal function improvement following a year of therapy (https://www.viforpharma.com/~/media/Files/V/Vifor-Pharma/documents/en/media-releases/2019/vifor-pharma-advocate-read-out-pr-nov-26.pdf).

Neutrophil extracellular traps directly induce epithelial and endothelial cell death mediated predominantly by histones (Kumar *et al.*, 2015). Neutrophil degranulation with subsequent release of NE and PR3 led to endothelial cell apoptosis (Yang *et al.*, 1996). Furthermore, a recent study showed that ANCA-induced NETs involve the RIPK1/3/mixed lineage kinase-domain like–dependent necroptosis signalling pathway whereas RIPK1 inhibition attenuated NET induced endothelial cell damage by ANCA stimulated neutrophils *in vitro* (Schreiber *et al.*, 2017). Finally, through NETosis, LDGs have increased capacity to kill endothelial

cells and to stimulate IFN-α synthesis by plasmacytoid dendritic cells.(Villanueva *et al.*, 2011)

1.3.6 Myeloperoxidase inhibition in vitro and preclinical models

Latterly, selective MPO inhibitors have been developed and, in experimental models of heart failure (Ali *et al.*, 2016), pulmonary hypertension (Klinke *et al.*, 2018) and vasculitis (Zheng *et al.*, 2015), have been shown to ameliorate disease. In the present study, I have investigated the role of MPO in mediating glomerular damage and T cell activation using a novel therapeutic MPO inhibitor, AZM198.

AZM198 belongs to a group of compounds that are 2-thioxanthines and act as suicide substrates of MPO. To explain the proposed mechanism of inhibition, illustrated in Figure1-7, I will refer to the MPO-H_2O_2-halide system explained in detail in section 1.2.2. During the respiratory burst, hydrogen peroxide reacts avidly with the iron of MPO (which is normally in the ferric form) to form a complex compound I. Compound I of MPO is unique among mammalian peroxidases because its high two-electron reduction potential enables it to oxidize the halides chloride, bromide, and iodide as well as thiocyanate, to their respective hypohalous acids. Its even higher one-electron reduction potential allows it to remove a single electron from physiological substrates (RH) such as nitric oxide, superoxide, and tyrosine to produce free radical intermediates (R*). In these reactions, compound I is reduced to compound II. Free radicals are also produced when substrates reduce compound II and recycle the enzyme back to its native state (Klebanoff, 2005; Aldib *et al.*, 2016).

2-thioxanthines react with compound I of MPO with a rate constant sufficiently large for it to compete with chloride, the most abundant halide, for oxidation. Reduction of compound I results in formation of compound II, which indicates that the 2-thioxanthines must undergo one-electron oxidation to produce a free radical intermediate. The proposed mechanism of action for the MPO inhibitor is that these free radicals then react with the heme part of MPO and inactivate it. In this way, they prevent production of hypochlorous acid without concomitant release of free radicals (Tidén *et al.*, 2011) .

In addition, this group of inhibitors has been shown to have good specificity and are oxidized to a limited extent before the enzyme is fully inactivated. They had only a moderate effect on bacterial killing by neutrophils in vitro even at concentrations that completely blocked extracellular production of hypochlorous acid. Importantly, they were able to inactivate MPO in plasma and reduce NET formation *in vitro* (Tidén *et al.*, 2011; Halla Björnsdottir *et al.*, 2015)
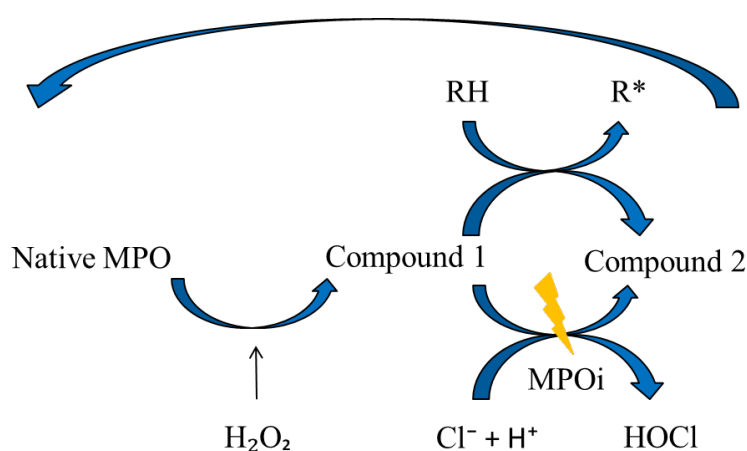
Figure 1-7 MPO complex formation and site of action of AZM198 (MPOi) (yellow sign). RH: physiological substrates, R*: substrate intermediates

1.4 Extra renal effects of neutrophils and myeloperoxidase in CGN

1.4.1 Incidence of athero-embolic disease in patients with crescentic glomerulonephritis

Patients with autoimmune diseases such as AAV and SLE have a significantly increased risk of developing cardiovascular atherosclerotic disease and thromboembolic events, often leading to premature mortality (Abou-Raya and Abou-Raya, 2006; Kang *et al.*, 2018).

In particular, we and others have found a 3-fold increase in coronary events (myocardial infarction and stroke) in patients with AAV compared with matched controls with chronic kidney disease (Morgan *et al.*, 2009; Kang *et al.*, 2018). Similarly, fatal myocardial infarction has been reported to be 3 times higher in

patients with SLE than in age- and gender -matched control subjects. Recent case- control series report that the risk of myocardial infarction in patients with SLE is increased between 9- and 50-fold over that in the general population (Esdaile *et al.*, 2001).

It remains unclear whether the high incidence of athero-embolic events in patients with autoimmunity is secondary to the disease itself or its treatment. Conditions associated with CGN are uniformly treated with corticosteroids that independently carry a high risk for cardiovascular disease. Evidence for the participation of histones and serine proteases in the development of atherosclerosis and thrombosis that can potentially identify them as promising steroid-sparing therapeutic targets not only in CGN but also in associated reno-cardiac disease, are presented in the following sections.

1.4.2 Neutrophils and serine proteases in cardiovascular disease.

Endothelial dysfunction is an early stage of atheromatous plaque development characterised by reduced vasodilation and a pro-inflammatory state displayed as enhanced expression of adhesion molecules and chemokines that eventually increase endothelial cell permeability (Soehnlein Oliver, 2012). Inflammatory stimuli such as TNFα and ANCA trigger β2-integrin activation which subsequently triggers neutrophil adhesion (Halbwachs and Lesavre, 2012). Adhesion of neutrophils to endothelial cells via β_2-integrin ligation results in rapid degranulation.

Neutrophil granule proteins are found in human atherosclerotic lesions, suggesting that activated neutrophils may directly contribute to lesion development (Mayadas, Cullere and Lowell, 2014). In addition, mice deficient in the neutrophil proteases such as PR3, NE and cathepsin G have lower inflammation and develop smaller atherosclerotic lesions (Herías *et al.*, 2015; Warnatsch *et al.*, 2015).

PR3 and azurocidin, both reside in azulophilic granules and are distributed into the surrounding on granule mobilization. Although no receptors for either protein have

been identified yet on endothelial cells, it was shown that the interaction of azurocidin and PR3 with the endothelium results in the activation of the latter. Azurocidin stimulates endothelial protein kinase C (Pereira, Moore and Grammas, 1996) which may explain enhanced expression of vascular cell adhesion molecule-1 (VCAM-1) and intercellular adhesion molecule-1 (ICAM-1) and subsequent recruitment of human monocytes (Lee *et al.*, 2003). Indeed, increased ICAM-1 and VCAM-1 expression are observed on glomerular endothelia from ANCA patients (Arrizabalaga *et al.*, 2008). Similarly, PR3 upregulates ICAM-1 expression, resulting in enhanced adhesion of neutrophils and monocytes to isolated endothelial cells (Taekema-Roelvink *et al.*, 2001). Neutrophils may also promote matrix degradation through PR3 and matrix metalloproteinases, leading to weakening of the fibrous cap on vascular atherosclerotic lesions (Soehnlein Oliver, 2012).

NETs have also been identified in human and murine atherosclerotic lesions (Megens *et al.*, 2012; Warnatsch *et al.*, 2015). Cholesterol crystals can induce NETs that prime macrophages for IL-1β and IL6 release, activating Th-17 cells that amplify immune cell recruitment in atherosclerotic plaques (Warnatsch *et al.*, 2015). Neutrophil elastase and cathepsin G are also known to process pro-IL-1β into its active form (Karmakar *et al.*, 2012). In addition to serine proteases, citrullinated histones are detected in atheromatous plaques (Sokolove *et al.*, 2013) and mice treated with PAD4 inhibitors, the enzyme that citrullinates histones during NETosis, have reduced atheroma formation (Knight *et al.*, 2014).

1.4.3   The role of myeloperoxidase in the development of atherosclerosis

Multiple lines of evidence support the role of MPO in atherogenesis in humans. Immunohistochemical evidence localises MPO and its oxidation products in human atherosclerotic plaques (Daugherty *et al.*, 1994; Hazen and Heinecke, 1997; Hazell, Baernthaler and Stocker, 2001; Sugiyama *et al.*, 2001). Individuals with total or subtotal MPO deficiency were protected from cardiovascular disease (Kutter *et al.*, 2000) whereas a polymorphism with a two-fold reduction in MPO

expression was associated with reduced angiographic evidence of coronary artery disease.

MPO promotes atheroma formation via low-density lipoprotein (LDL) oxidation (Smith *et al.*, 2014). Oxidised LDL accumulates in the subendothelial space and is subsequently taken up by macrophages to become foam cells, the first cellular hallmark of the atherosclerotic plaque. MPO also reduces NO bioavailability leading to endothelial cell dysfunction while pharmacological MPO inhibition attenuates endothelial cell dysfunction (Cheng David *et al.*, 2019) in a preclinical model of atherosclerosis.

MPO may also participate in ischemic complications of atherosclerosis via generation of HOCL that promotes endothelial cell apoptosis, leading to breakdown of the fibrous cap (Sugiyama *et al.*, 2004). Mechanistic links with activation of tissue factor (TF) and the coagulation cascade are also reported. Studies with MPO knockout mice and models of myocardial infarction have supported a role for MPO in progression of myocardial necrosis to adverse ventricular remodelling and heart failure via its ability to activate proteases and promote degradation of the extracellular matrix (Askari *et al.*, 2003). In addition, MPO inhibition improved ventricular function and remodelling after experimental myocardial infarction (Ali *et al.*, 2016). Figure 1-8 illustrates multiple processes throughout the evolution of atherosclerosis in which MPO is implicated.
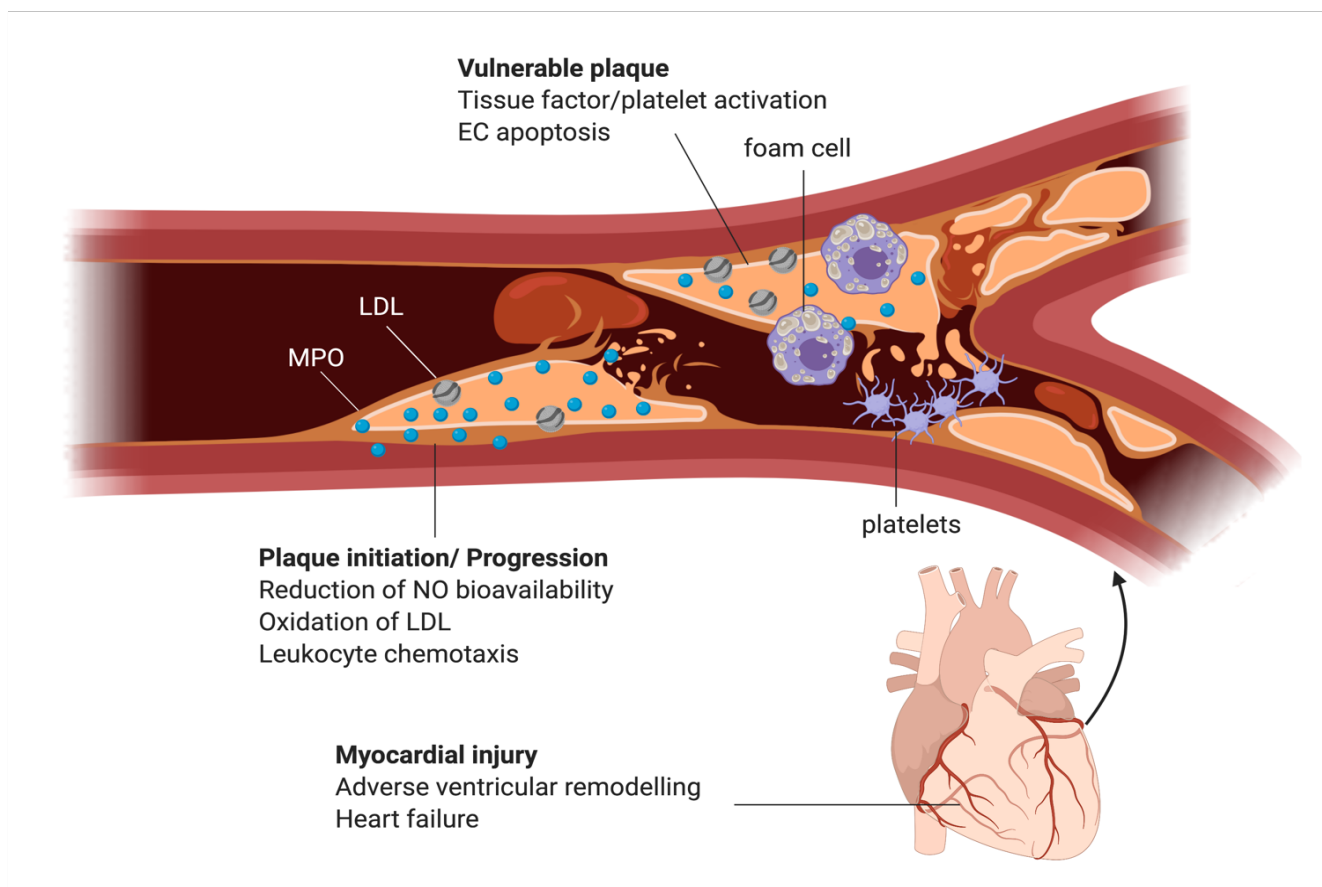
Figure 1-8 Scheme that illustrates the multiple processes throughout the evolution of atherosclerosis in which MPO is implicated.

1.4.4   The role of neutrophils and myeloperoxidase in thrombosis.

Neutrophil interaction with platelets plays a central role in inflammation and also provides an important link between inflammation and thrombosis. Impaired DNase1-mediated degradation of neutrophil extracellular traps is associated with acute thrombotic microangiopathies (Askari *et al.*, 2003) and DNase treatment or PAD4 inhibitors block DVT formation in mice (Martinod *et al.*, 2013). Neutrophils that accumulate at sites of vascular inflammation promote thromboxane A2 production by platelets, which induces endothelial cell expression of ICAM1 and strengthens neutrophil-endothelial cell interactions. In turn, this process triggers further NETosis (Papayannopoulos, 2018). In addition, NETs promote the expression of tissue factor which activates platelets and coagulation factors promoting thrombosis. Indeed, NETs are shown to co-localize with fibrin strands in

vitro, providing scaffolding for thrombus formation while histones can bind vWF to recruit platelets and red blood cells (Fuchs *et al.*, 2010)

1.5 Project hypothesis

As described above, MPO released through neutrophil degranulation and NETosis and its oxidation products can lead to direct host tissue damage in both CGN as well as associated atheroma formation.

My hypothesis is that selective MPO inhibition will reduced neutrophil degranulation, ROS production and NET formation while it will have a protective role in a preclinical model of CGN. Inflammation enhances atheroma formation which might suggest that chronic immune-mediated glomerular inflammation could be an independent risk factor for the development of atherosclerosis

The next chapters will aim to address the following key questions:

1. In MPO a marker of disease severity in CGN?
2. What is the effect of selective MPO inhibition on neutrophil degranulation, NET formation and neutrophil-mediated endothelial cell damage?
3. What is the effect of delayed MPO inhibition on glomerular inflammation and adaptive immune responses in a preclinical model crescentic glomerulonephritis?
4. What is the effect of chronic nephritis on atheroma formation?

2 Materials and Methods

2.1 Materials

2.1.1 Animals

C57BL/6 wild-type (WT), DO11.10 mice, BALB/C, ApoE$^{-/-}$ and MPO$^{-/-}$ mice, were obtained from The Jackson Laboratory (Bar Harbor, ME). Mice were 12 weeks old with an average weight of 25g. All animals were bred at UCL, housed in individually ventilated cages and fed a standard chow diet or a high fat diet provided by Special Diet Services (SDS) (AFE 45%FAT +0.15% Cholesterol, # 824063, Special Diets Services).

Studies adhered to the Animals (Scientific Procedures) Act 1986 (A(SP)A) and UCL Animal Welfare and Ethical Review Body (AWERB) guidelines for animal experimentation. All animal work described in this thesis was carried out under project license (PPL) P6377F606 and personal license (PIL) ICF36C587.

2.2 Methods

2.2.1 Human studies

2.2.1.1 Patient samples

Blood and tissue samples from patients presenting with AAV and other forms of glomerulonephritis, CKD disease controls, and healthy controls attending the Royal Free Hospital, London, UK were included in this study. All samples and biopsy specimens were obtained following informed consent (National Research Ethics Committee Reference 05/Q0508/6).

In all cases the diagnosis of AAV was confirmed by renal biopsy with a positive ANCA result. MPO activity during active AAV and two-month remission was measured using a sandwich ELISA(abcam) in PR3-ANCA positive patient serum enrolled in the RAVE trial (Stone *et al.*, 2010). Eighteen renal biopsies were obtained from patients with various forms of CGN (MPO-ANCA (n=5), Proteinase

3 (PR3)-ANCA (n=3), ANCA-negative pauci-immune GN (n=2), IgA (n=4) and SLE (n=4)) and stained for CD15 and MPO as described below. Clinical and laboratory data were collected from hospital records and pathology archives.

2.2.1.2.   Immunohistochemistry of renal biopsies

Sections (2 μm) of formalin-fixed, paraffin-embedded tissue specimens were mounted on superfrost plus slides (Menzel, Germany), dewaxed, rehydrated, and pre-treated with antigen retrieval solution Tris-EDTA pH 9 in a pressure cooker for 20 min, washed thrice, blocked in 5% casein solution for 1 hour and probed with antibodies against CD15 (Biolegend, cat#301902) for 2 hours in a humidified chamber (1:50 dilution) and MPO (DAKO, A0398) overnight at 4 °C. Isotype control antibody was used as a negative control at the same dilution as the primary antibody. Sections were subsequently washed thrice and visualized with a VECTOR Red alkaline phosphatase substrate kit (Vector, SK-5100) for CD15 and DAB substrate for MPO and counterstained with hematoxylin. The slides were then rinsed in water and counterstained with filtered Harris' haematoxylin (Cell Path plc, Powys, UK), then dehydrated and mounted with DAKO mounting medium and coverslips where then placed. Images were acquired on an Olympus CX-41 upright microscope. MPO deposition was expressed as a percentage of total captured area from ten random high power-fields using Colour Deconvolution, FIJI software (NIH, Bethesda, MD). Total and extracellular glomerular MPO deposition was expressed as a percentage of glomerular area from all glomeruli present on each biopsy section. The macro evaluated area stained, correcting for background threshold and expressed results as area fraction percentage of assessed area. Intra-leukocyte MPO was defined being associated with CD15 (CD15+MPO+ cells). Extracellular MPO was measured as MPO+CD15− staining.

2.2.1.3.   Purification of ANCA and control human immunoglobulin

Human anti-PR3 IgG from the plasma exchange fluid of three patients with crescentic PR3-ANCA GN and pulmonary haemorrhage and healthy control IgG from serum were purified using HiTrap Protein G column (GE Healthcare) chromatography. The 5ml protein G column was connected to a 20ml syringe via a suitable adapter and was washed with 50mls binding buffer (20mM sodium phosphate pH 7.0). Each sample was diluted at a ratio of 1:1 in binding buffer.

Plasma diluted in binding buffer from anti-PR3 patients and healthy control were processed on columns and IgG isolated from each sample, eluted by adding 5ml of elution buffer (0.1M glycine-HCl, pH 2.7) in 1.5mL reaction tubes containing 120μl alkalising agent (1M Tris-HCl, pH 9.0). The amount of IgG eluted was determined using a spectrophotometer, measuring absorbance at 280nm. The sample was dialysed overnight using a dialysis membrane in sterile PBS. After dialysis, the samples were endotoxin-depleted (see below) and quantified again using a spectrophotometer at 280nm and then stored at -20°C until used.

2.2.1.4. Endotoxin removal and detection assay

In order to ensure there was no LPS contamination of the isolated IgG, the preparations when incubated in Detoxi-Gel™ AffinityPak™ columns as pre manufacturer instructions. To test for the presence of LPS, the limulus amebocyte lysate assay (Lonza) was used. Standard LPS concentrations were obtained by following manufactures' instructions and diluting E.coli endotoxin into the following concentrations: 1.0, 0.5, 0.25 and 0.1EU/mL. The assay was performed in a water bath at 37°C. The Limulus amebocyte lysate was added to 50μl of sample or standard and following 10 minutes incubation, a chromogenic substrate supplied in the kit was added. The absorbance was then read at 405nm. The final concentration of the LPS-free IgG was determined using a spectrophotometer at 280nm.

2.2.1.5. Neutrophil isolation from human blood

10mls of peripheral blood anticoagulated with EDTA was mixed with 6% dextran to separate the blood cells (RBC). The upper layer containing the granulocytes was washed in PBS (centrifuged at 350g for 6 min) and transferred onto a Percoll (Sigma) gradient made up of 3mls each of the following percentages; 81%, 68% and 55%. After centrifugation at 700g for 20 minutes with no brake, the layers between 68% and 81% were collected, washed and counted for subsequent manipulation or analysis. Viability was ≥95%, assessed by trypan blue exclusion (Life Technologies).

2.2.1.6.   Neutrophil stimulation and inhibition experiments

Peripheral blood anticoagulated with EDTA was mixed with 6% dextran and granulocytes isolated on a Percoll (Sigma) gradient as mentioned above. Human neutrophils were suspended in RPMI medium (2% AB serum (Sigma), 500U/mL penicillin-streptomycin (Gibco Life technologies)). They were plated alone or stimulated with PMA (20 µM) (Sigma) or TNFα (2 ng/mL) (Bio-Rad Laboratories) and endotoxin-depleted ANCA or normal human IgG (both at 0.2 mg/mL) in the absence or presence of 10 µM AZM198, a concentration that has been reported to inhibit both intragranular and extracellular MPO activity, as well as NETosis (Halla Björnsdottir *et al.*, 2015). Cells were incubated with the inhibitor or vehicle control for 30 minutes prior to priming. The supernatants were collected at 30 minutes and peroxidase activity measured as described below. In flow cytometry experiments, isolated neutrophils were stained in 96 wells for viability then washed and stained for surface expression of MPO (2C7 FITC, ab11729) , CD11b (M1/70, BioLegend) and CD16 (3G8 BioLegend) for 30minutes at room temperature. The cells were not fixed prior to flow cytometry which carried out immediately after staining.

2.2.1.7.   ROS production (Dihydrorhodamine (DHR) assay)

DHR 123 is a non-reduced non-fluorescent molecule that in the presence of hydrogen peroxide is converted to rhodamine 123, which fluoresces at a wavelength of approximately 534nm and can therefore be detected in the FITC (FL-1)-light channel on a flow cytometer. Neutrophils (2.5×10^6 cells/ml) were loaded with 17µg/mL DHR123 (Calbiochem, UK) together with 5µg/mL Cytochalasin B as well as 2mM sodium azide and incubated in the dark for 10 minutes at 37°C. Cells were primed by incubation with 2ng/ml TNFα for 15 minutes and subsequently incubated with PR3-ANCA(200µg/ml) for 45 minutes and subsequently analysed by flow cytometry.

2.2.1.8.   Circulating MPO and HNP 1-3 levels, MPO enzymatic activity and ROS

Circulating MPO was measured by ELISA (AbCam) in serum samples. In neutrophil supernatants, HNP 1-3 levels were measured by ELISA (Hycult) as per manufacturer's instructions.

2.2.1.9.   MPO enzymatic activity

Peroxidase activity with 3,3′,5,5′-Tetramethylbenzidine (TMB, Sigma) was measured as described before (Suzuki *et al.*, 1983). Briefly, 10 µl sample were combined with 80 µl 0.75 mM H_2O_2 (Sigma) and 110 µl TMB solution (2.9 mM TMB in 14.5% DMSO [Sigma] and 150 mM sodium phosphate buffer at pH 5.4), and the plate was incubated at 37°C for 20 min. The reaction was stopped by adding 50 µl 2 M H_2SO_4, and absorption was measured at 450 nm to estimate MPO activity. A standard curve of MPO was made with human MPO (Sigma, #M6908), diluted in PBS.

2.2.1.10.   β-Glucuronidase activity assay

β-Glucuronidase activity of the supernatant was assessed by the cleavage of *P*-nitrophenolate from *P*-nitrophenyl-β-glucuronide (Sigma, N1627), which can be measured spectrophotometrically at a wavelength of 405 nm. The assay was performed using 96-well microtiter plates. Each well contained 50 µl of a 0.01 M solution of *P*-nitrophenyl-β-glucuronide in 0.1 M sodium acetate, pH 4.0, which was mixed with 50 µl of the cell-free supernatant. After an 18-h incubation period in the dark at 37°C, the reaction was stopped by adding 100 µl of a 0.4 M solution of glycine buffer, pH 10, to each well. Finally, the plates were scanned at 405 nm with a microtiter plate reader. Non-stimulated primed neutrophils provided a baseline, whereas the total neutrophil β-glucuronidase content was obtained by incubating the same amount of neutrophils with 1% Triton X-100 (Sigma). Results are expressed as percentage of the total β-glucuronidase content released per 8 × 10^5 cells/ml.

2.2.1.11.   NET visualisation and quantification

After the neutrophil supernatants were collected, cells were stained with Sytox Green (0.5 µM) (Invitrogen, cat#S7020) or fixed and stained with MPO (DAKO) and elastase (DAKO, M0752) visualised by anti-rabbit FITC and anti-mouse Alexa fluor 647 IgG respectively and counterstained with DAPI (2 µg/mL). NETs were visualised under a fluorescent microscope.

Ten consecutive high-power fields (HPFs) at 20x magnification were captured. For each image, DAPI and Sytox green (Alexa 488) were visualized. Acquired images

were automatically analysed by Fiji analysis software by determining the area of extracellular DNA, using a pixel threshold to exclude potential intracellular staining. Extracellular DNA of NETs was quantified as the cumulative area of positive Sytox green. The ratio of Sytox Green stained area: number of nuclei was calculated, representing the NET area index corrected for the number of imaged neutrophils. A higher index ratio indicates a larger NET area present.

2.2.1.12. Analysis of endothelial cell damage in EC-neutrophil co-culture

Human umbilical vein endothelial cells (EC), a gift from Dr Xu Shiwen, Centre for Rheumatology, UCL, were cultured on 0.1% gelatine-coated culture plates in basal EC medium containing low serum (2% FCS) and EC growth supplement (PromoCell). Bromodeoxyuridine / 5-bromo-2'-deoxyuridine (BrdU)-labelled EC were seeded into 96-well microtiter plates at 10^4 cells/well. Confluent EC were cultured for 16 h in the presence of TNFα (2 ng/well), then rinsed to remove all traces of TNFα and cultured for an additional 16 hours under the following conditions: EC alone; EC + unstimulated PMNs; EC + activated PMN; EC + activated PMN + AZM198; EC + activated PMN + DNAse. The PMNs (2 × 10^5 cells/well) were primed by TNFα (2ng/mL) for 15 minutes and stimulated with PR3-ANCA (200μg/mL). DNase (Sigma) was used at 500 U/mL (Sigma) and AZM198 at 10μM, both incubated with neutrophils for 30 minutes prior to priming. Supernatants were collected for analysis of BrdU-labelled DNA fragments using a cellular DNA fragmentation ELISA (Roche Diagnostics GmbH, Germany) and von Willebrand Factor release measured by ELISA (RayBiotech). Immunofluorescence staining of the EC monoculture and EC-PMN co-culture was performed using Vascular Endothelial Cadherin (MAB9381, R&D) and MPO (DAKO) counterstained with DAPI.

2.2.2. Animal models

2.2.2.1 Nephrotoxic nephritis (NTN)

Thirty two C57BL/6 mice were pre-immunised subcutaneously with sheep IgG (0.2mg) (Sigma-Aldrich, cat# I5131) in Complete Freunds Adjuvant (CFA) (Sigma-Aldrich, cat#F5881) and five days later received intravenous sheep nephrotoxic serum (NTS, 200 µL) mixed 1:1 with Lipopolysaccharide (LPS) (E.Coli R515, Hycult) diluted in 0.9% NaCl (5µg/mL, final concentration). One day post-immunisation with NTS 16 mice received AZM198 by gavage and the remaining animals were dosed with vehicle (0.5% hydroxypropyl methyl cellulose in water) every 12hr for 7 days. Two different AZM198 dose regimens were used: 133µmol/kg (n=8) or 400µmol/kg (n=8). Both doses are predicted to inhibit at least 80% of the extracellular MPO-activity over 12h, and the high dose is predicted to also inhibit intragranular activity more than 80% during 4 out of 12h (Halla Björnsdottir *et al.*, 2015). The allocation of animals to groups and the order of dosing were random. The animals were placed in metabolic cages on day 7 for urine collection and were culled on day 8. Kidneys were collected in buffered formalin and stained with periodic acid Schiff (PAS) and haemotoxylin-eosin (Sigma) or paraformaldehyde-lysine-periodate (PLP) for immunofluorescence.

2.2.2.2 DO11.10 T cell adoptive transfer model

Lymphocytes were harvested from the lymph nodes of BALB/c DO11 mice, that are transgenic for an MHC class II-restricted T cell receptor (DO11.10) recognizing an ovalbumin peptide, and stained with KJ126, a monoclonal antibody against the DO11.10 T cell receptor. KJ+CD4+cells were subsequently injected intravenously into six BALB/c mice ($1.2x10^6$ cells/mouse). The following day, the mice were immunised subcutaneously with 50µL ovalbumin peptide (2mg/mL) mixed 1:1 in incomplete Freund's adjuvant on each side of the chest wall. Subsequently, the mice were dosed twice daily by oral gavage with vehicle or AZM198 (400umol/kg) for 7 days, following which they were sacrificed, and their draining lymph nodes were harvested. Cells were stained for DO11.10, CD4, and CD44 and analysed using flow cytometry (BD) and FlowJo software.

2.2.2.3. Glomerular neutrophil accumulation

Eight C57BL/6 mice were dosed with either vehicle (n=4) or AZM198 (n=4) twice a day at 133 µmol/kg for 48 hours prior to the injection of nephrotoxic serum (NTS) as described above. Twelve hours after the last dosing and 2 hours after NTS injection kidneys were collected and frozen sections stained for Ly6g (Abcam ab25377), a murine neutrophil marker

2.2.2.4. Pharmakokinetic study for AZM198

Nine C57BL/6 mice received a single dose of 133µmol/kg AZM198 via oral gavage. Free plasma AZM198 was measured at 2, 12 and 19 hours post dose (n=3 at each tome point) to define the maximal (C_{max}) and trough (C_{min}) levels, and to bridge the data to the terminal samples of the NTN study.

2.2.2.5. Atheroma model in non-accelerated nephrotoxic nephritis

Six ApoE^{tm1Un} mice (three females, three males) and 5 C57BL/6 mice (three females, two males) were immunised intravenously with sheep nephrotoxic serum (NTS, 200 µL) mixed 1:1 with Lipopolysaccharide (E.Coli R515, Hycult) diluted in 0.9% NaCl (7.5µg/mL, final concentration) and 6 ApoE^{tm1Un} mice (three females, three males) received intravenous 200 µL 0.9% NaCl. Mice will be 10-12 weeks old, housed in individually ventilated cages with food and water provided ad libitum. After immunisation all mice received the same pelleted high fat diet (AFE 45%FAT +0.15% Cholesterol, # 824063, Special Diets Services) for 10 weeks. Weekly weights were recorded, and mice were placed in metabolic cages for 16hr urine collection every two weeks for the duration of the study. At week 11, urine and blood were collected and murine kidneys, hearts and aortas were harvested.

2.2.2.6. Measurement of proteinuria and creatinine

Sixteen hours prior to sacrifice, the mice were placed in individual metabolic cages and urine collected. Mice had access to food and water. Proteinuria was quantified using the sulphosalicylic acid assay. Standards were obtained using several

concentrations of bovine serum albumin (BSA)(Sigma-Aldrich). The following dilutions prepared: 1, 0.8, 0.6, 0.4, 0.2, 0.1, 0.05, 0.02 and 0mg/ml. Urine from individual animals was plated into a 96 well plate in triplicate at either a dilution of 1:10 (or 1:100 if significant proteinuria on urine dipstick analysis (Multistix 8 SG, Siemens)). 10µl per well of 25% sulphosalicylic acid was added to 2 wells, with water added to the third well. The optical density was then analysed using an ELISA plate reader (Lab Tech International, UK) at 450nm and proteinuria concentration

calculated from the standard curve generated by BSA. Plasma creatinine was measured at the MRC Harwell Institute, Mary Lyon Centre, Harwell Campus, Oxfordshire.

2.2.2.7.   Histological scoring

Images were acquired on an Olympus CX-41 upright epi-fluorescent microscope. Murine kidney sections were scored for glomerular thrombosis by counting 25 consecutive glomeruli from 10 randomly chosen high power fields (HPFs) and scoring each glomerulus (number of glomerular quadrants with thrombosis, score 0-4). Glomerular MPO and F4/80 staining was expressed as corrected total cell fluorescence (CTCF) and number of CD4 positive cells was counted per glomerulus using Fiji software. Ten randomly chosen HPFs were used to score 25 adjacent glomeruli per section. One section was scored per animal.

2.2.2.8.   Immunofluorescence staining of frozen kidney sections

Direct immunofluorescence was performed on PLP fixed- frozen kidney sections for MPO (DAKO), macrophages (using anti-F4/80, Invitrogen cat#14-4801-81), CD4 cells (using rat anti-mouse CD4 clone GK1.5, BD) and sheep IgG (Sigma) . Frozen kidneys were sectioned at 5µm thickness and fixed in 2% paraformaldehyde. 5 % goat serum (Sigma) was applied to block non-specific binding, followed by incubation with the primary antibody: F4/80, FITC CD4 and sheep IgG for 2 hours at room temperature and rabbit anti-mouse/human MPO (DAKO) at 4°C in a humidified chamber overnight). Post incubation the sections

were treated with a secondary antibody (goat anti-rat AF488 and goat anti-rabbit FITC) for 2 hours and subsequently visualised under a fluorescent microscope

2.2.2.9. Isolation and processing of murine splenocytes

The spleens were harvested, and each mouse spleen was passed through a 70µM and subsequently 40µM cell strainer. The isolated splenocytes were spun down for 5 minutes at 350g followed by re-suspension in 5ml (red blood cell) RBC lysis buffer (4.17g NH4Cl, 0.00185g EDTA, 0.5g NaHCO3, 500ml sterile water). Red cells were lysed for 1 minute, followed by the addition of media (RPMI-1640 (Sigma) including 10% FCS (Gibco) and 5% penicillin/ streptomycin (10,000 U/mL, Thermofisher) to a final volume of 15mls. Splenocytes were then spun down at 350g for 5 minutes and re-suspended in 20mls of media. After counting the cells, a final suspension of $5x10^6$ cells per ml/media. 500,000 splenocytes in 100µl were plated out per well in a 96-well plate in duplicate. Splenocytes were plated alone in duplicate, or with 50µg/ml of aggregated (heated to 60°C for 5 minutes to aggregate) sheep IgG (Sigma). The cells were stimulated at 37°C, 5% CO2 for 72 hours. Following the stimulation, lymphocytes were plated in 96-well plates, stained for viability and T cells populations for expression of CD4 (GK1.5), CD44 (IM7) and CD62L (MEL-14), and analysed by flow cytometry (FlowJo software) for 30min on ice , fixed in 2% paraformaldehyde and analysed with flow cytometry.

2.2.2.10. Circulating antibodies
Circulating serum levels of mouse anti-sheep globulin IgG subclasses, IgG1, IgG2b and IgG3 were assessed by ELISA (Invitrogen) according to the manufacturer's protocol.

2.2.2.11. En face lesion quantification

For en face lesion quantification the aorta was cleaned of peripheral fat and branching arteries under a dissection microscope and cut open longitudinally to expose the inner surface of the aorta from the aortic arch through thoracic and abdominal aorta. Aortas were pinned on a silicone disc with insect pins and immersed in deionised H_2O for 1 minute to remove PFA, 60% isopropanol for 2

minutes and 12 minutes in O-red-oil on an agitating device in the dark. They were subsequently destained by briefly immersing in 60% isopropanol and deionised H_2O. The sections containing whole aortas were then mounted with aqueous medium and outsourced to be scanned by LD path Operations Team using a 3DHistech P250 scanner. One image was captured per animal.   The relative lesion area was calculated using ImageJ software proportional to the total area of the whole aorta or the total volume of the aortic root, respectively

2.2.2.12.   Genotyping MPO -/-

Ear clips were digested for 30 minutes in 75μl alkaline lysis buffer (1.25M NaOH, 10mM EDTA, pH12) at 95°C. After digestion they were subsequently neutralised with 75μl neutralising solution (2M Tris-Cl, pH 5) and kept on ice. PCR (polymerase chain

reaction) was conducted with 5μl of the crude lysates and illustraTM puReTaq Ready-To-Go PCR Beads and the addition of 1.25μl $MgCl_2$ and 0.6μl of each 20mM primer in each tube. Primer sequences and cycling conditions were specified by The Jackson Laboratory (Oligonucleotide synthesis, Sigma Aldrich).

Primers: 5' TGA-CAC-CTG-CTC-AGC-TGA-AT 3'

 5' TGC-AGGCAG-CTG-GTC-TCG-CA- 3'

 5' CTA-CCG-GTG-GAT-GTG-GAA-TGT- 3'

PCR conditions:

Hot-start	95°C for 5 minutes	
35 cycles	Denaturation	94°C for 1 minute
	Primer annealing	60°C for 1 minute
	DNA extension	72°C for 1 minute
Final extension	72°C for 5 minutes	
Hold	4°C indefinitely	

A 1.5% agarose (Thermo Fisher 93 Scientific) with 1μl/mL Syber in TAE buffer was prepared. Gels were run in TAE buffer at 100V for 30 minutes and visualised using a UV light source.

Expected results
Mutant = ~350 bp

Heterozygote = ~155 bp and ~350 bp

Wild type = ~155 bp

2.2.2.13.   Genotyping ApoE -/-

Ear clips were digested for 30 minutes in 75μl alkaline lysis buffer (1.25M NaOH, 10mM EDTA, pH12) at 95°C. After digestion they were subsequently neutralised with 75μl neutralising solution (2M Tris-Cl, pH 5) and kept on ice. PCR (polymerase chain

reaction) was conducted with 5μl of the crude lysates and illustraTM puReTaq Ready-To-Go PCR Beads and the addition of 1.25μl $MgCl_2$ and 0.4μl of each 20mM primer in each tube. Primer sequences and cycling conditions were specified by The Jackson Laboratory (Oligonucleotide synthesis, Sigma Aldrich).

Primers: 5' GCC TAG CCG AGG GAG AGC CG 3'

        5' TGT GAC TTG GGA GCT CTG CAG C 3'

        5' GCC GCC CCG ACT GCA TCT 3'

PCR conditions:

Hot-start	94°C for 3 minutes	
35 cycles	Denaturation	94°C for 30 seconds
	Primer annealing	68°C for 40 seconds
	DNA extension	72°C for 1 minute
Final extension	72°C for 2 minutes	
Hold	10°C indefinitely	

A 1.5% agarose (Thermo Fisher 93 Scientific) with 1μl/mL Syber in TAE buffer was prepared. Gels were run in TAE buffer at 100V for 30 minutes and visualised using a UV light source.

Expected results

Mutant = ~245 bp

Heterozygote = ~155 bp and ~245 bp

Wild type = ~155 bp

ApoE$^{-/-}$ were crossed with MPO$^{-/-}$ to obtain ApoE$^{-/-}$/MPO$^{-/-}$, to be used for future experiments with the atheroma model of non-accelerated nephrotoxic nephritis (section 2.2.3.4)

2.2.3. Statistical analysis

The Shapiro Wilk test was used to determine if data sets were well-modelled by a normal distribution and to compute how likely it is for a random variable underlying the data set to be normally distributed. If the data were normally distributed parametric tests of significance were applied. If the data were not normally distributed or the number of variables was less than five non-parametric tests were applied.

The results from animal and patient studies are expressed as medians (interquartile range, IQR) for non-parametric data or as mean (± standard deviation, SD) for parametric data. All statistics were performed using GraphPad prism 8.0 (GraphPad Software, San Diego California, USA).

For comparing two groups, Mann-Whitney U test or t test was used, for groups of three or more, Kruskal Wallis or one-way analysis of variance (ANOVA) was carried out for non-parametric and parametric data respectively. Two-way ANOVA was used to analyse differences among groups from more than one experiment for parametric data and Friedman test for non-parametric data. Wilcoxon signed-rank test was used to compare non-parametric paired data and paired t test was used to compare parametric paired data. Correlations were assessed using the non-parametric Spearman rank correlation analysis. A significant value was defined $p < 0.05$ with 95% confidence.

Power calculations

Initial power calculations for measuring serum MPO levels and MPO deposition on human biopsies were based on the number of subjects used previously in our laboratory to quantify serum concentration and deposition of calprotectin, a neutrophil granule protein. All power calculations carried out in this thesis used a significance value of less than 0.05 and power greater than 80% (Pepper *et al*., 2013). I subsequently used the smallest effect size from this analysis (effect size 1.3 for MPO concentration differences between patients and healthy controls) and representative subject numbers for degranulation assay read outs published in literature (Falk *et al.*, 1990) to perform the power calculations for the degranulation assays described in Chapter 4.

For the *in vivo* experiments power calculations were based on the average effect size from our *in vitro* experiments in Chapter 4 and previous experience of animal numbers used to show a significant difference between treatment groups from different interventions in the nephrotoxic nephritis model carried out in our laboratory. Based on these calculations we decided to proceed with 8 animals per group, in order to have a minimum effect size of 1.4, significance level less than 0.05 and power greater than 80%.

2.2.4. Buffers and solutions

2.2.4.2.   Polymerase chain reaction

Lysis buffer for ear samples

Alkalising lysis buffer (50x)

1.25M NaOH, 10mM EDTA, pH 12, To use in DNA electrophoresis was diluted down to 1x with nuclease free H_2O.

Neutralising solution (50x)

2M Tris-Cl, pH **5**. To use in DNA electrophoresis was diluted down to 1x with nuclease free dH$_2$0.

TAE buffer (50x)

40mM Tris-acetate, 1mM EDTA (pH 8.0) To use in DNA electrophoresis was diluted down to 1x with dH$_2$O.

2.2.4.3.   Tissue fixation

Neutral buffered formalin (pH 7.0)

100ml formalin, full strength (37-40% formaldehyde), 6.5g of Na$_2$HPO$_4$, 4g NaH$_2$PO$_4$ and 900mLdH$_2$O.

Paraformaldehyde lysine periodate (PLP) fixative

Lysine stock solution: prepare 0.2M lysine monohydrochloride (3.65g/100ml) and add to an equal volume of 0.1M disodium hydrogen orthophosphate (1.41g/100ml for anhydrous). Adjust to pH 7.4 and store at 4°C.

4% Paraformaldehyde: Paraformaldehyde was dissolved in dH$_2$0 at 4g/100mL with stirring at 60°C in a fume hood. The solution was cleared by adding a few drops of 1M NaOH and then stored at 4°C.

Immediately prior to use, add 1 volume of 4% paraformaldehyde to 3 volumes of lysine stock solution and add sodium metaperiodate 0.214g/100ml (10mM).

2.2.4.4.   Immunohistochemistry

Phosphate buffered saline (PBS)

137mM NaCl, 0.27mM KCl, 8.1mM Na$_2$PO$_4$, 1.5mM KH$_2$PO$_4$, adjust to pH 7.2

Tris-EDTA

10 mM Tris base, 1 mM EDTA solution, 0.05% Tween 20, pH 9.0

Diaminobenzine (DAB) solution

0.05% DAB, 0.001% 30%H_2O_2 in PBS (pH 7.5)

Acid alcohol

1% HCl mixed with 70% ethanol

2.2.4.5.　　ELISA

Wash buffer

0.05% Tween 20 in PBS (pH 7.5)

Blocking buffer

3% BSA in PBS (pH 7.5)

Reagent diluent

1% BSA in PBS (pH 7.5)

Substrate solution

1:1 mixture of colour Reagent A (H_2O_2) and colour Reagent B (Tetramethylbenzine) (R&D Systems)

Stop Solution

1M H_2SO_4 diluted in dH_2O

2.2.4.6.　　Tissue culture

Neutrophil medium

RPMI (2% AB serum (Sigma), 500U/mL penicillin-streptomycin (Gibco Life technologies))

Endothelial cell medium

Basal EC medium containing low serum (2% FCS) and EC growth supplement (PromoCell)

2.2.4.7. FACS solutions

FACS Wash buffer

0.5% BSA, 0.1% NaN_3 diluted in PBS

Fixation solutions

4% and 2% paraformaldehyde

3 Myeloperoxidase as a marker of disease severity in crescentic glomerulonephritis

3.1 Introduction

Myeloperoxidase is the only peroxidase that uses H_2O_2 to oxidize several halides and to form different hypohalous acids such as hypochlorous acid (HOCL). So, the antibacterial activities of MPO involve the production of ROS and reactive oxygen intermediates. Controlled MPO release at the site of infection is of prime importance for its microbicidal role. Any aberrant degranulation exaggerates the inflammation and can also lead to tissue damage even in absence of inflammation. Several types of tissue injuries and the pathogenesis of several other major chronic diseases such as rheumatoid arthritis, cardiovascular diseases, liver diseases, diabetes, and cancer have been reported to be linked with MPO-derived oxidants (Khan, Alsahli and Rahmani, 2018). Thus, the enhanced level of MPO activity has gained importance as a possible biomarker of inflammation and oxidative stress in these conditions.

MPO has been detected in renal biopsies of patients with active vasculitis (Brouwer *et al.*, 1994; Kessenbrock *et al.*, 2009; Kawashima *et al.*, 2013; O'Sullivan *et al.*, 2015) and renal and skin biopsies of patients with active lupus

nephritis (Villanueva *et al.*, 2011). In addition, enzymatically active MPO and/or its products such as HOCL-modified proteins are upregulated at sites of inflammation in rheumatoid arthritis joints (Stamp *et al.*, 2012), and lungs of patients with cystic fibrosis (Kettle *et al.*, 2004). NETs and neutrophil granule proteins, including azurocidin, LL-37, and α-defensins, are also found in murine and human atherosclerotic lesions, suggesting that activated neutrophils may directly contribute to lesion development in cardiovascular disease (Edfeldt *et al.*, 2006; Warnatsch *et al.*, 2015).

In addition to its presence in tissue at sites of inflammation, MPO and MPO-containing NETs have been found in the circulation of patients with AAV and positively correlated with disease activity and neutrophil count (Kessenbrock *et al.*, 2009; Söderberg *et al.*, 2015). In rheumatoid arthritis increased MPO-containing NETs were found in peripheral blood, synovial fluid, rheumatoid nodules, and skin of RA patients, and NET levels were positively associated with the levels of anti-citrullinated antibody (Khandpur *et al.*, 2013). In sterile inflammation, serum levels of MPO have been shown to predict risks of subsequent major adverse cardiac events (nonfatal myocardial infarction, death, and need for revascularization) in patients presenting with acute coronary syndromes (Baldus *et al.*, 2003).

It is therefore plausible that NET-bound MPO contributes to organ inflammation and injury in those conditions given the ability of enzymatically active MPO to produce tissue damaging HOCl in the presence of H_2O_2, as well as to the development of autoimmunity where granule derived peptides presented on NETs, can be recognised as autoantigens.

In this chapter I explore the role of MPO as a marker of disease activity in diverse forms of crescentic GN including ANCA negative vasculitis, lupus nephritis and crescentic IgA nephropathy.

3.2   Aims

To investigate if MPO is a marker of disease activity in patients with diverse forms of crescentic GN

3.3   Experimental design

Levels of free myeloperoxidase were measured in the serum of patients with AAV and compared to renovascular disease, CKD controls and healthy controls. In order to assess if MPO levels vary according to disease activity I measured serum MPO in patients with PR3-ANCA disease from the RAVE trial during active disease and disease in remission at two months. I then performed immunohistochemistry staining for MPO in active renal biopsies of patients with crescentic GN secondary to various causes including ANCA positive and ANCA negative vasculitis, SLE, crescentic IgA nephropathy and post-infectious GN. This allowed me to detect the presence of total MPO deposition (leukocyte-associated and extracellular) in the glomeruli and in the tubulo-interstitium of patients with crescent GN. A sub-cohort of these biopsies were stained for both MPO and CD15, a neutrophil marker to detect the presence of extracellular MPO deposition. Image J software was used to quantify MPO deposition. Patient biopsy reports and clinical records were reviewed and correlated total MPO deposition in whole kidney, glomeruli as well as extra-leukocyte glomerular MPO with markers of clinical and histological disease severity eGFR (estimated glomerular filtration rate), proteinuria, percentage of active crescents and percentage of interstitial fibrosis and tubular atrophy).

3.4   Results

3.4.1   Serum MPO levels are elevated in patients with active AAV

Serum levels of MPO in patients with AAGN, renovascular disease controls and healthy controls were measured by ELISA. Increased MPO levels were found in patients with active PR3-AAGN 482 (330.0-1397) ng/mL compared with active MPO-AAGN 204.3(42.6-396.7) ng/mL (p=0.04) and healthy controls, 96.2 (53.5-176.3) ng/mL ($p < 0.001$). There was no significant difference in MPO levels

between active PR3- AAGN patients and renovascular disease controls 290.5 (182.8 – 419.5) ng/mL (p= 0.55). (Figure 3-1).

During inhibition studies we found that MPO-ANCA-containing serum inhibited MPO detection in the immunoassay by up to 40% (Figure 3.2), suggesting that the MPO-concentration in MPO-AAGN samples is potentially underestimated.
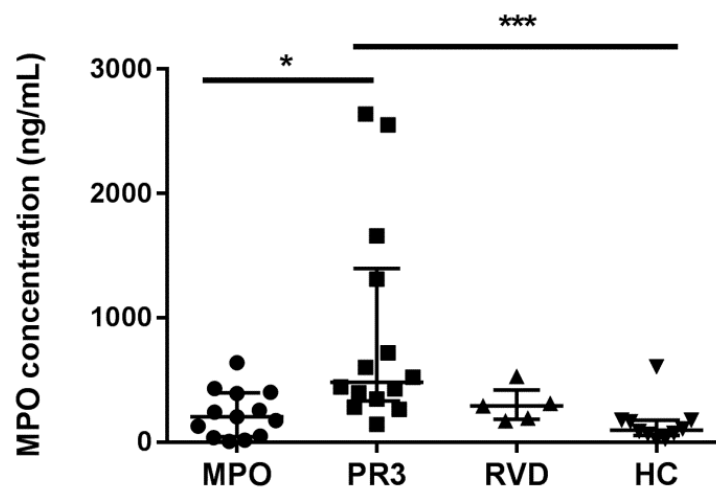
Figure 3-1. Serum MPO levels in patients with AAV, healthy and disease controls.

Median (IQR) serum concentration of circulating MPO in A) MPO (n=13) and PR3 (n=14) AAV ANCA-subtypes, renovascular disease controls (n=5) and healthy controls (n=10), non-parametric Kruskal-Wallis test and Dunn's multiple comparison post-test, *P<0.05, ***P<0.001
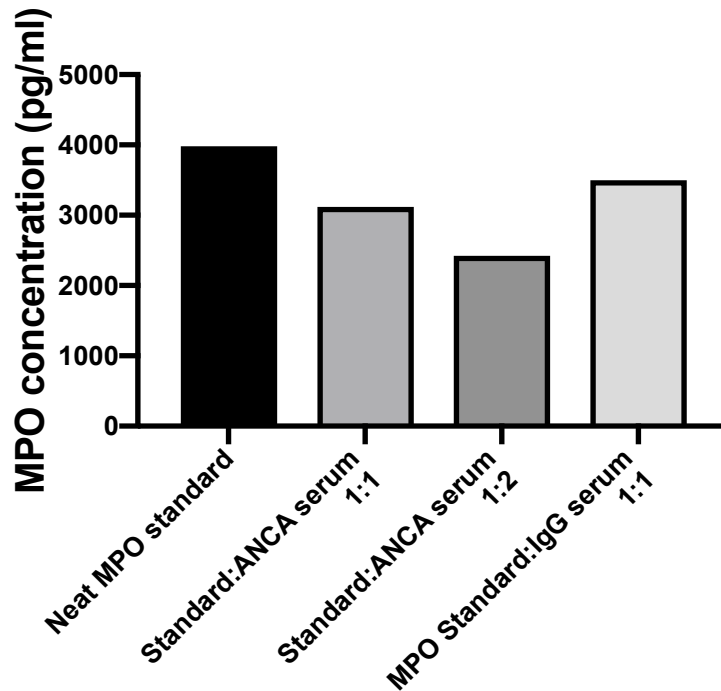
Figure 3-2. Inhibition studies of MPO by MPO-ANCA containing serum

Inhibition studies showing MPO concentration detected when human MPO standard (4000pg/mL) was incubated neat or after 1- hour incubation with MPO-ANCA containing serum in two dilutions and human IgG from a healthy control on pre-coated Elisa plates (MPO Elisa, DY3174).

Therefore, only patients with PR3-ANCA AAGN were included when differences between MPO levels in active AAGN and in disease remission were analysed (Figure 3-3).

MPO levels in PR3-ANCA patients with active disease from the RAVE trial were significantly reduced when measured at two-months following treatment (active AAGN 262.9 (211.5-355.2) ng/mL *vs* remission 177.5 (128.5-275.2) ng/mL, p= 0.002)
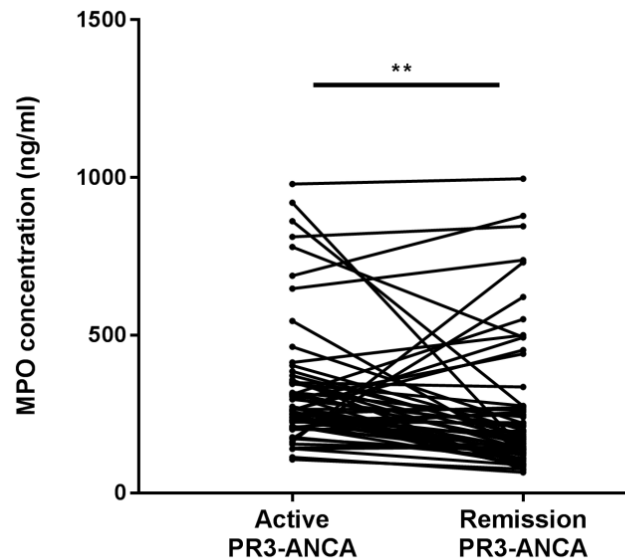
Figure 3-3. Serum MPO levels in patients from the RAVE trial.

Serum MPO levels in patients from the RAVE trial during active PR3-ANCA AAV and PR3-ANCA AAV in remission (n=58), non-parametric Kruskal-Wallis test and Dunn's multiple comparison post-test, Wilcoxon test ***P < 0.01.*

3.4.2 MPO deposition is seen in various forms of crescentic glomerulonephritis

MPO was detected by immunohistochemistry in renal patient biopsies with diverse forms of crescentic GN due to MPO-ANCA GN (n=5), PR3-ANCA GN (n=3), ANCA-negative pauci-immune GN (n=2), crescentic IgA (n=4) and SLE (n=4). MPO deposition (leukocyte associated and extracellular) was detected in all kidney biopsies (Figure 3-4). Most MPO that was detected was associated with leukocytes, with some non-leukocyte associated MPO deposited along the glomerular capillary walls. There was significant MPO deposition in biopsies with post infectious GN (3-4 D), consistent with the extensive neutrophil infiltration within the glomerular capillaries that characterises this form of crescentic GN.
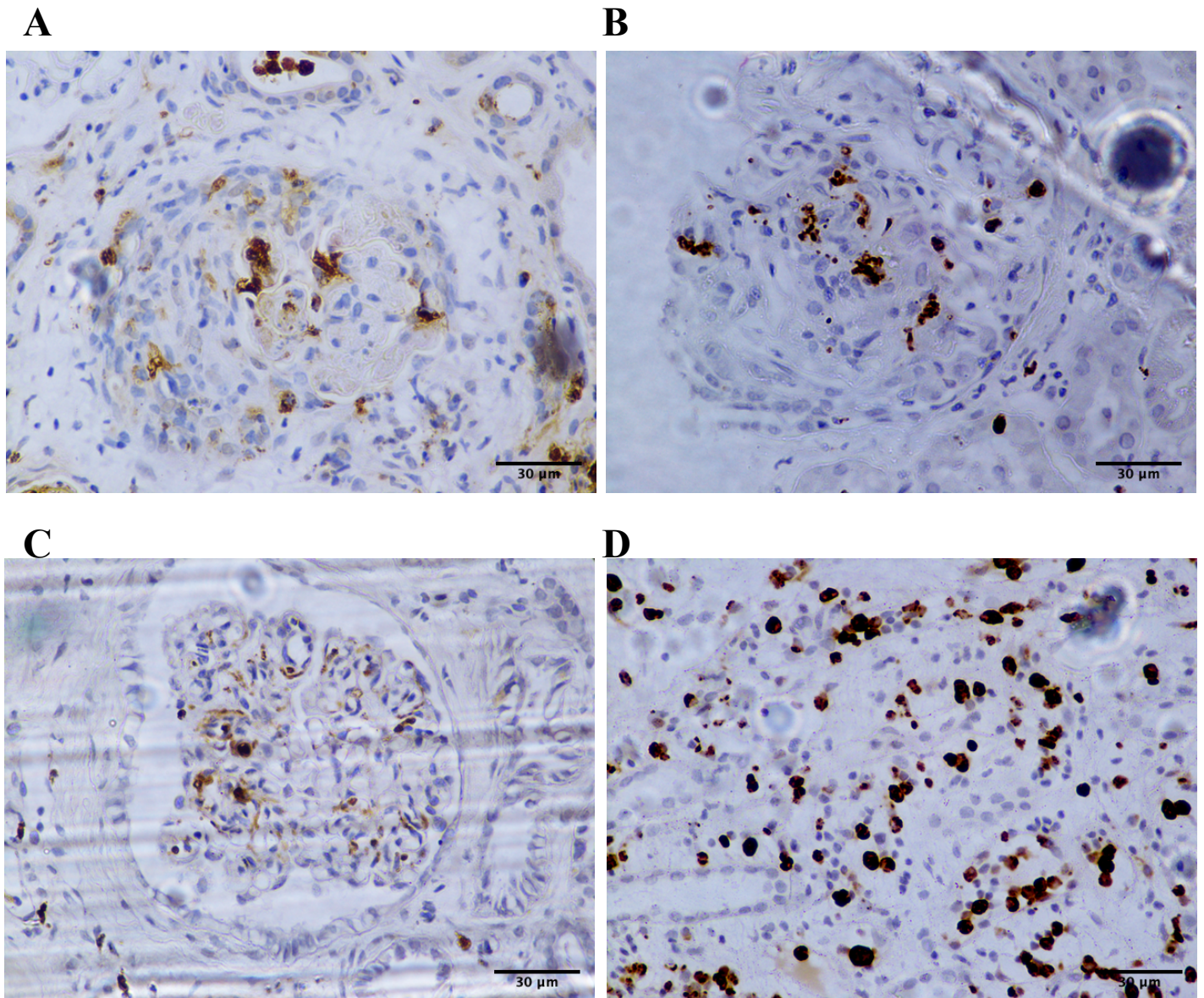
Figure 3-4 MPO deposition in patient biopsies with diverse forms of CGN.

Immunohistochemistry for MPO (brown) in inflamed glomeruli from patients with crescentic glomerulonephritis due to A) MPO-ANCA B) PR3-ANCA, C) ANCA negative disease and D) post-infectious GN.

Double staining was performed in a sub-cohort of these biopsies for both MPO and CD15, a neutrophil marker to detect the presence of extracellular MPO. Extracellular glomerular MPO, defined as MPO staining (brown) that was not co-localized with CD15 (red) was detected in all kidney biopsies. Extracellular MPO was found close to intra-glomerular CD15+ cells and it was also deposited independently along the glomerular capillaries (Figure 3.5 yellow arrows and Figure 3.6) and on tubular epithelial cells. CD15 was also detected along the brush border of tubular epithelial cells.
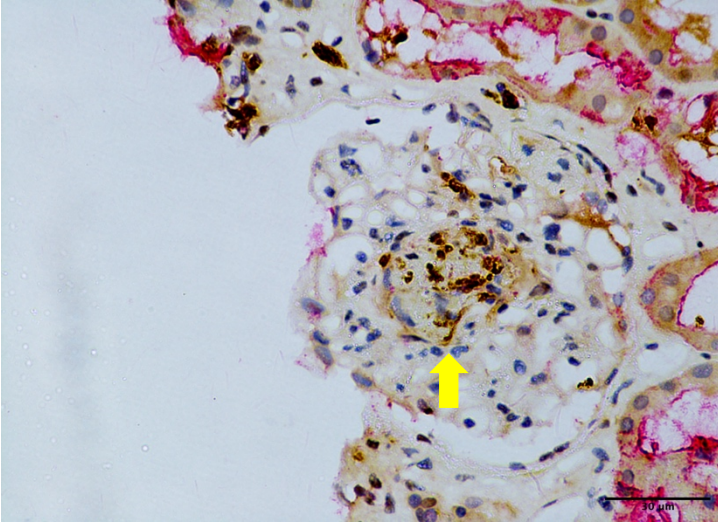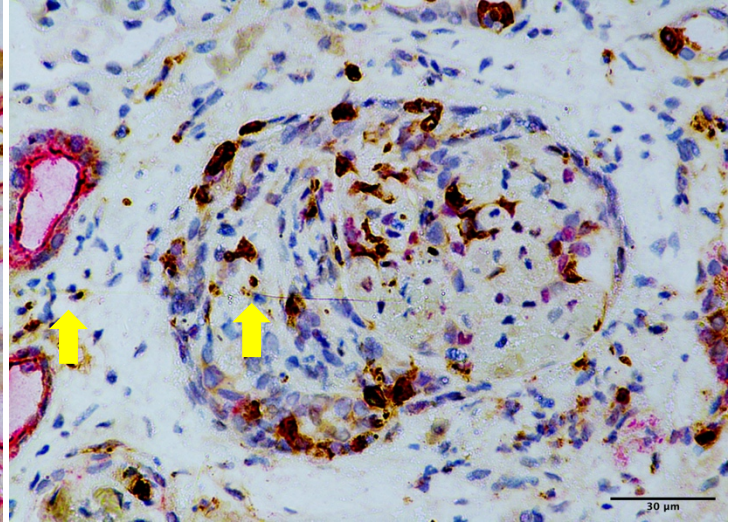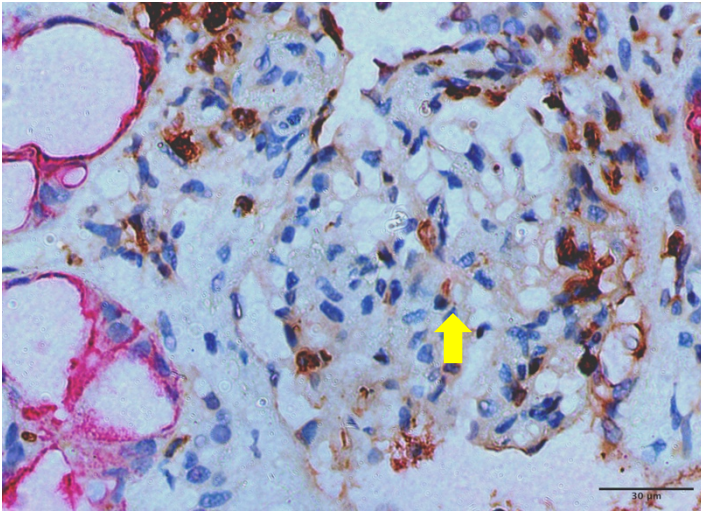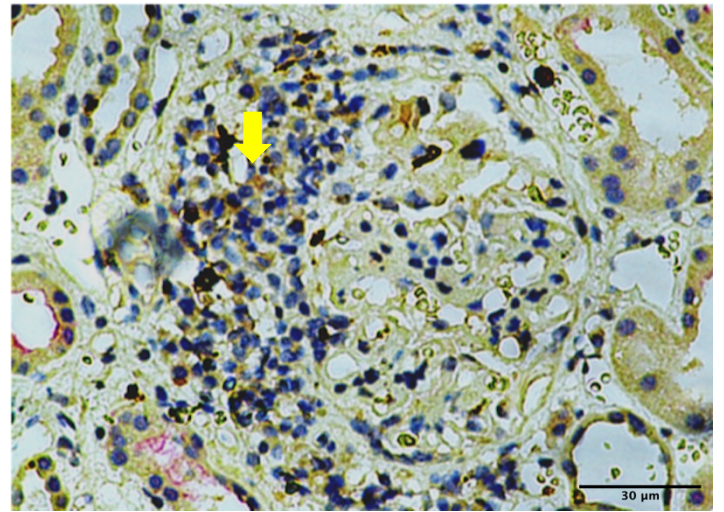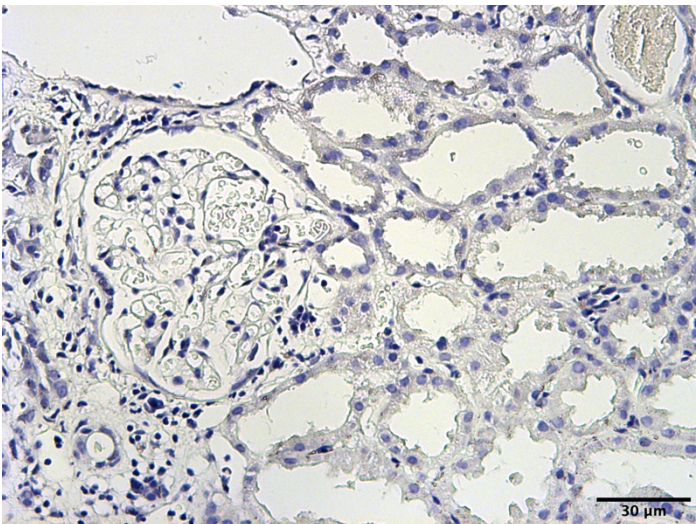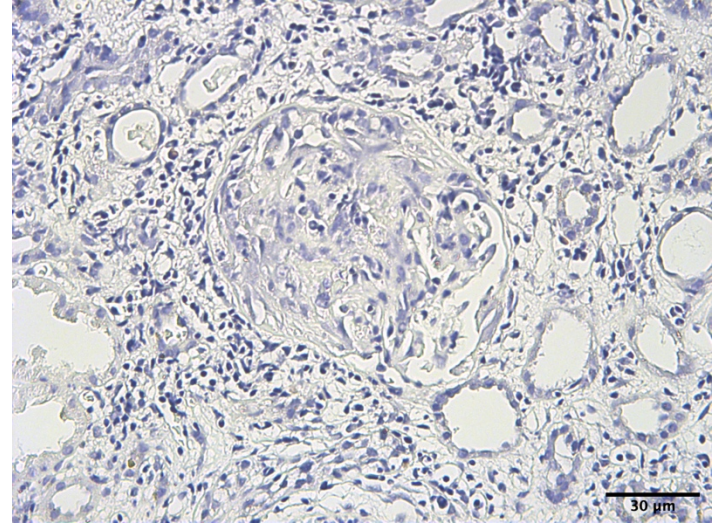
Figure 3-5 Extracellular MPO deposition in patients with diverse forms of CGN

Immunohistochemistry for MPO (brown) and CD15 (red) in inflamed glomeruli from patients with crescentic glomerulonephritis due to A) PR3-ANCA, B) MPO-ANCA, C) ANCA negative disease and D) crescentic IgA nephropathy. Extracellular (extra-leukocyte) deposition along capillary walls can be seen in various areas (highlighted by yellow arrows). Immunohistochemistry staining with isotype IgG for E) MPO and F) CD15. Scale bars shown in right hand corner of each image (40x magnification).
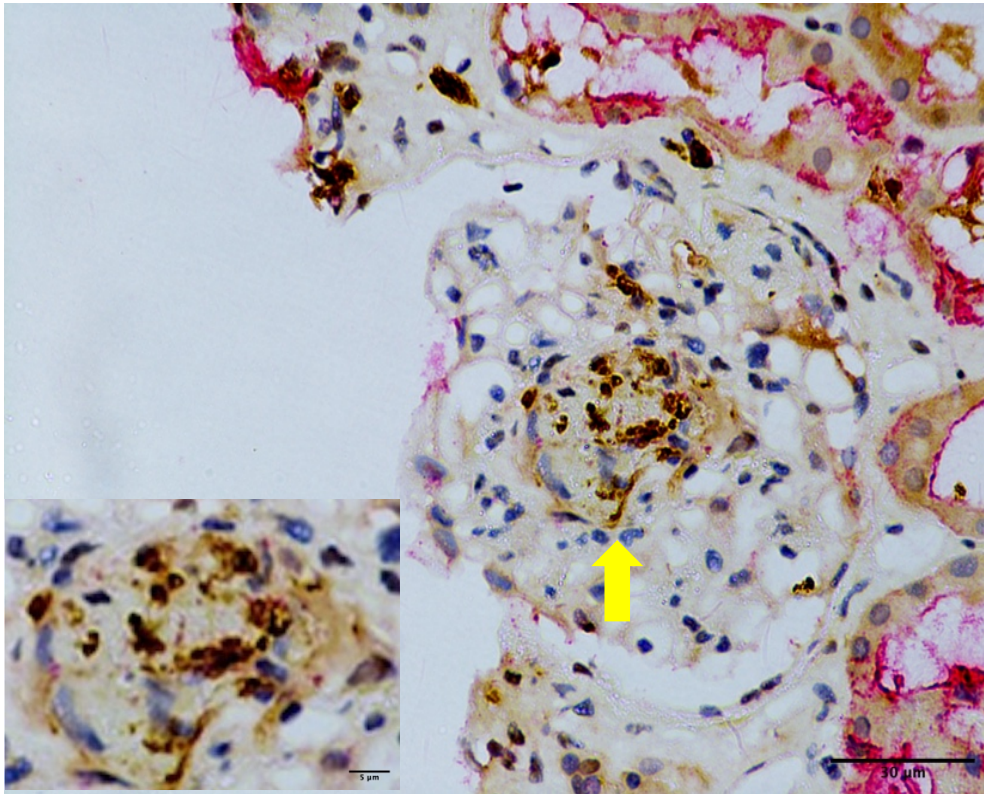
Figure 3-6 Immunohistochemistry for MPO (brown) and CD15 (red) in inflamed glomeruli from patients with crescentic glomerulonephritis due to PR3-ANCA disease (40x magnification). A zoomed out inset of the central glomerular area is shown on the bottom left hand corner highlighting the area of extracellular MPO deposition along the glomerular capillary wall (100x magnification).

MPO deposition was correlated with clinical and histological markers of disease severity. Table 3-1 shows the patient clinical and histological features and percentage area of MPO deposition in their renal biopsies. Total (leukocyte and non-leukocyte associated) whole kidney MPO deposition significantly correlated with estimated Glomerular Filtration Rate (eGFR) (r = -0.68, p<0.001) and proteinuria (r=0.51, p=0.02), as well as percentage of glomeruli with active cellular crescents (r= 0.58, p=0.01) (Figure 3.7) and interstitial fibrosis and tubular atrophy (IFTA) on the renal biopsy, (r = 0.66, p= 0.001, Figure 3.8).

Glomerular MPO deposition correlated with eGFR (r=-0.45, p=0.03, Figure 3.7), percentage of active crescents (r=0.42, p=0.04, Figure 3.7) and IFTA (r= 0.53, p=0.01, Figure 3.8). When extracellular (non-leukocyte associated) glomerular MPO deposition was analysed, it correlated inversely with eGFR (r= -0.58, p=0.03, Figure 3.7) and positively with crescent formation (r=0.63, p=0.02, Figure 3.7).

Total tubulointerstitial MPO deposition correlated significantly with eGFR only (Table 3-2). As CD15 is also expressed on tubular epithelial cells the quantification of extracellular tubulointerstitial MPO was not possible.

Diagnosis	eGFR at biopsy mls/min/1.73m^2	uPCR at biopsy mg/mmol	% Crescents	% IFTA	Total whole kidney MPO	Total tubulo-interstitial MPO	Total glomerular MPO	Extra-leukocyte glomerular MPO
MPA	35	240	30	50	2.66	5.31	10.37	4.4
MPA	34	393	45	40	2.27	6.5	8.45	
MPA	88	10	5	5	0.2	2.1	3.6	
MPA	37	228	50	40	2.02	9.5	13.5	2.5
MPA	28	274	70	20	3.66	12.3	12.9	5.9
GPA	13	737	85	50	3.042	5.7	14.5	6.9
GPA	46	235	85	30	2.25	9	10.8	4.6
GPA	52	489	65	10	0.97	2	3.15	
ANCA negative	11	1747	40	40	4.674	7.8	13.16	6.3
ANCA negative	7	529	25	10	6.644	14	17.7	6.4
SLE	49	128	10	5	0.337	9	5.7	0.5
SLE	15	266	40	40	5.29	14	5.1	1.6
SLE	15	883	15	44	1.5	10.2	6.9	1.34
SLE	71	466	15	5	1.68	2.3	8.08	
IgA	90	51	27	10	2.05	5	12.9	2.5
IgA	14	416	30	5	0.82	2.4	3.2	
IgA	95	147	0	5	0.299	7.8	4	
IgA	90	150	12	5	0.897	7.5	5.9	

Table 3-1 Clinical, histological features and percentage area of myeloperoxidase deposition in the renal biopsies of patients with various forms of CGN

A

r = - 0.68 ***

B

r = 0.58 **

C

r = - 0.45 *

D

r = 0.42 *

E

r = -0.58 *

F

r = 0.64 *
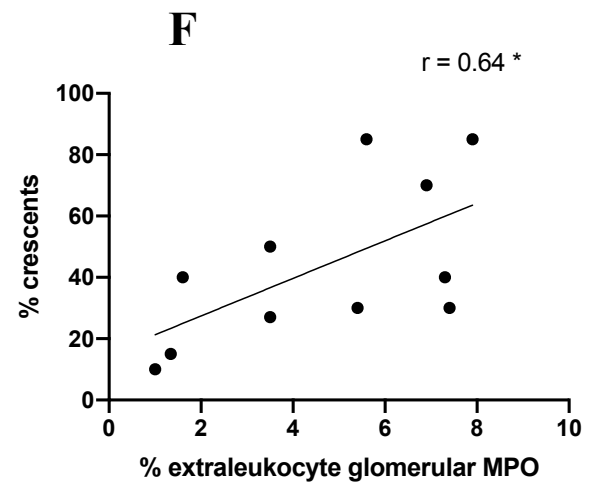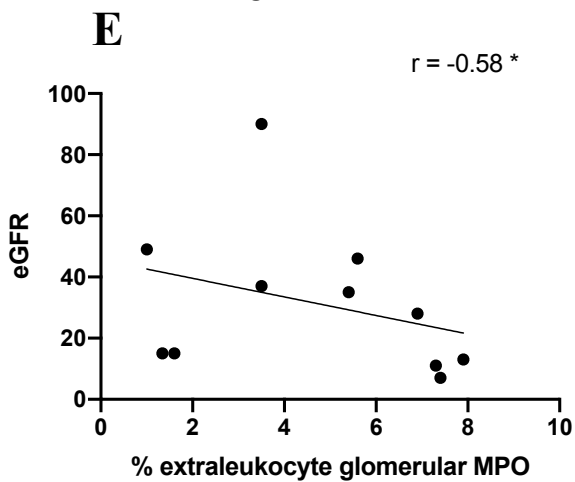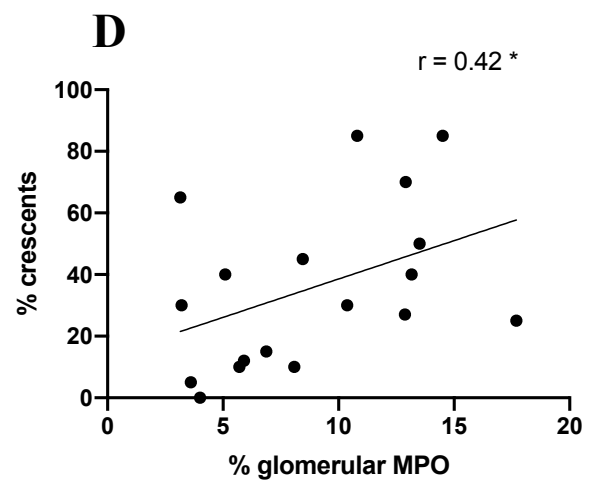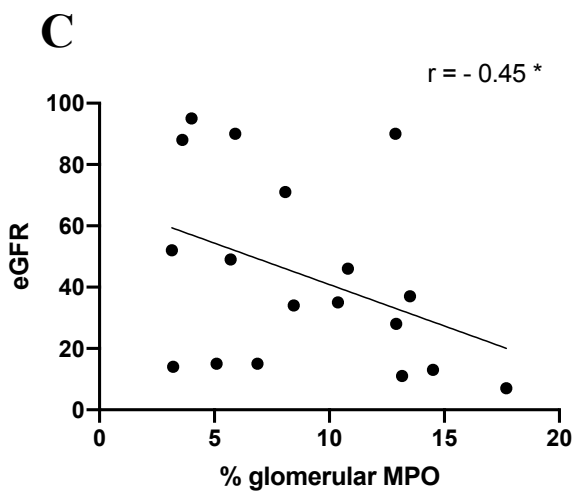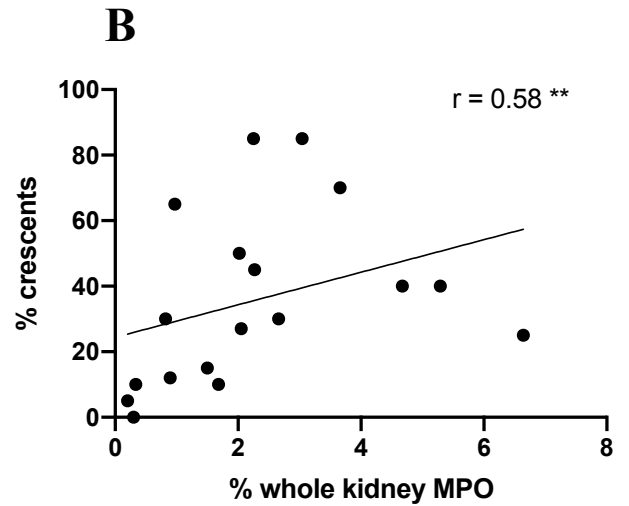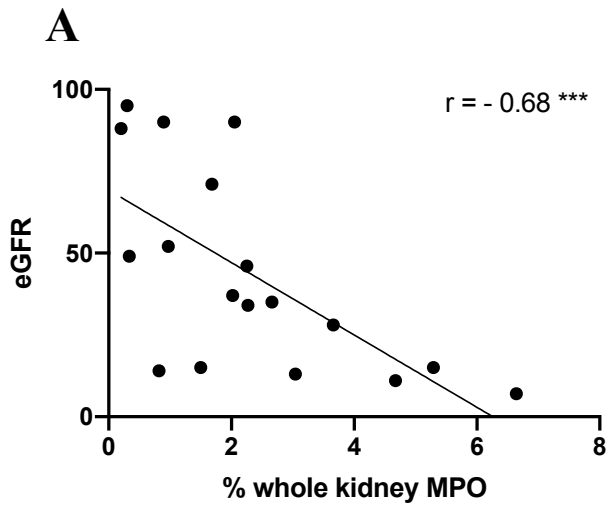
Figure 3-7 Correlation between MPO deposition with eGFR and percentage of glomerular crescents

Correlation between MPO and markers of disease severity in patients with diverse forms of CGN (MPO-ANCA=5, crescentic IgA=4, SLE =4, PR3-ANCA=3, ANCA negative =2). Percentage of total whole kidney (n=18) and glomerular intra- and extra-leukocyte MPO deposition (n=11) (percentage of myeloperoxidase stained area per whole kidney section or glomerulus) with eGFR(mL/min/1.73 m[2)] (A, C, E respectively) and percentage of active cellular crescents (B,D,F respectively). Non-parametric Spearman rank correlation analysis, *P < 0.05, **P < 0.01 *** P < 0.00*
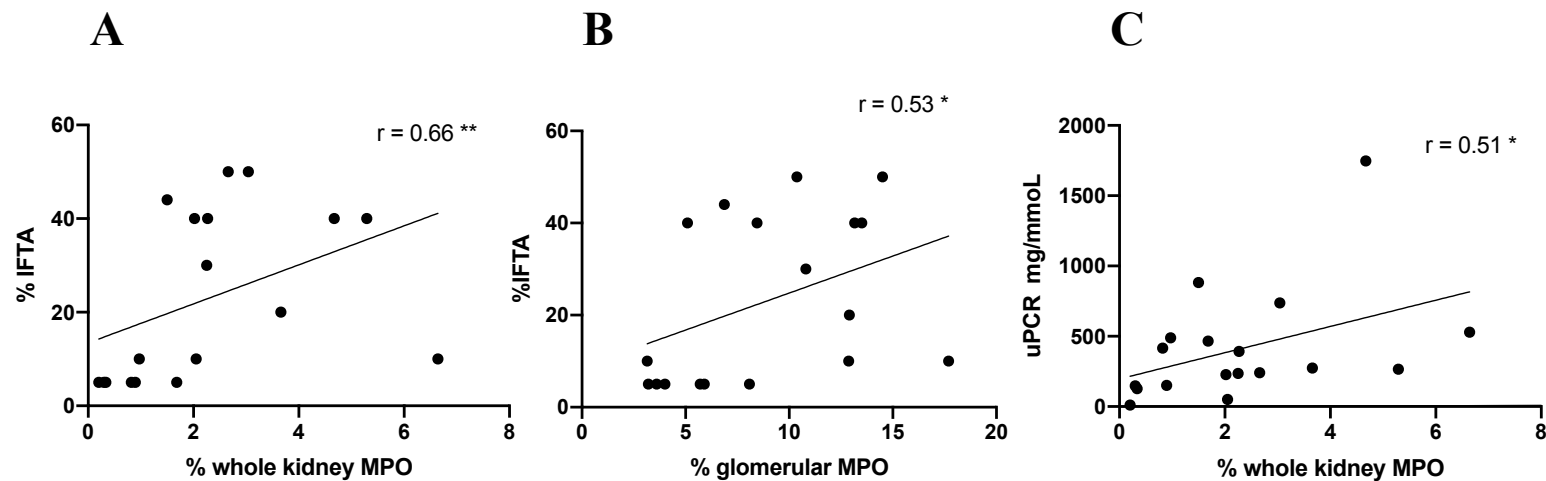
Figure 3-8 Correlation of intrarenal MPO deposition with interstitial fibrosis and tubular atrophy and urinary protein: creatinine.

Correlation between total whole kidney (A) or glomerular MPO deposition (B) (n=18) (percentage of myeloperoxidase stained area per whole kidney section or glomerulus) and interstitial fibrosis and tubular atrophy (IFTA) on renal biopsy, and C) between total whole kidney MPO and urinary protein: creatinine ratio (mg/mmol). Non-parametric Spearman rank correlation analysis, *P < 0.05, **P < 0.01.* Biopsies from patients with diverse forms of CGN (MPO-ANCA=5, crescentic IgA=4, SLE =4, PR3-ANCA=3, ANCA negative =2).

		% crescents	% IFTA	eGFR at biopsy	uPCR at biopsy
Total MPO whole kidney	r	0.5822[c]	0.6623[c]	-0.6839[c]	0.5067[c]
	P value	0.0056	0.0014	0.0009	0.0159
Total tubulointerstitial MPO	r	0.1124	0.312	-0.4299[c]	0.1168
	P value	0.3285	0.1037	0.0375	0.3222
Total glomerular MPO	r	0.424[c]	0.532[c]	-0.4525[c]	0.2879
	P value	0.0398	0.0115	0.0297	0.1233
Extracellular glomerular MPO	r	0.6376[c]	0.1871	-0.5845[c]	0.492
	P value	0.0192	0.2885	0.0313	0.0632

[c] Indicates a significant correlation

Table 3-2 Correlation of intrarenal myeloperoxidase with clinical and histological parameters

3.5   Discussion

In this chapter I have shown that MPO can be detected intra- and extracellularly in inflamed glomeruli, in biopsies from patients with the most common form of CGN in adults, ANCA-Associated Vasculitis, as well as in ANCA-negative pauci-immune glomerulonephritis, crescentic IgA nephropathy and Lupus Nephritis. Total, neutrophil-associated and extracellular MPO deposition in the whole kidney, and total glomerular MPO deposition, correlated with clinical and histological disease severity in the initial renal biopsy. Extracellular glomerular MPO deposition alone correlated with eGFR and crescent formation, suggesting that extracellular MPO could be an important driver mediating renal inflammation. It is important to acknowledge here that the use of immunohistochemistry instead of confocal microscopy in combination with the choice of similar colour substrates for MPO

and CD15 staining has made the distinction between the two markers difficult for the reader. When quantifying MPO and CD15 staining on the sections, this difficultly was overcome to some extent with the use of Colour Deconvolution, FIJI software.

Our data on the distribution of extracellular and intracellular MPO within kidneys of AAV patients confirm and extend previous observations (Brouwer *et al.*, 1994; Kessenbrock *et al.*, 2009; Arimura *et al.*, 2013; O'Sullivan *et al.*, 2015). MPO deposition has been detected in the biopsies of patients with active vasculitis (Brouwer *et al.*, 1994; Kessenbrock *et al.*, 2009; Kawashima *et al.*, 2013; O'Sullivan *et al.*, 2015). In MPO-ANCA disease, most of the MPO is detected within the leukocyte populations known to express MPO such as neutrophils and monocyte/macrophages. Leukocytes were prominent in almost all glomeruli and were associated with fibrin deposition (O'Sullivan *et al.*, 2015). Consistent with our data, the authors found that a proportion of deposited MPO was extracellular (not leukocyte-associated) and was found in the glomeruli, peri-glomerular regions and tubulointerstitium. Extracellular MPO co-localised with histones in renal biopsies suggesting the presence of NETs but it also co-localised with C3 and IgG deposition along the glomerular capillary walls (Kawashima *et al.*, 2013) suggesting that not only MPO itself released from the neutrophils but also immune complexes composed of MPO and anti-MPO antibody may play some pathogenic role for the glomerular injuries especially in the early, neutrophil-mediated phase of human MPO-ANCA-associated GN. A causative role for MPO in mediating glomerular damage is also supported by murine models of CGN in which acute disease is attenuated in MPO-deficient animals, despite augmentation of adaptive (T cell) immunity (Odobasic *et al.*, 2007).

In addition, in PR3-ANCA disease, activated PMN, assessed by their capacity to produce H_2O_2 in situ, are present in renal biopsies from patients with active disease and they correlate with serum creatinine levels (Brouwer *et al.*, 1994). Extracellular MPO deposition has also been demonstrated in the kidneys of

patients with active lupus nephritis. Interestingly, in this cohort patients with a higher proportion of glomeruli infiltrated by netting neutrophils had higher levels of circulating anti-dsDNA antibodies and higher activity index in renal biopsies (Villanueva *et al.*, 2011).

Circulating MPO levels were increased in AAV patients with active disease compared with disease in remission, confirming it as a modifiable marker of disease activity. Indeed, in addition to its presence in the renal biopsies, MPO and MPO-containing NETs have been found in the circulation of patients with crescentic GN (Kessenbrock *et al.*, 2009; Söderberg *et al.*, 2015). In particular, increased levels of circulating NET remnants, defined as free MPO associated with histones in the circulation were found in patients with active AAV and positively related to disease activity and neutrophil count. Furthermore, AAV patients exhibit an increased propensity for spontaneous NETosis (Söderberg *et al.*, 2015).

In summary, I have shown that MPO is elevated in the serum of patients with active AAV and is reduced when disease is in remission. Both leukocyte-associated and extracellular MPO deposition is detected in renal biopsies of patients with diverse forms of crescentic GN and correlates with clinical and histological markers of disease activity.

4 The effect of myeloperoxidase inhibition on neutrophil degranulation, ROS production, NET formation and neutrophil-induced endothelial cell death *in vitro*

4.1 Introduction

In this chapter the effect of myeloperoxidase inhibition on neutrophil degranulation and NET formation as well as neutrophil-associated endothelial cell damage is examined, in healthy controls and patients with ANCA-associated vasculitis (AAV), the most common form of crescentic GN in adults.

AAV is characterized by autoantibodies against the neutrophil granule proteins PR3 or MPO. ANCAs can activate TNFα-primed neutrophils to degranulate and ROS (Falk *et al.*, 1990), induce the formation of NETs (Kessenbrock *et al.*, 2009) and mediate the release of microparticles from polymorphonuclear leucocytes (PMNs) (Hong *et al.,* 2012) . Neutrophil microparticles are membrane vesicles released upon activation or apoptosis and have been shown to express neutrophil membrane surface markers as well as MPO and PR3.

Activation of neutrophils by ANCA seems to involve both the Fc portion of the antibody, as well as the F(ab) portion binding to its antigen on the neutrophil surface (Kettritz, 2012). The pathogenicity of ANCAs seems to vary with epitope specificity (Roth *et al.*, 2013) and affinity (Nakazawa *et al.*, 2014) and both of these parameters change with disease activity suggesting that ANCA play different roles at different stages of AAV (Söderberg and Segelmark, 2016).

Following FcR ligation intracellular signalling via MEK (MAPK/ERK kinase) pathway induces ROS production. The induction of ROS then initiates an MPO pathway which leads to NETosis. In this pathway, MPO triggers the activation and translocation of NE from azulophilic granules to the nucleus. In the nucleus, NE proteolytically processes histones to disrupt chromatin packaging. Subsequently, MPO binds chromatin and synergizes with neutrophil elastase in chromatin decondensation and NET formation. Chromatin decondensation is also promoted

by MPO and the activation of protein-arginine deiminase type 4 (PAD4), which citrullinates histones (Papayannopoulos *et al.*, 2010b).

Whether MPO depends on its enzymatic activity to initiate NETosis is debatable in current literature. A report where the enzymatic activity of MPO was inhibited by the non-specific MPO inhibitor aminobenzoic acid hydrazide (ABAH) suggests that the activity of MPO might be non-essential to induce NETosis (Papayannopoulos *et al.*, 2010). However, others have shown that NET-associated MPO is enzymatically active and can produce HOCl in the presence of its substrate, H_2O_2 (Parker *et al.*, 2012).

AZM198 is a membrane permeable MPO inhibitor with intra-granular action that has been shown to abolish PMA-triggered NET formation in vitro (Halla Björnsdottir *et al.*, 2015). MPO contains ferric heme in its resting state. In the presence of H_2O_2, MPO gets oxidised to its enzymatically active compound I. MPO-compound I oxidizes Cl^- to $HOCl^-$ and no further intermediates are formed in this reaction, as compound I gets converted directly to its native form (Khan, Alsahli and Rahmani, 2018). AZM198 reacts with compound I of MPO with a rate constant sufficiently large for it to compete with chloride for oxidation. Reduction of compound I by AZM198 results in formation of compound II, which indicates that AZM198 must undergo one-electron oxidation to produce a free radical intermediate. The proposed mechanism of action for AZM198 is that these free radicals then react with the heme part of MPO and inactivate it. In this way, it prevents production of hypochlorous acid without concomitant release of free radicals (Tidén *et al.*, 2011)

One of the hallmarks of CGN is endothelial injury and rupture of the glomerular capillary loops due to aberrant leucocyte activation. Cytokine-activated EC produce IL-8, which has a significant role in promoting neutrophil recruitment and migration (Csernok *et al.*, 1994; Halbwachs and Lesavre, 2012). Recent reports have shown that activated EC can also induce NET formation that can promote EC death (Woodfin *et al.*, 2009; Gupta *et al.*, 2010; Woodfin, Voisin and Nourshargh, 2010). Both ROS and serine proteases released during neutrophil

degranulation and presented on NETs have been previously proposed as initiators of endothelial cell damage in vasculitic lesions *in vivo* (Lu *et al.*, 2006; Al Laham *et al.*, 2010).

4.2   Aims

To investigate the effect of MPO inhibition on neutrophil degranulation and ROS production as well as NET formation and neutrophil-associated endothelial cell death

4.3   Experimental design

Neutrophils were isolated from patients and healthy controls using a Percoll gradient. Cells were subsequently stimulated with either PMA or primed with TNFα for 15 minutes prior to stimulation with PR3-ANCA. In experiments where the effect of MPO inhibition using AZM198 was investigated, neutrophils where incubated with 10μM AZM198 for 30minutes prior to stimulation. The AZM198 concentration of 10μM was chosen as it has been shown to abolish NETosis *in vitro* (Halla Björnsdottir *et al.*, 2015). The effect of AZM198 on ROS production and neutrophil degranulation was assessed using markers of degranulation such as β-glucuronidase, neutrophil elastase (NE), and human neutrophil peptide levels 1-3. Additionally, NETosis was induced in neutrophils from patients and healthy controls using PMA and PR3-ANCA and the effect of AZM198 tested on NET formation and expression of neutrophil proteins on NETs and neutrophil surface. Finally, an assay where endothelial cells (EC) and neutrophils (PMN) were co-cultured to test the effect of neutrophil stimulation by ANCA on EC death in the presence and absence of MPO inhibition was established.

4.4   Results

4.4.1 MPO inhibition inactivates enzymatically active MPO *in vitro*

In order to confirm that AZM198 inactivates enzymatically active MPO as previously reported (H. Björnsdottir *et al.*, 2015) , neutrophils from patients and healthy controls were isolated and stimulated with PMA, a synthetic activator of

protein kinase C, in the presence or absence of AZM198 for 30 minutes. I confirmed that AZM198 attenuated enzymatically active myeloperoxidase activity from PMA-stimulated neutrophils (Figure 4-1)
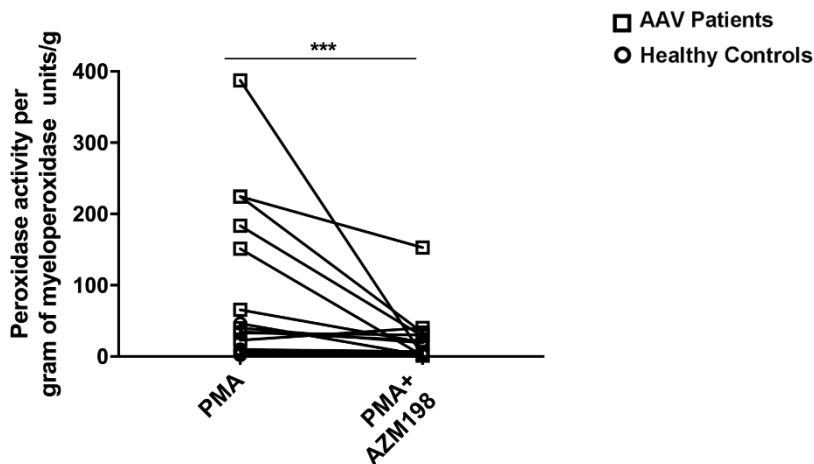
Figure 4-1 Effect of AZM198 on enzymatic myeloperoxidase activity

Effect of AZM198 on enzymatic myeloperoxidase activity (units/ g myeloperoxidase) in the supernatants of neutrophils from patients with AAV and healthy controls following 30-minute stimulation using PMA (n=16, 7 healthy controls, 6 MPO-ANCA, 3 PR3- ANCA), Wilcoxon test, *** $P < 0.001$

4.4.2 MPO inhibition reduces ROS production and HNP 1-3 release *in vitro*

In all subsequent experiments, TNFα priming/PR3-ANCA stimulation was used to stimulate neutrophils. I tested several degranulation assays to assess the effect of MPO inhibition on neutrophil degranulation in the presence of ANCA stimulation. Markers of neutrophil degranulation independent of MPO, such as β-glucuronidase, neutrophil elastase and human neutrophil peptides 1-3 (HNP 1-3), that are released upon neutrophil activation were chosen. β-glucuronidase is a lysosomal enzyme whose activity was assessed by the cleavage of *P*-nitrophenolate from *P*-nitrophenyl-β-glucuronide. NE is a serine protease exclusively found in neutrophils and monocytes. HNP 1-3 are part of the α-defensin family of peptides that are stored in the azulophilic granules and are

therefore specific markers of neutrophil degranulation. All assays were performed on Percoll gradient isolated neutrophils.

PR3-ANCA was purified from the plasma exchange fluid of three patients who presented with PR3-ANCA GN and pulmonary haemorrhage. The effect of purified PR3-ANCA stimulation on neutrophils was confirmed by comparing ROS production induced by PR3-ANCA with that induced by purified IgG isolated from a healthy control. Rhodamine release was used as a marker of ROS production. DHR 123 is a non-reduced non-fluorescent molecule that in the presence of hydrogen peroxide is converted to rhodamine 123, which fluoresces at a wavelength of approximately 534nm and can therefore be detected in the FITC (FL-1)-light channel on flow cytometry. Figure 4-2 shows a variable effect amongst the three purified patient IgGs on rhodamine 123 expression from stimulated healthy control neutrophils that was higher when compared to unstimulated neutrophils and neutrophils stimulated with IgG control.
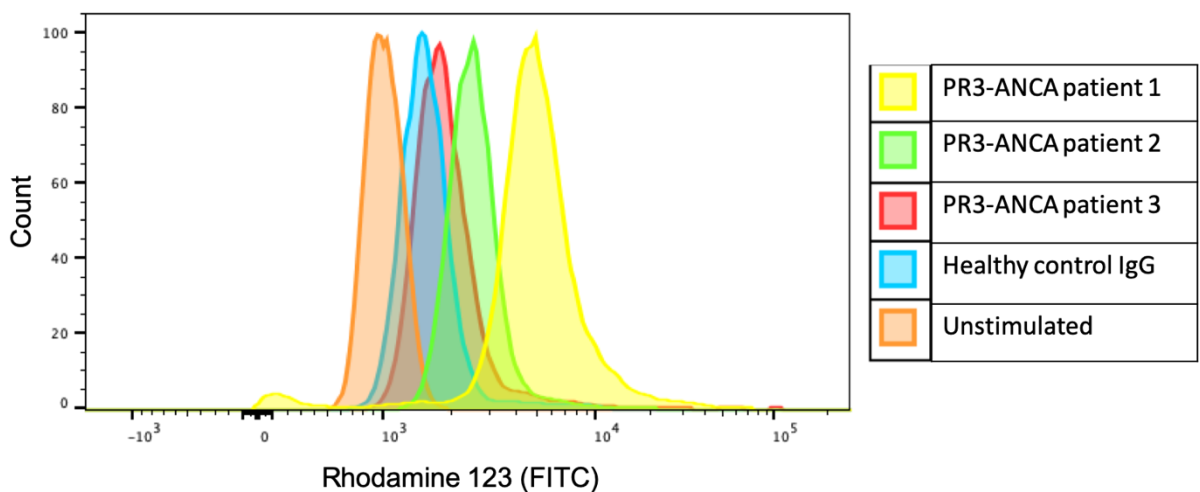
Figure 4-2 Purified human immunoglobulin-induced neutrophil degranulation

Histogram of rhodamine 123 (FITC) expression from unstimulated neutrophils or neutrophils stimulated with purified endotoxin-deplete PR3-ANCA from three different patients with crescentic GN and pulmonary haemorrhage or healthy

control IgG (all used at 200mg/mL) analysed by flow cytometry demonstrating ANCA-induced neutrophil degranulation

In all subsequent stimulation experiments the PR3-ANCA IgG from patient 1 (yellow histogram, Figure 4-2) was used. NE and β-glucuronidase release was measured in the supernatants of TNFα-primed/ PR3-ANCA stimulated neutrophils collected after one hour of stimulation. No significant difference between PR3-ANCA stimulation and PR3-ANCA stimulation in the presence of AZM198 was found; Neutrophil elastase: (Mean ±SD); PR3-ANCA 88.27±91.8ng/mL vs PR3-ANCA+AZM198 74.94±72.48ng/mL, p=0.09) and β-glucuronidase release Median (IQR) OD absorbance, PR3-ANCA 0.11 (0.06- 0.3) AU vs PR3-ANCA+AZM198 0.06 (0.05-0.2) AU p= 0. 33) (Figure 4-3).

A

B

□ AAV Patients
O Healthy Controls
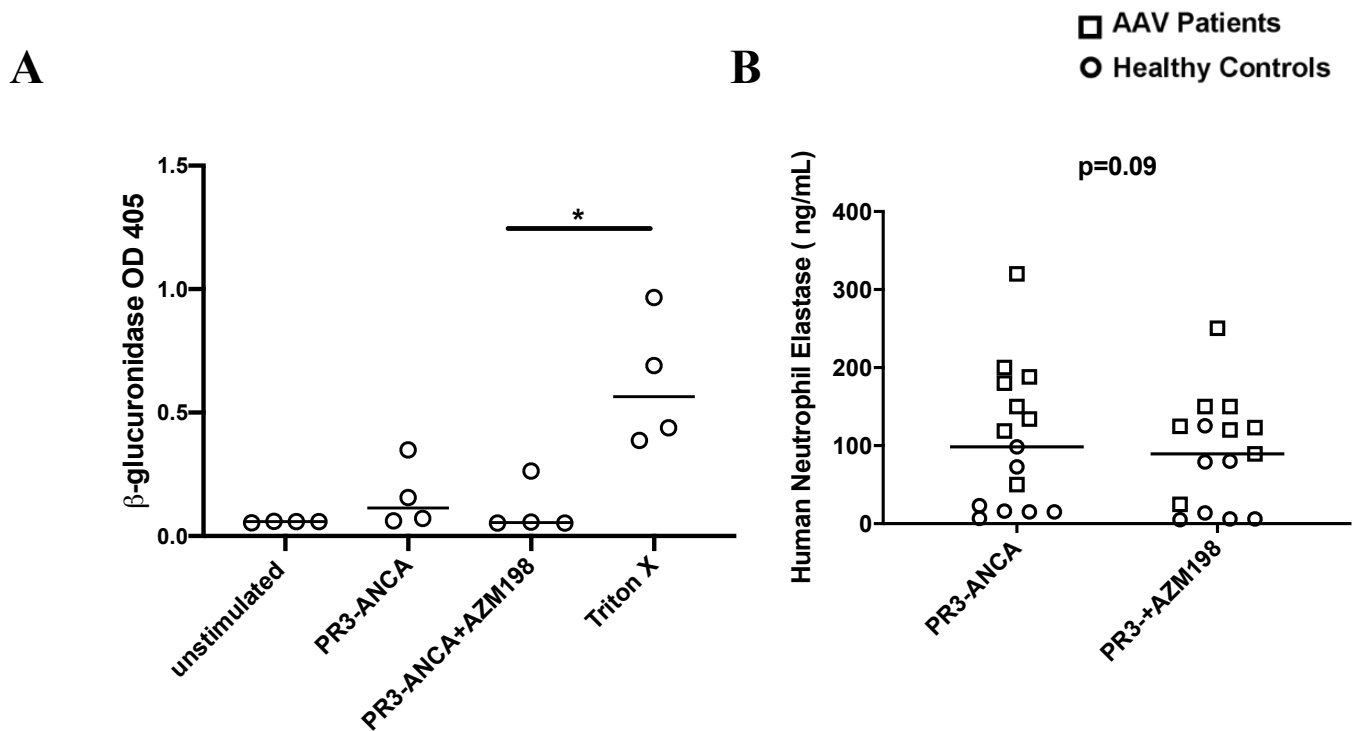
Figure 4-3 Effect of AZM198 on β-glucuronidase and neutrophil elastase (NE) release by PR3-ANCA stimulated neutrophils

Median β-glucuronidase and mean neutrophil elastase (NE) release in the supernatants of neutrophils from patients and healthy controls after one-hour TNFα-primed/ PR3-ANCA stimulated neutrophils stimulation in the presence and absence of AZM198, Friedman test, Paired t test, *P< 0.05

I subsequently went on to measure ROS production as well as HNP 1-3 levels in TNFα-primed/ PR3-ANCA stimulated neutrophils as different markers of degranulation specific to the azulophilic granules of neutrophils.

In TNFα-primed/PR3-ANCA stimulated neutrophils, the addition of AZM198 led to a significant reduction in ROS production , MFI Rhodamine 123(IQR): PR3-ANCA: 10675 (4481-13196) AU, *vs* unstimulated:1749 (515-3808) AU (p=0.004) and

PR3-ANCA with AZM198: 2123 (643-6275) AU (p=0.04), vs IgG control: 4000 (2500-5003)AU (p=0.34) (Figure 4-4)
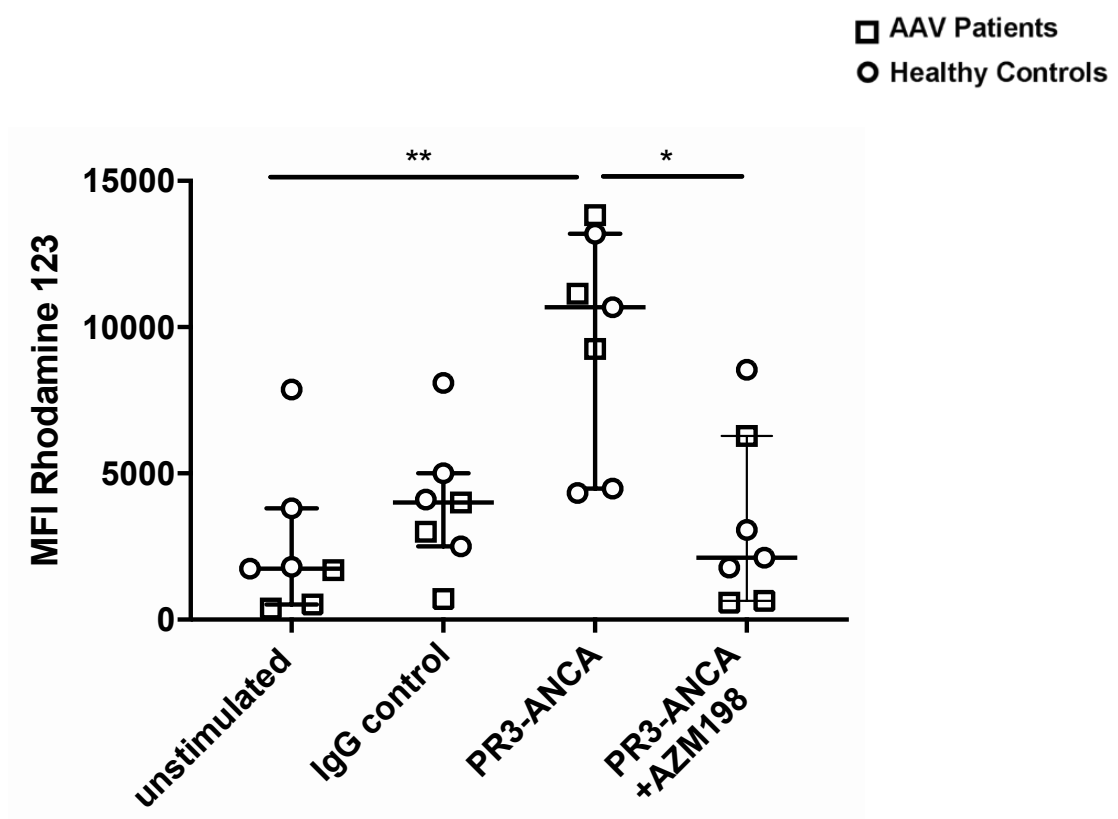
Figure 4-4 Effect of AZM198 on ROS production by PR3-ANCA stimulated neutrophils

Rhodamine 123 (FITC) MFI expression in TNFα primed/PR3-ANCA-stimulated neutrophils analysed by flow cytometry (n=7, 4 healthy controls, 3 PR3-ANCA patients)

In addition to ROS production, AZM198 also led to a reduction in the release of HNP 1-3 levels, HNP 1-3 levels: PR3-ANCA: 135 (116-217) pg/mL *vs* unstimulated:106 (97-160) /mL, p=0.003 and PR3-ANCA with AZM198: 127(104-189) pg/mL, p=0.03) (Figure 4-5)
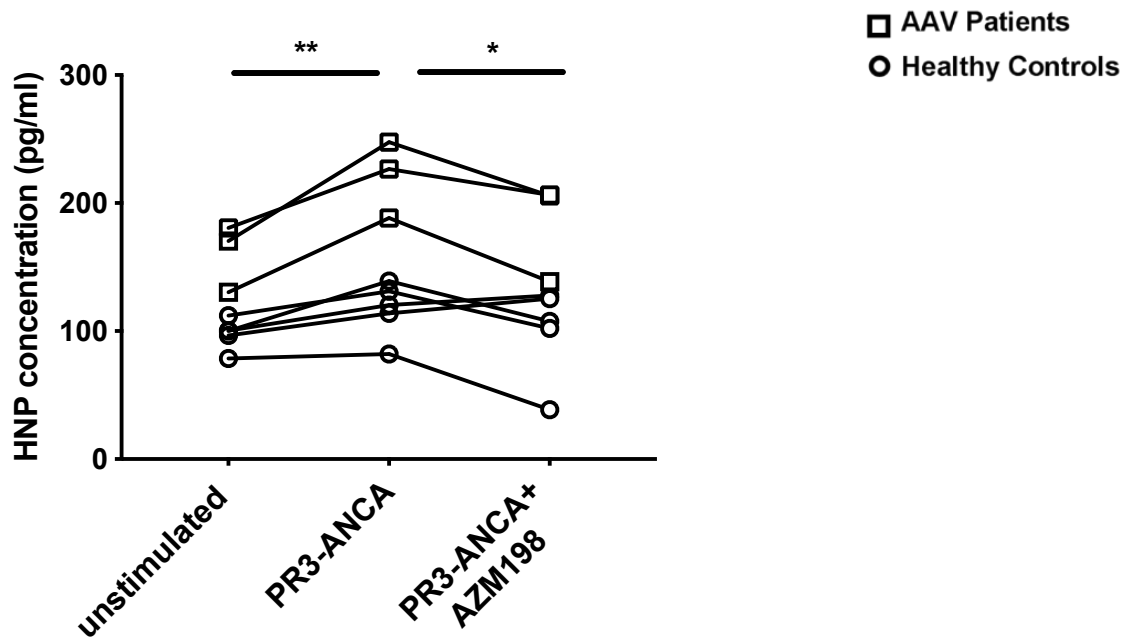
Figure 4-5 Effect of AZM198 on Human Neutrophil Peptide (HNP) 1-3 release

Human Neutrophil Peptide 1-3 (pg/ml) release in the supernatants from TNFα primed/PR3-ANCA stimulated neutrophils (n=8, 5 healthy controls, 3 PR3-ANCA patients), Friedman test, *P < 0.05, **P < 0.01,*

4.4.3 Myeloperoxidase inhibition reduces NET formation in vitro

As previously stated, neutrophils were isolated from patients with PR3-ANCA disease and healthy controls, then primed with TNFα for 15 minutes and stimulated with purified PR3-ANCA for one hour. I then assessed NET production by calculating the NET area index, defined as area that stains positive for Sytox green (that binds extracellular DNA), corrected for the total number of neutrophils (Figure 4-7).

TNFα/PR3-ANCA stimulation triggered NET formation in neutrophils from active AAV patients and healthy controls, while AZM198 reduced NETosis (Figure 4-6) (NET area index PR3-ANCA: 6.3 (5.6-7.2) AU *vs* unstimulated: 2.7 (0.9-3.3) AU and PR3-ANCA with AZM198:3.3(1.9-4.2) AU, p= 0.01, vs IgG control 3.6(3-4.2) p=0.02)). Representative images of NETosis induced by TNFα/PR3-ANCA stimulation in the presence and absence of AZM198 are shown in Figure 4-7.
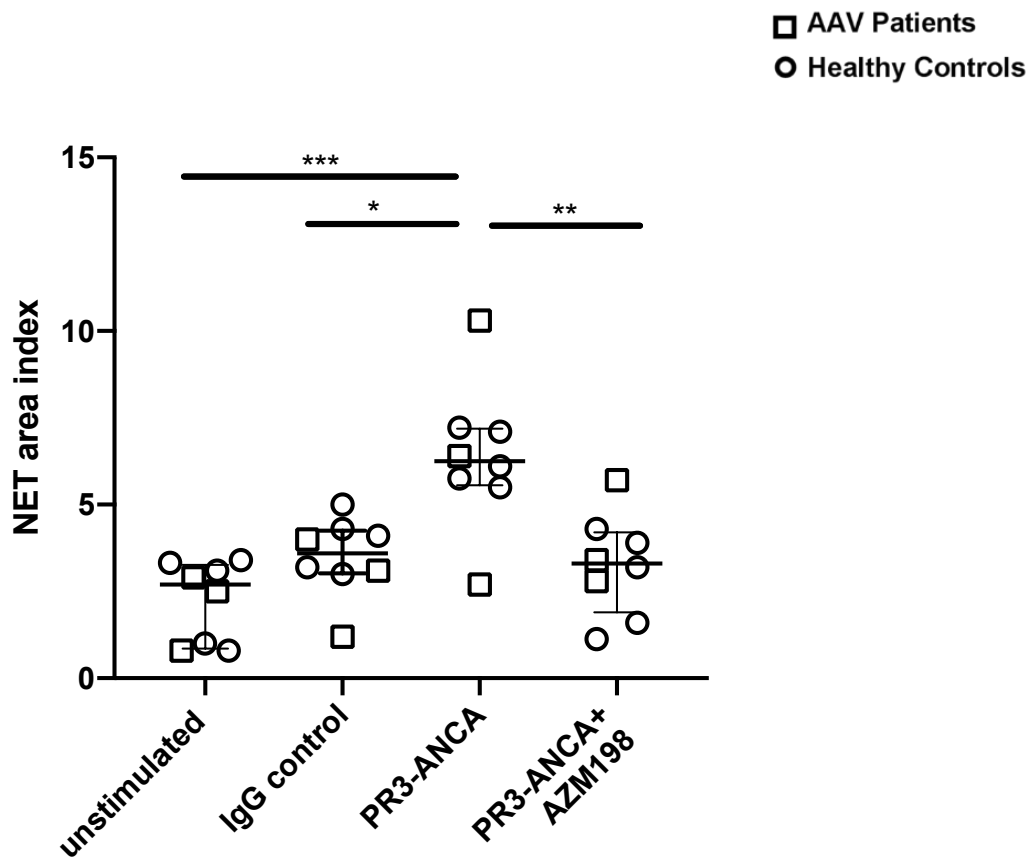
Figure 4-6 Effect of AZM198 on NET formation in patients and healthy controls

Median (IQR) NET formation in unstimulated neutrophils or in the absence or presence of AZM198 (10µM) after 1hr neutrophil stimulation with TNFα/PR3-ANCA. NET index was defined as the ratio between the cumulative Sytox Green stained area, corrected for the number of imaged neutrophils, Friedman test, *P<0.05, **P < 0.01, ***P < 0.001
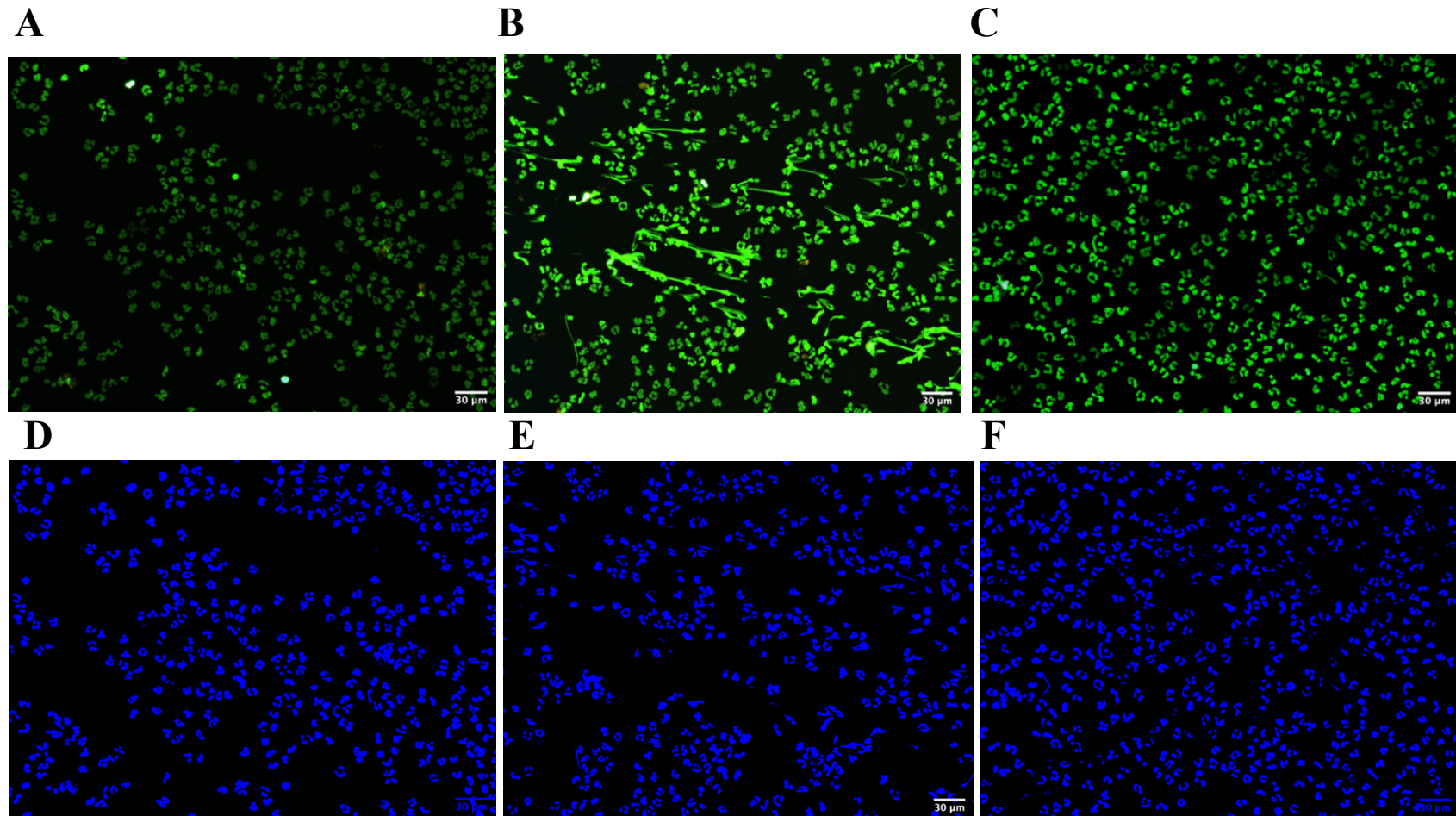
Figure 4-7 Visualisation of NET formation in the presence and absence of AZM198

Immunofluorescence of NET formation in unstimulated neutrophils (A) or in the absence (B) or presence (C) of AZM198 (10µM) after 1hr neutrophil stimulation with TNFα/PR3-ANCA from a healthy control. Extracellular DNA and permeable cells (Sytox) shown in green. Nuclei were stained blue with DAPI (D-F).

Additionally, immunofluorescence staining for NE and MPO was performed on the PMA stimulated neutrophils to visualise the effect of MPO inhibition on NETs and apoptotic neutrophils. A recent report has shown that NE is essential to initiate NET formation and that it synergizes with MPO to drive chromatin decondensation (Metzler *et al.*, 2014). Both of these proteins are then presented on NETs. Representative images of NETosis induced by PMA stimulation in the presence and absence of AZM198 are shown in Figure 4-8. MPO and NE co-localised on NETs and the cell surface of activated/NETotic neutrophils. MPO inhibition reduced NET formation and subsequently the expression of these proteins on NETotic neutrophils.
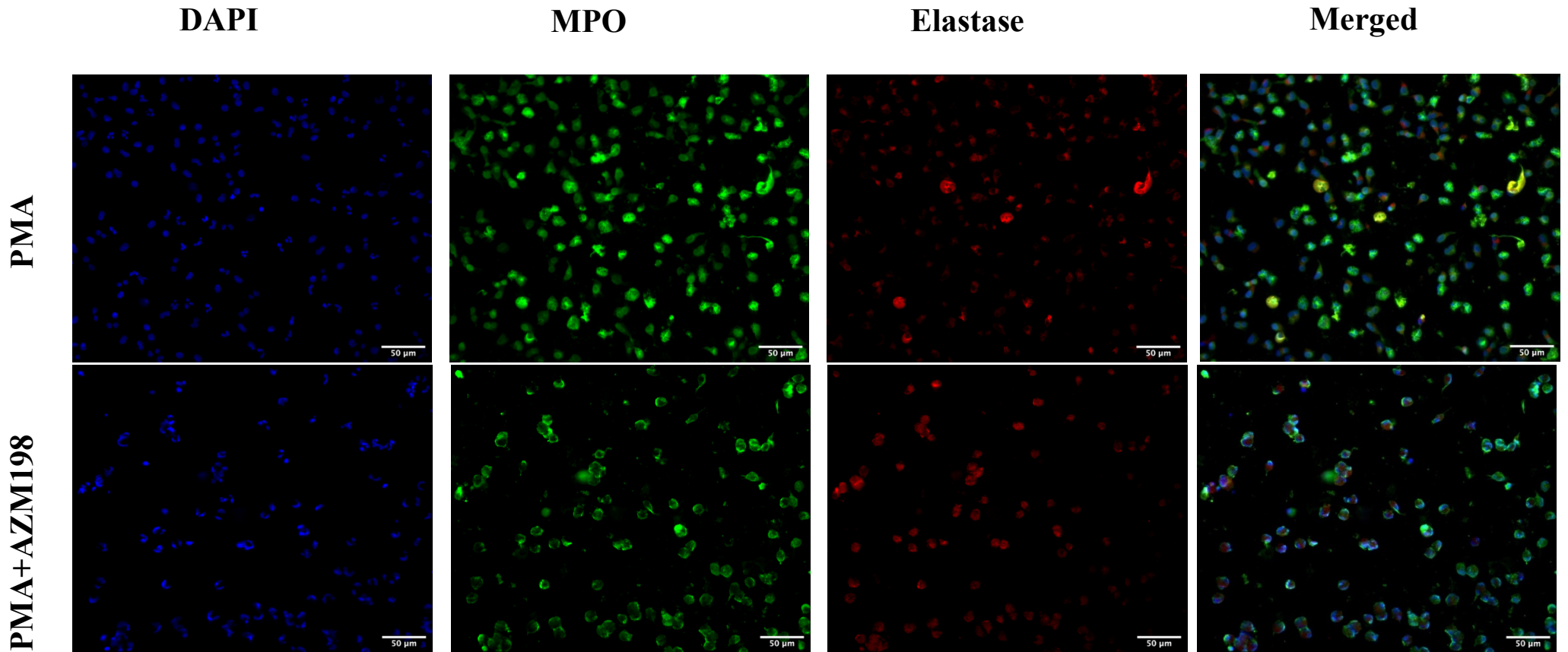
Figure 4-8 Immunofluorescence of MPO and NE in the absence and presence of MPO inhibition

Single channel and merged microscopic images (x20 magnification) show NET formation and MPO (green)/elastase (red) co-localisation on NETs in the absence or presence of AZM198 (10µM) after 30min neutrophil stimulation with PMA from a patient with active MPO-ANCA disease

4.4.4 MPO cell surface expression after inhibition of MPO enzymatic activity

Neutrophils from six patients with PR3-ANCA disease in remission were isolated using a Percoll gradient and stimulated with PR3-ANCA in the presence and absence of AZM198.

Neutrophils were stained for CD16, CD11b and MPO and the expression of MPO on CD11b^{high}CD16^{high} was analysed using FlowJo software (Figure 4-10). I found no difference in the percentage of MPO expression on CD11b^{high}CD16^{high} stimulated cells when the enzymatic activity of myeloperoxidase was inhibited with AZM198 (Figure 4-9).
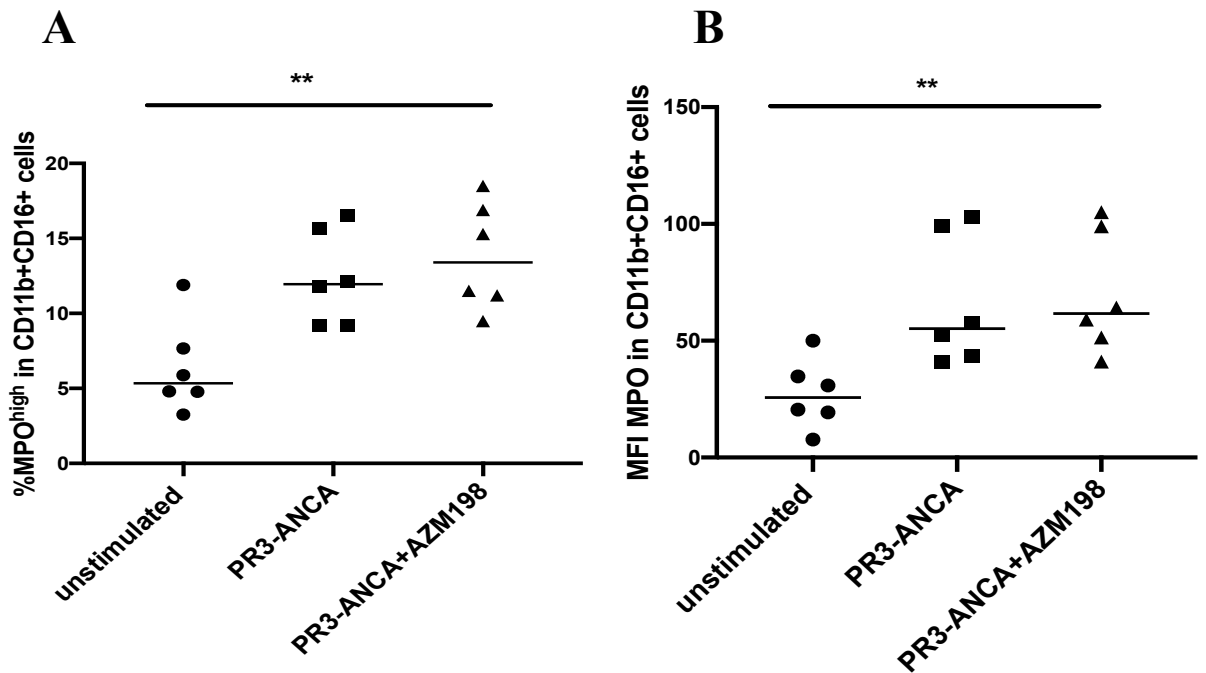
Figure 4-9 MPO expression on CD11b^{high}CD16^{high} cells in the presence and absence of AZM198.

Percentage of MPO^{high}CD11b^{high}CD16^{high} cells on isolated neutrophils (A) as well as (Mean Fluorescent intensity) MFI of MPO on CD11b^{high}CD16^{high} (B) in the presence or absence of AZM198.
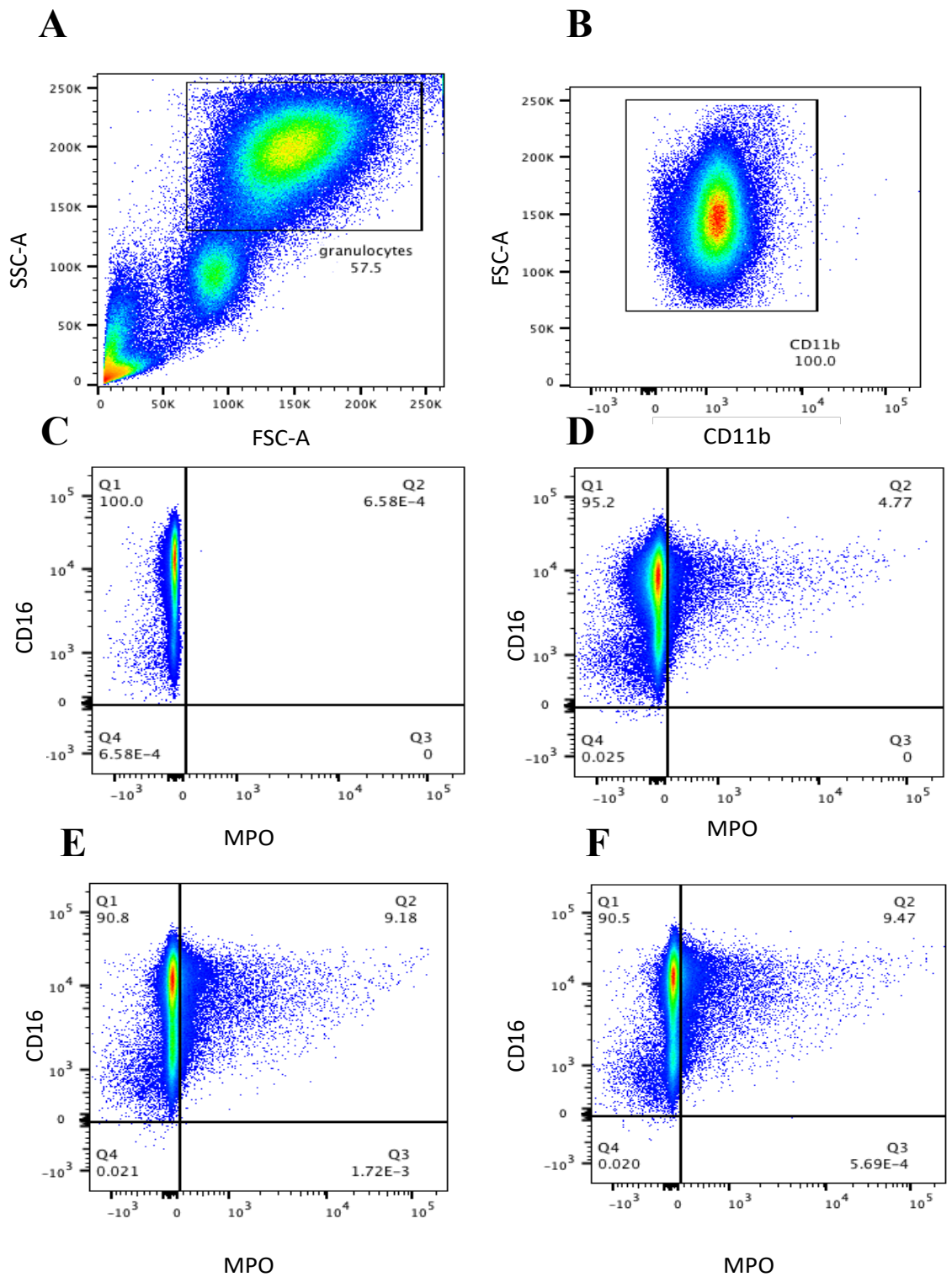
Figure 4-10 Flow cytometry plots demonstrating MPO expression on CD11b^{high}CD16^{high} neutrophils.

Neutrophils were identified by forward and side scatter (A) and high expression on CD11b and CD16. The plots show MPO expression on unstimulated CD11b^{high}CD16^{high} cells (D) or TNFα/PR3-ANCA stimulated cells in the presence

(E) or absence of AZM198 (F). C shows the fluorescence minus one (FMO) gating for MPO.

4.4.5 Endothelial cell/ PR3-ANCA-stimulated neutrophil co-culture results in EC damage that is reduced by MPO inhibition

I initially carried out pilot experiments to achieve the optimal conditions for the EC-PMN co-culture. First, the effect of EC stimulation on EC death was tested. BrdU-labelled EC were incubated in the presence or absence of TNFα stimulation for 4 hours and subsequently co-cultured with PMNs in the following conditions: EC only, EC+PMN unstimulated, EC+ TNFα/PR3-ANCA stimulated PMN, EC+ TNFα/PR3-ANCA stimulated PMN+ AZM198, EC+ TNFα/PR3-ANCA stimulated PMN+ DNAse. EC death was quantitated by measuring BrdU release in the co-culture supernatants. Comparable results were found (Table 4-1). In order to mimic the proinflammatory micro-environment of small vessels in crescentic GN (Halbwachs and Lesavre, 2012) , I decided to proceed with TNFα EC priming and extend the incubation time to 16 hrs.

	Unstimulated EC BrdU release (AU)	P value	TNFα primed EC BrdU release (AU)	P value
EC only	0.103	0.47	0.102	0.056
EC + PMN unstimulated	0.113	>0.99	0.106	>0.99
EC + PMN TNFα/PR3-ANCA	0.108		0.11	
EC + PMN TNFα/PR3-ANCA +AZM198	0.108	>0.99	0.114	*0.007**
EC +PMN TNFα/PR3-ANCA +DNAse	0.101	0.58	0.082	0.101

Table 4-1 Effect of EC stimulation on EC death in the EC-PMN co-culture.

Median BrdU release (AU) from unstimulated and TNFα-primed EC, that were subsequently cocultured with unstimulated PMN or stimulated with PR3-ANCA in the presence or absence of AZM198, Friedman test, **P < 0.01,* EC+PMN PR3-ANCA was used as the comparator group.

Subsequently, the effect of the duration of the EC/PMN co-culture on EC death was tested. TNFα-primed EC were co-cultured with PMNs in the conditions listed above for 4 and 16 hours. EC death was increased in the co-culture with TNFα/PR3-ANCA activated neutrophils that was reduced with MPO inhibition in both assays, however the results were more consistent in the prolonged 16-hour co-culture (Table 4-2, Figure 4-11)

In addition, von Willebrand Factor (vWF) release was measured in the co-culture supernatants as an additional marker of EC death. However, there was no significant reduction in supernatant vWF levels in the presence of AZM198 in the 16-hour assay (PR3-ANCA: 259±40 ng/mL *vs* PR3-ANCA with AZM198: 197±28 ng/mL, p=0.06, Figure 4-12).

EC morphology was visibly disrupted during the EC-PMN 16hr co-culture when PMN were stimulated, but this was attenuated in the presence of AZM198 (Figure 4-12).

	4-hour coculture	p value	16- hour coculture	p value
EC only	0.099	0.056	0.277	*<0.0001****
EC + PMN unstimulated	0.105	>0.999	0.367	*0.008***
EC + PMN TNFα/PR3-ANCA	0.126		0.45	
EC + PMN TNFα/PR3-ANCA +AZM198	0.097	*0.007***	0.35	*0.003***
EC +PMN TNFα/PR3-ANCA +DNAse	0.099	0.101	0.38	*0.008***

Table 4-2 Effect of duration of EC-PMN co-culture on EC death

Median BRDU release (AU) from TNFα-primed EC for 16 hours, that were subsequently co-cultured for 4 or 16 hours with unstimulated PMN or PMN stimulated with TNFα/PR3-ANCA in the presence or absence of AZM198, Friedman test, **P < 0.05,**P<0.01, ***P < 0.001* EC+PMN TNFα/PR3-ANCA were used as the comparator groups respectively
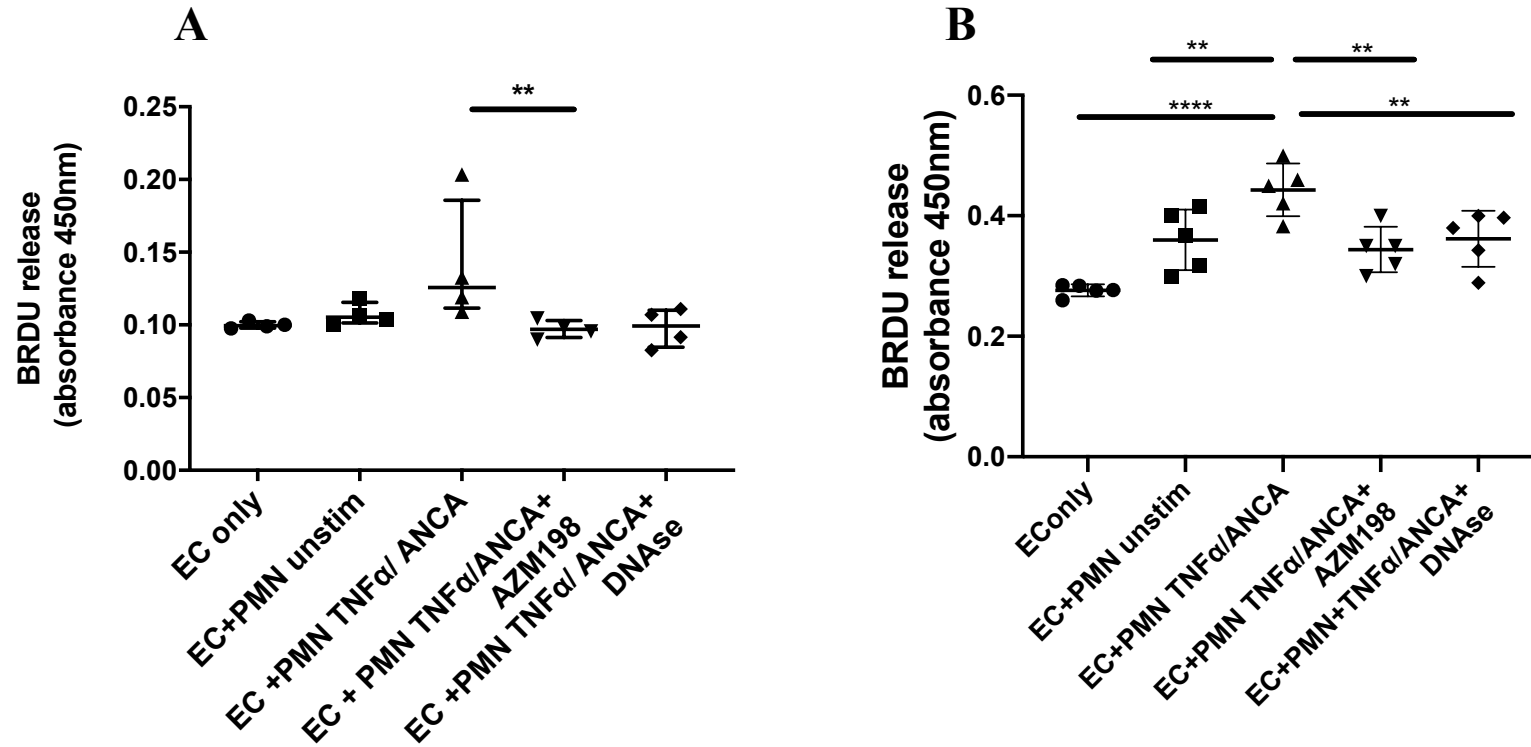
Figure 4-11 Effect of AZM198 on EC death in the co-culture of EC- TNFα/PR3-ANCA stimulated neutrophils.

Median (IQR) BRDU release in the supernatants of EC/PMN co-culture at A) 4 and B) 16 hours. BrdU-labelled EC were primed with TNFα for 16 hours. After rinsing to remove all traces of TNFα EC were cultured without or with inclusion of PMN in the absence or presence of TNFα/PR3-ANCA, and with AZM198 or DNAse for a further 4 or 16 hours after which BrdU-labelled DNA fragments from EC was analysed, Friedman test *P < 0.01, *** P < 0.001*.
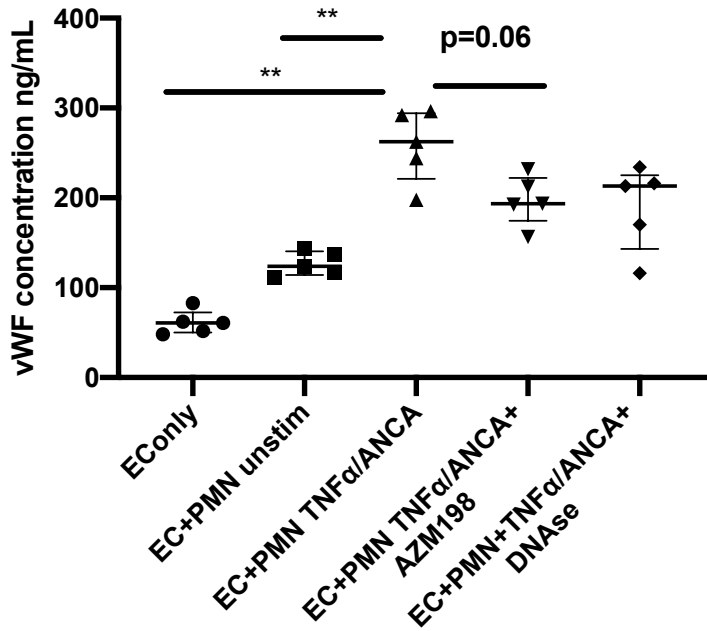
Figure 4-12 vWF release in the supernatants of the EC/PMN co-culture

Median (IQR) vWF release in the supernatants of EC/PMN co-culture at 16 hours. EC were primed with TNFα for 16 hours. After rinsing to remove all traces of TNFα EC were cultured without or with inclusion of PMN in the absence or presence of TNFα/PR3-ANCA, and with AZM198 or DNAse for a further 16 hours after which vWF release was analysed, Friedman test ***P < 0.01*
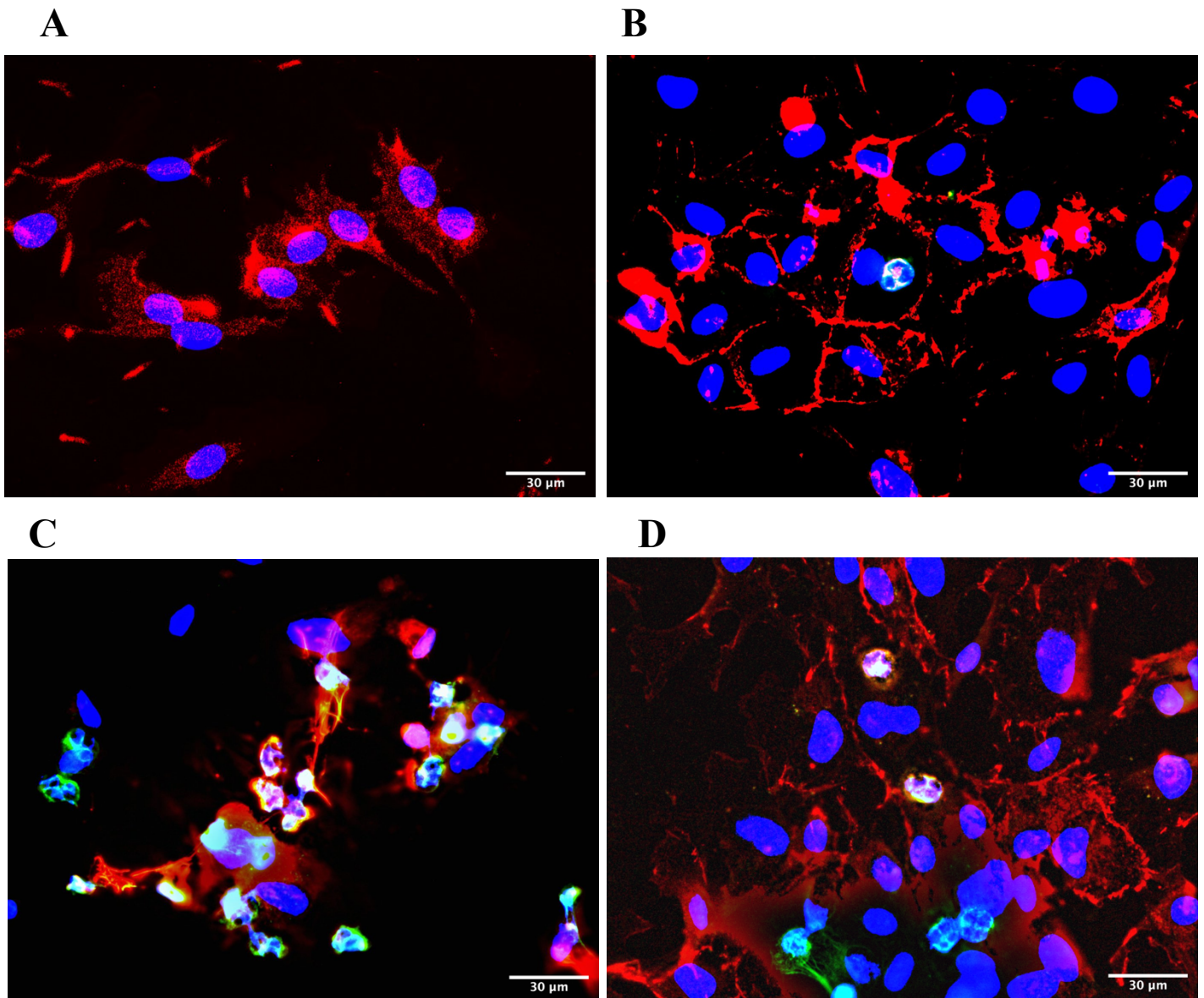
Figure 4-13 Immunofluorescence of the EC-PMN co-culture.

Merged microscopic images of TNFα primed EC in monoculture (A) or co-culture (B-D) with unstimulated PMN (B), TNFα/PR3-ANCA stimulated PMNs in the absence (C) or presence (D) of AZM198. EC stained with Vascular Endothelial (VE) Cadherin (red), PMN with MPO (green), nuclei with DAPI (blue).

4.5   Discussion

The experiments included in this chapter demonstrate that MPO inhibition with AZM198 inactivated enzymatically active MPO and reduced ROS production, NET formation and had a modest effect on neutrophil degranulation, in cytokine- and ANCA-stimulated neutrophils from AAV patients and healthy controls.

There was no difference in the read-outs between patients and healthy controls, so the data from both groups were plotted together. This lack of difference between the two groups can be explained by the fact that the vasculitis samples analysed were from patients whose disease was in remission. As explained in greater detail later in this section, PR3 can be expressed on the cell surface of resting neutrophils in both patients and healthy controls (Kettritz, 2016). Membrane PR3 expression is higher in active disease and decreases when disease reaches remission suggesting that patient neutrophils with inactive disease might behave similarly to healthy controls.

I purified IgG from three different patients with PR3-ANCA containing serum and found a variable effect of ANCA stimulation in donor neutrophil activation. In addition, I tried four different assays of neutrophil degranulation and found that AZM198 reduced HNP 1-3 release and ROS production in TNFα-primed/ PR3-ANCA stimulated neutrophils but had no significant effect in neutrophil elastase and β-glucuronidase release. It is possible that the lack of significant difference between conditions is secondary to inadequate neutrophil stimulation in these assays. However, others have similarly shown that neutrophils are not consistently activated by ANCA in *in vitro* assays (Popat and Robson, 2019). In addition, neutrophil degranulation and ROS production, although both triggered by neutrophil activation, are distinct processes. In fact, a report showed that neutrophils from AAV patients produce more intracellular ROS that correlated with NET formation, but degranulate to a similar extent as neutrophils from healthy controls (Ohlsson *et al.*, 2014).

Selective myeloperoxidase inhibition with AZM198 reduced NET formation in patient and healthy control neutrophils. Together with elastase, MPO has been demonstrated to associate with nuclear DNA/ histones and play a role in NET-formation and NET-mediated bacterial killing (Parker *et al.*, 2012). Neutrophils from donors who are completely deficient in MPO fail to form neutrophil extracellular traps (NETs), indicating that MPO is required for NET formation (Metzler *et al.*, 2011). Similarly, the induction of NETs in neutrophils from healthy donors via pro-inflammatory cytokines such as TNFα, IL-8, or IL-1β, in the absence of any infectious stimuli, required the presence of enzymatically active MPO (Keshari *et al.*, 2012). As mentioned previously, a recent study has added to our understanding of how MPO contributes to NET formation inside human neutrophils by showing that MPO activates elastase allowing it to enter the nucleus where it can then associate with DNA/histones (Papayannopoulos *et al.*, 2010).

Recent studies support the central role for NETs in the pathophysiology of different forms of crescentic glomerulonephritis. Impaired NET degradation in patients with SLE has been associated with higher dsDNA titres and frequency of flares (Hakkim *et al.*, 2010b). In MPO-ANCA CGN a reduced degradation of NETs has been observed, implicating NETs as a means of breaking tolerance to ANCA autoantigens (Nakazawa *et al.*, 2014). The latter was corroborated in animal studies where presentation of extracellular DNA derived from NETotic neutrophils to myeloid dendritic cells led to MPO-ANCA and PR3-ANCA production, with subsequent vasculitis-like renal lesions in C57BL/6 mice (Sangaletti *et al.*, 2012). In addition, augmented NET formation following infection in dectin-/- mice leads to a vasculitic phenotype, which can be attenuated by inhibiting NET generation (Branzk *et al.*, 2014).

Many studies exploring the membrane expression of ANCA antigens have been performed. MPO and PR3 reside in azurophilic granules, which can be mobilized during activation (Sengeløv, Kjeldsen and Borregaard, 1993). In contrast to MPO, PR3 is also stored in specific granules and in secretory vesicles that are mobilized more easily (Witko-Sarsat *et al.*, 1999). Moreover, significant PR3 amounts are already expressed on the surface of resting cells with a strong increased

expression after activation (Witko-Sarsat *et al.*, 1999), whereas MPO is not detected on the plasma membrane of resting neutrophils (Kindzelskii *et al.*, 2006). Furthermore, the membrane MPO that increases after cell activation is small compared to PR3. In this chapter, MPO inhibition with AZM198 had no effect on MPO membrane expression in TNFα-primed PR3-ANCA stimulated neutrophils. This could be partly explained by some of these differences in the expression and mobilisation between MPO and PR3 listed above. It is also possible that the translocation of MPO to the cell surface triggered by neutrophil priming by TNFα, is not dependent on enzymatically active MPO.

Endothelium-neutrophil interactions are essential to allow neutrophils to move toward inflammatory sites and regulate neutrophil recruitment. The rolling of neutrophils through the endothelium is converted by ANCA into firm adhesion even at minimal TNF-α concentration. Firm adhesion mainly involves neutrophil β2-integrins interacting with endothelial ICAM-1 (Halbwachs and Lesavre, 2012) . The synergy between signals promoted by TNFα, β2-intergrin engagement and ANCA-bound FcγR leads to intense neutrophil degranulation and release of proteases and reactive intermediates highly toxic for the endothelium. Indeed, ROS and serine proteases released during neutrophil degranulation and presented on NETs have been shown to induce endothelial cell damage in vasculitic lesions (Lu *et al.*, 2006; Al Laham *et al.*, 2010).

I found that TNFα/PR3-ANCA-stimulated neutrophils led to EC injury that was attenuated by enzymatic NET degradation using DNAse, as well as pharmacological inhibition of MPO. In fact, others have similarly shown that inhibiting other serine proteases such as cathepsin G (Jerke *et al.*, 2019), also presented on NETs, as well as signalling pathways upstream of ROS generation such as receptor-interacting serine/threonine-protein kinase 1 (RIPK1) (Schreiber *et al.*, 2017) and spleen tyrosine kinase (SyK) (Prendecki *et al.*, 2019) reduced ROS production and ANCA-stimulated neutrophil-induced endothelial cell damage.

Aberrant neutrophil degranulation and spontaneous NETosis has been reported in patients with crescentic GN (Ohlsson *et al.*, 2014; Carmona-Rivera *et al.*, 2015;

Grayson *et al.*, 2015). The *in vitro* experiments included in this chapter suggest that MPO inhibition can reduce neutrophil degranulation and NET formation as well as attenuate EC damage induced by ANCA-stimulated neutrophils.

5 Investigation of myeloperoxidase inhibition in a pre-clinical model of crescentic glomerulonephritis

5.1 Introduction

In this chapter, the effect of delayed myeloperoxidase inhibition on murine glomerular inflammation is examined *in vivo*. The murine model of nephrotoxic nephritis (NTN) is used which is a T cell and neutrophil mediated preclinical model of crescentic immune complex GN.

NTN is induced by administration of nephrotoxic serum, obtained from sheep (or rabbits) immunised with murine glomeruli. When administered to mice, it 'plants' an antibody in the glomerular basement membrane. NTN can be divided into 2 phases, the heterologous and autologous phases. During the initial, or heterologous, phase of the disease, glomerular injury is characterized by proteinuria which is mediated by infiltrating neutrophils whose accumulation in glomeruli peaks 2 hours after nephrotoxic serum administration (Cochrane, Unanue and Dixon, 1965). The subsequent autologous phase of the disease is initiated by a T helper cell 1 (Th1)-polarized, delayed-type hypersensitivity (DTH)-like adaptive immune response against the immunizing antigen that develops 7 days later. During this phase, severe glomerular injury, characterized by crescent formation and glomerular thrombosis, is mediated by infiltrating $CD4^+$ T cells and macrophages.

The pathogenic role of neutrophils in nephrotoxic nephritis is supported by early work that demonstrated that neutrophil depletion attenuated glomerular injury (Naish *et al.*, 1975). While murine neutrophils contain 5-10-fold lower levels of MPO than human neutrophils (Rausch and Moore, 1975), histones and MPO have been detected in murine glomeruli of experimental models of crescentic GN, and their deposition was decreased with pharmacological inhibition of NETosis (Knight *et al.*, 2015; O'Sullivan *et al.*, 2019). In addition, a causative role for MPO in mediating glomerular damage is supported by the results of NTN in MPO-deficient animals, which demonstrated less proteinuria in the acute heterologous phase.

However, during the autologous phase these animals demonstrated augmentation of adaptive (T cell) immunity (Odobasic *et al.*, 2007). If pharmacological MPO inhibition has the same effect on adaptive immunity as MPO deficiency, using the former as a therapeutic strategy in crescentic GN could be problematic as many conditions associated with crescentic GN are characterised by autoreactive T and B cells (Tipping and Holdsworth, 2006; Dörner, Giesecke and Lipsky, 2011). In this chapter, the effect of selective MPO inhibition on both cellular and humoral immunity in the nephrotoxic nephritis model as well as on antigen specific T cell responses are examined.

Latterly, selective MPO inhibitors have been developed and tested in experimental models of heart failure (Ali *et al.*, 2016), pulmonary hypertension (Klinke *et al.*, 2018) and vasculitis (Zheng *et al.*, 2015) and have been shown to ameliorate disease.

5.2   Aims

To investigate the effect of myeloperoxidase inhibition on glomerular inflammation and adaptive immune responses in a T cell and neutrophil mediated model of crescentic glomerulonephritis.

5.3   Experimental design

Nephrotoxic nephritis was induced in C57BL/6 mice. In order to assess the impact on crescentic nephritis, mice were pre-immunised with sheep IgG in Complete Freunds Adjuvant (accelerated model) and one day after immunisation with nephrotoxic serum, mice received AZM198 at two different doses (133 µmol/kg or 400 µmol/kg) or vehicle via gavage every 12 hours. Mice were sacrificed on day 8 and blood and 16 hr urine were collected, and kidneys and spleen harvested. Renal sections were analysed for histology, glomerular macrophage and T cell infiltration and MPO deposition. In order to assess the effect of MPO inhibition on cellular immunity, splenocytes from these mice were stimulated in vitro with sheep IgG to induce a recall response and analysed for the expression of memory T cell markers, CD44^{high}CD62L^{low}. In order to further assess the effect of MPO inhibition

on antigen specific T cell responses, the adoptive transfer model of DO11.10 lymphocytes into ovalbumin immunised mice was used in the presence and absence of AZM198. Lymphocytes were isolated from draining lymph nodes and analysed for the expression of CD44^{high}KJ^{high}, using KJ126, a monoclonal antibody against the DO11.10 T cell receptor. The two doses of AZM198 used are predicted to inhibit at least 80% of the extracellular MPO activity over 12 hours. The higher dose is predicted to also inhibit intragranular activity more than 80% for 4 out of 12 hours (Halla Björnsdottir *et al.*, 2015). In order to assess the effect of AZM198 on glomerular neutrophil influx, mice were pre-treated with AZM198 or vehicle for 2 days, subsequently immunised with nephrotoxic serum and culled 2 hours later where kidneys were harvested. Kidney sections were analysed to count the corrected total cell fluorescence (CTCF) of neutrophils per glomerulus, identified by Ly6G staining.

5.4   Results

5.4.1   MPO inhibition attenuates glomerular inflammation in the accelerated NTN model

One day following NTS injection and following the time of early neutrophil entry into the kidney mice received vehicle (n=16) or AZM198, at 133µmol/kg (n=8) or 400µmol/kg (n=8) by gavage twice a day for 7 days. Two animals in the vehicle group (on day 6 and 7) and one in the 400µmol/kg AZM198 group (day 2) died, while two vehicle animals were anuric.

MPO inhibition using AZM198 at either dose led to a reduction in renal injury. In particular, median (IQR) glomerular thrombosis score in the 133 µmol/kg group was 0 (0-0.1) and in the 400 µmol/kg group 0.8 (0.5-1.3) *vs* vehicle 2.6 (1.0-3.3) (p<0.001 and p=0.24, respectively (Figure 5-1A and 5-2). There was also a reduction in proteinuria in both AZM198-treated groups compared with vehicle (133 µmol/kg 1.3 (1.0-1.9) mg/24hrs and 400µmol/kg 1.0 (0.1-1.2) mg/24hrs *vs* vehicle 3.5 (1.0-7.1) mg/24hrs, p=0.22 and p=0.02, respectively) (Figure 5-1B). Plasma creatinine was lower in both AZM198 groups compared with vehicle (plasma creatinine 133 µmol/kg 12.5 (9.0-14.8) µmol/L and 400 µmol/kg 6.0 (1.2-

8.0) µmol/L and vs vehicle 16.1 (8.4-52.8), p=0.26 and p=0.04, respectively, Figure 5-1C).
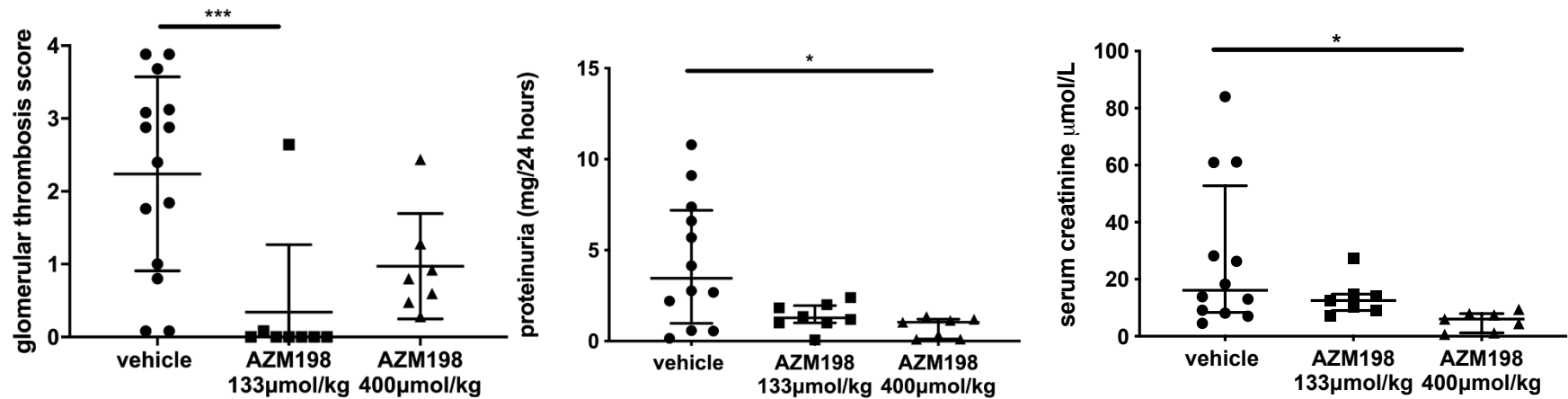
Figure 5-1 Effect of AZM198 on glomerular thrombosis score, proteinuria and serum creatinine in mice with nephrotoxic nephritis.

Median (IQR) A) glomerular thrombosis score B) proteinuria and C) plasma creatinine in mice with crescentic glomerulonephritis secondary to nephrotoxic nephritis treated with vehicle (n=14) or AZM198 dosed at two different doses, 400μmol/kg (n=7) and 133μmol/kg (n=8, but only 6 analysed for urine protein). Kruskal Wallis*P < 0.05, ***P < 0.0
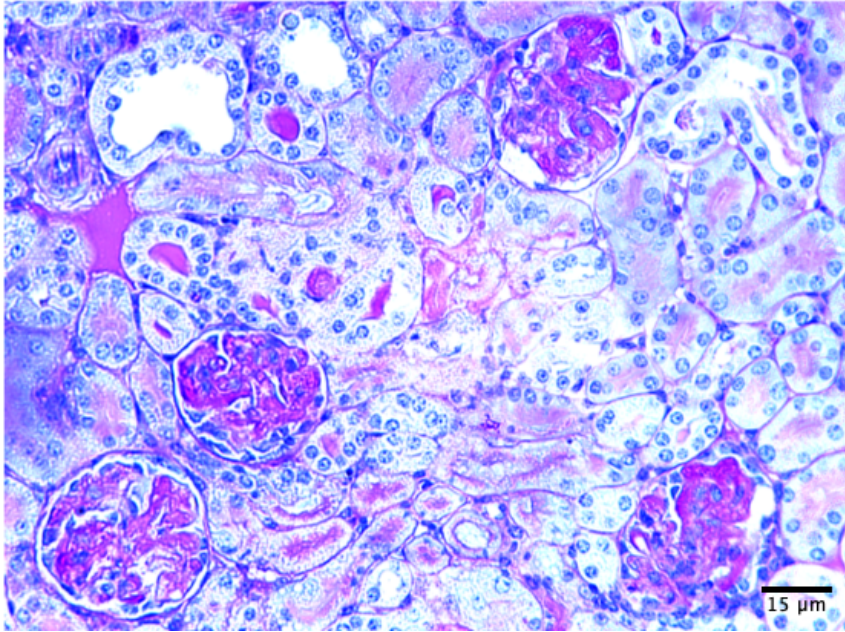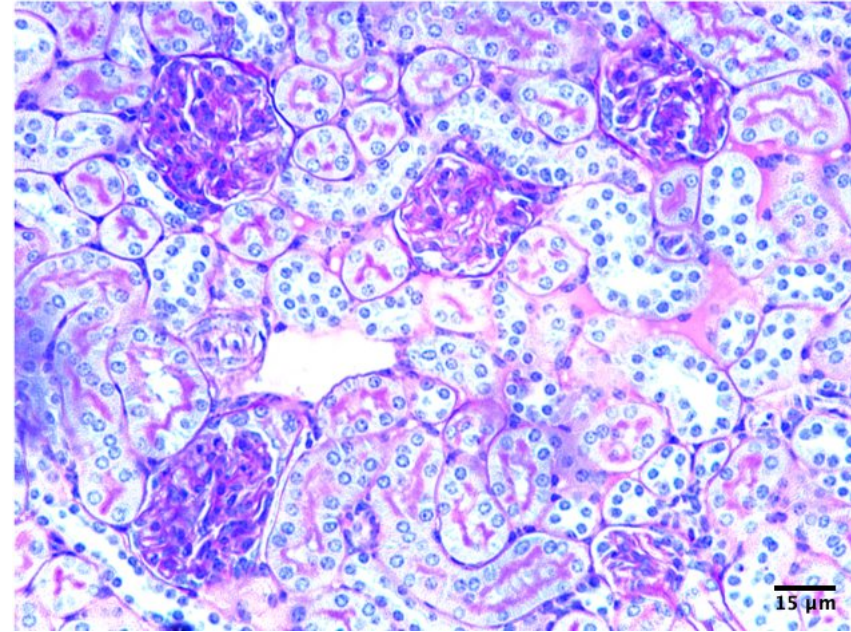
Figure 5-2 Representative histology of kidney sections from mice with nephrotoxic nephritis in the presence and absence of AZM198

Periodic acid–Schiff (PAS) stain showing glomerular thrombosis in kidney sections of mice with NTN treated with vehicle (A) or B) AZM198.

5.4.2 MPO inhibition reduces MPO deposition as well as T cell and macrophage infiltration in nephrotoxic nephritis

Immunofluorescence staining showed a significant reduction in macrophage (Figure 5-3) and CD4$^+$ T cell infiltration (Figure 5-4) as well as glomerular MPO deposition (Figure 5-5) in the kidneys of the animals that were treated with AZM198 133µmol/kg compared with vehicle controls. F4/80 CTCF (Corrected Total Cell Fluorescence) in AZM198 treated: 41.1 (24.0-42.3) AU *vs* vehicle: 68.2 (58.3-75.6) AU p=0.01, number of T cells per glomerulus AZM198 treated : 0 (0-0.4) *vs* vehicle: 1 (0 -2.1) and MPO CTCF in AZM198: 45.9 (40.6-51.6) AU *vs* vehicle: 67.7 (61.0-102.0) AU, p=0.01).
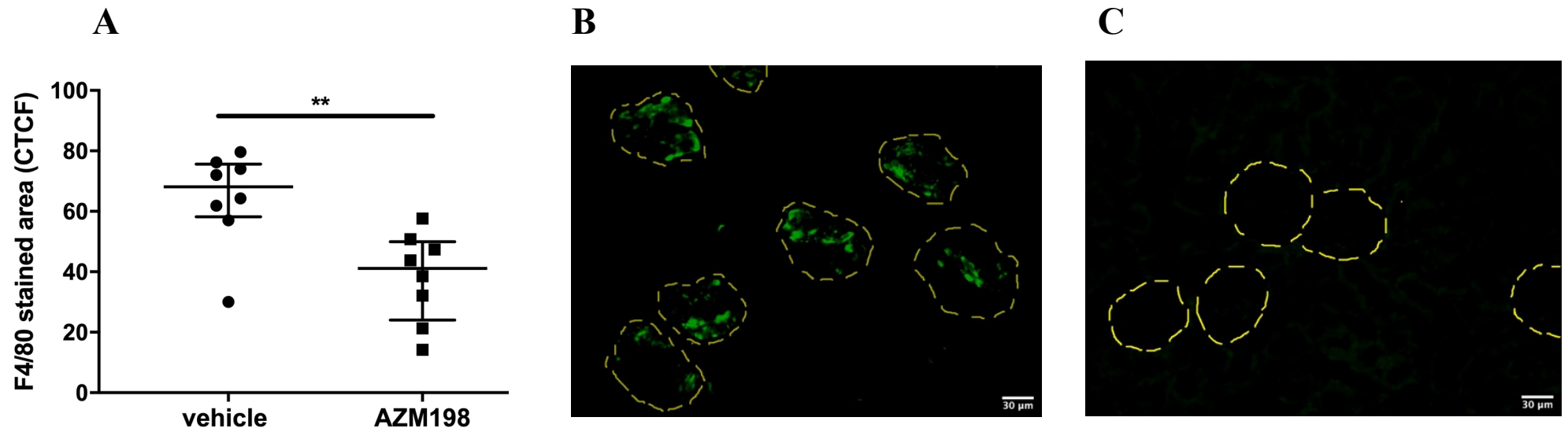
Figure 5-3. Macrophage infiltration in the nephrotoxic nephritis model in the presence or absence of AZM198.

Median (IQR) glomerular corrected total cell fluorescence (CTCF) (A) and immunofluorescence staining for F4/80 expressing macrophages in the glomeruli of mice with NTN treated with vehicle (B) or AZM198 at 133µmol/kg (C), Mann Whitney test, **$P <$ 0.01. Yellow lines outline glomeruli. Glomerular F4/80 staining was expressed as corrected total cell fluorescence (CTCF) using the Fiji software for each glomerulus. Ten randomly chosen HPFs were used to score 25 adjacent glomeruli per section. One section was scored per animal.
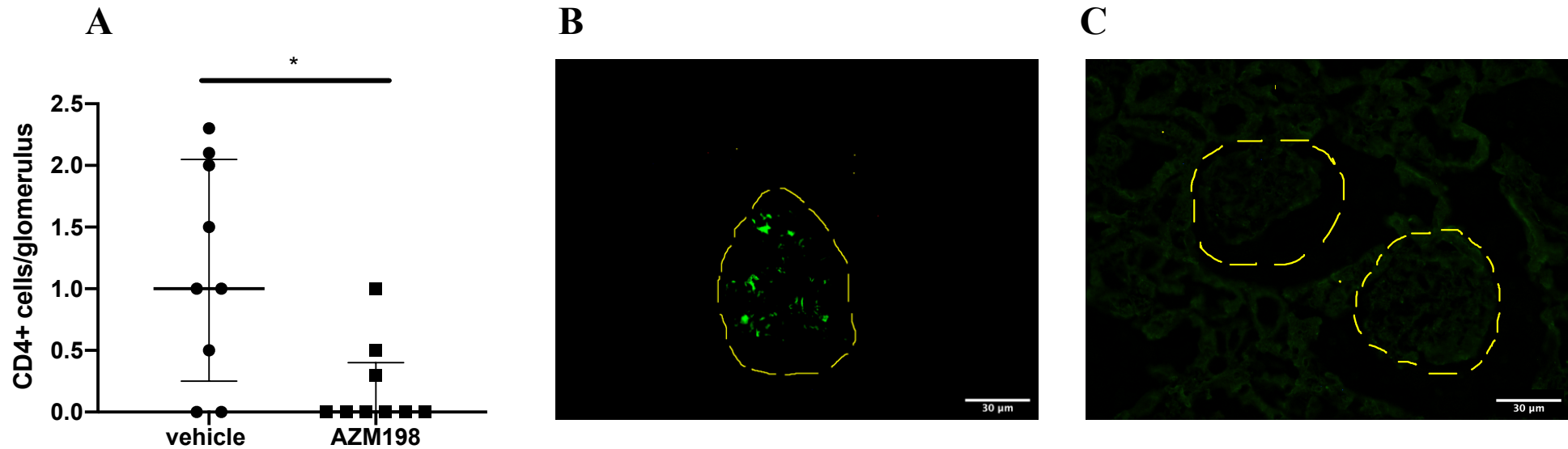
Figure 5-4. T cell infiltration in the nephrotoxic nephritis model in the presence and absence of AZM198.

Median (IQR) glomerular corrected total cell fluorescence (CTCF) (A) and immunofluorescence staining for CD4 positive cells in the glomeruli of mice with NTN treated with vehicle (B) or AZM198 at 133µmol/kg (C), Mann Whitney test, *P < 0.05. Yellow lines outline glomeruli. Glomerular CD4 positive cells was counted in each glomerulus using the Fiji software. Ten randomly chosen HPFs were used to score 25 adjacent glomeruli per section. One section was scored per animal.
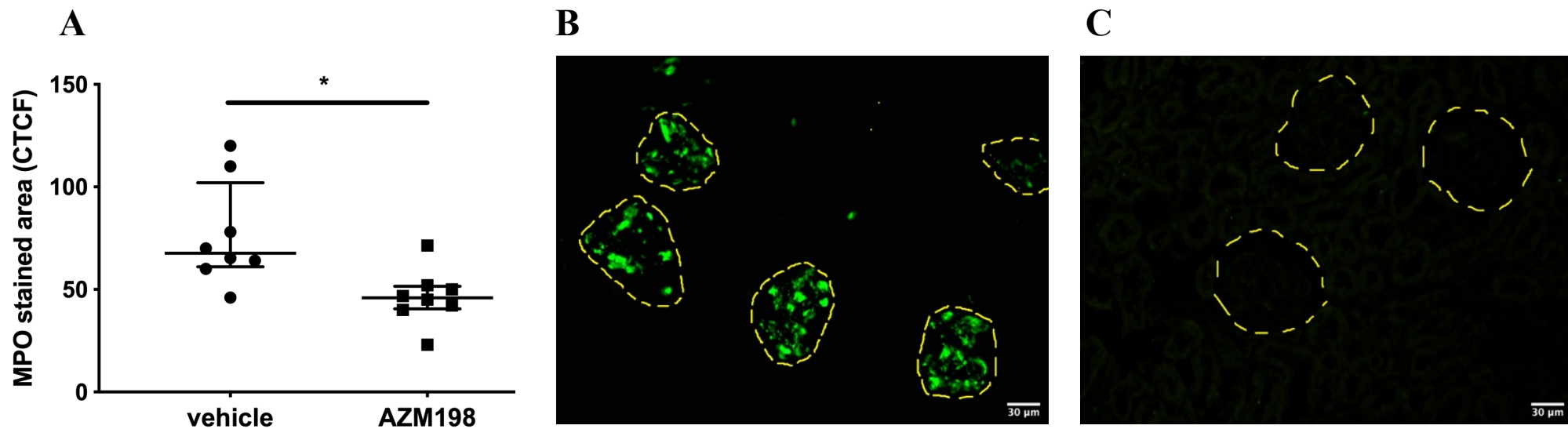
Figure 5-5. MPO deposition in the nephrotoxic nephritis model in the presence and absence of AZM198.

Median (IQR) glomerular corrected total cell fluorescence (CTCF) (A) and immunofluorescence staining for MPO in the glomeruli of mice with NTN treated with vehicle (B) or AZM198 at 133µmol/kg (C), Mann Whitney test, $*P < 0.05$. Yellow lines outline glomeruli. Glomerular MPO was expressed as corrected total cell fluorescence (CTCF) using the Fiji software for each glomerulus. Ten randomly chosen HPFs were used to score 25 adjacent glomeruli per section. One section was scored per animal.

5.4.3 MPO inhibition does not affect neutrophil recruitment in NTN

To assess the effect of AZM198 on glomerular neutrophil accumulation, mice were dosed with either vehicle (n=4) or AZM198 133μmol/kg (n=4) for 48 hours. On day 3, NTS was administered and kidneys were collected 2 hours later for assessment of glomerular neutrophil infiltration. Neutrophils were identified by Ly6g positive staining in murine glomeruli. A non-significant reduction in glomerular neutrophil infiltration was found in those treated with AZM198 (Ly6g CTRF AZM198 26.5(23-70.7) AU *vs* vehicle 71.0(45.3-152.8) AU, p=0.11), Mann Whitney test (Figure 5-6)
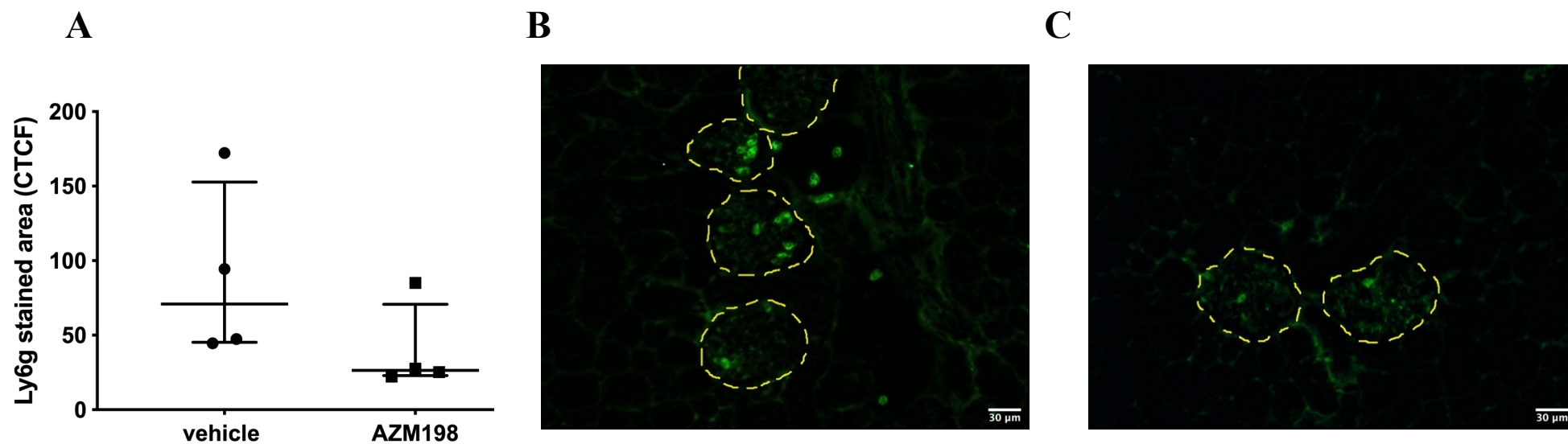
Figure 5-6 Effect of AZM198 on glomerular neutrophil accumulation

Mice were dosed with either vehicle (n=4) or AZM198 (n=4) twice a day at 133µmol/kg for 48 hours following the injection of nephrotoxic serum (NTS) (12 hours after the last dosing). Median (IQR) glomerular corrected total cell fluorescence (CTCF) (A) and immunofluorescence staining for Ly6g in the glomeruli of mice with NTN treated with vehicle (B) or AZM198 at 133µmol/kg (C), Mann Whitney test, *P < 0.05. Yellow lines outline glomeruli. Yellow lines outline glomeruli.

5.4.4 Effect of MPO inhibition on adaptive immunity

Previous reports have suggested that in murine models of crescentic GN, acute glomerular disease is attenuated in MPO-deficient animals, but there is augmentation of adaptive T cell immunity (Odobasic *et al.*, 2007). To investigate if this also occurs after pharmacological inhibition of MPO, the effect of AZM198 on T and B cell responses was determined in context of two different models. First, the effect on humoral and cellular immunity in the Th1 and Th17-mediated and immune complex-driven NTN model described above was investigated, and second the effect on antigen-specific T cell responses in an adoptive transfer model of T cell receptor transgenic T cells recognizing an ovalbumin peptide, i.e. the DO11.10 mice.

There was no significant increase in the concentration of IgG1, IgG2b and IgG3 subclasses in the AZM198-treated animals compared with vehicle controls (IgG1: 354.5 (33.6-465.2) µg/mL *vs* vehicle 347.3 (212.5-994.5) µg/mL, p=0.38 and IgG2b 191.8 (73.9 -305.3)µg/mL *vs* vehicle 163.0 (30.9-297.7) µg/mL p=0.51, IgG3 8.4 (5.1-50.6) µg/mL *vs* vehicle 16.0 (3.4-46.6) µg/mL p>0.99 (Figure 5-7).
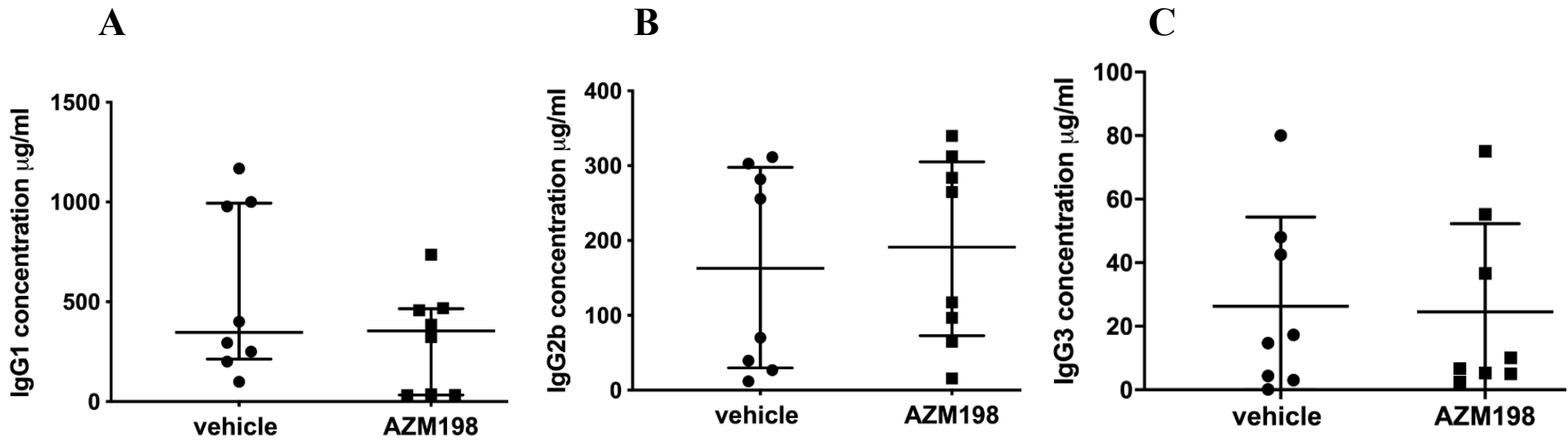
Figure 5-7 Effect of AZM198 on serum humoral immune responses to sheep globulin

Median (IQR) IgG subclass concentrations IgG1 (A), IgG2b (B) and IgG3 (C) respectively (n=8 per group).

CD4$^+$ splenocytes from the NTN mice that received vehicle or AZM198 133 µmol/kg, were isolated and re-stimulated with sheep globulin *in vitro* for 72 hours, after which expression of CD44 and CD62L were assessed by flow cytometry (Figure 5-8, 5-9). There was no difference in the median frequency of CD44^{high}CD62L^{low} T cells (memory T cells) amongst the vehicle and treatment group, suggesting that AZM198 attenuated glomerular inflammation without an increase in adaptive T cell responses (median CD44^{high}CD62L^{low} % of CD4+cells: AZM198 49.6(42.9-55.9)% *vs* vehicle 47.6(38.6-58.2)%, (p=0.78)).
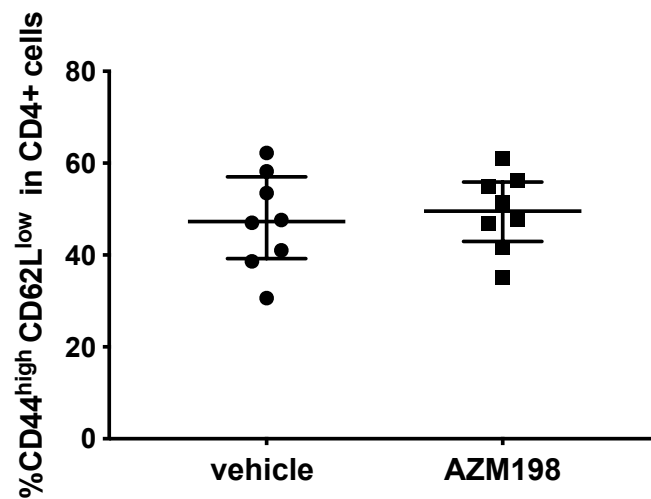
Figure 5-8 Effect of AZM198 on cellular immunity in the nephrotoxic nephritis model

Median (IQR) frequency of CD44^{high} CD62L^{low} CD4+ splenocytes from mice with NTN (n=8 per group).
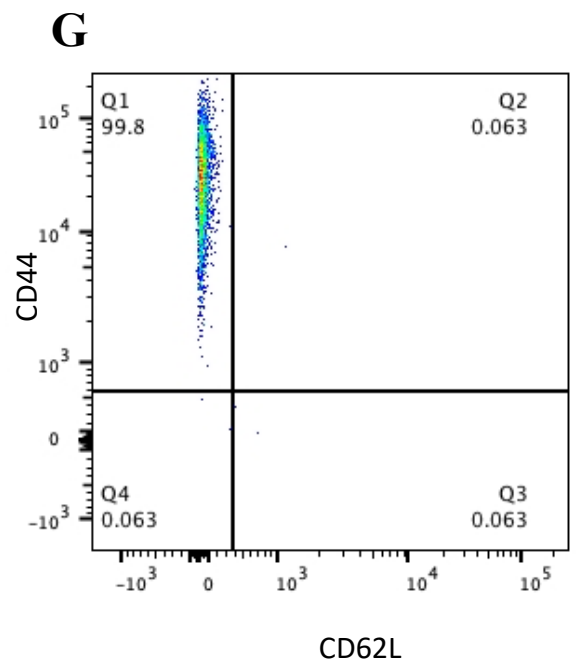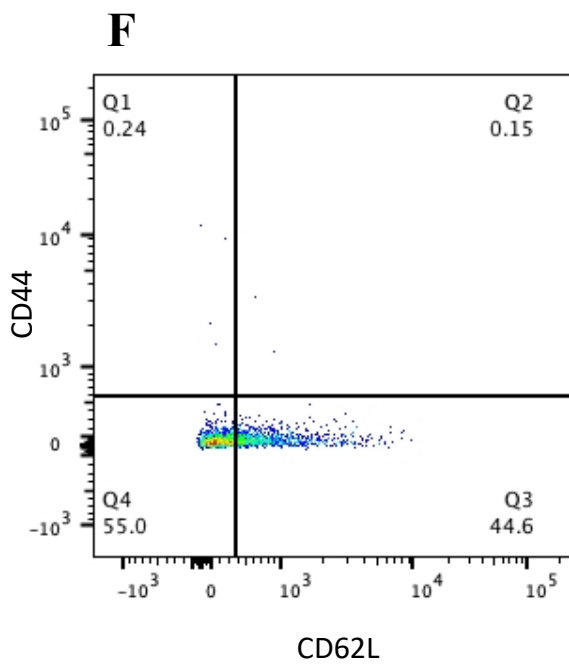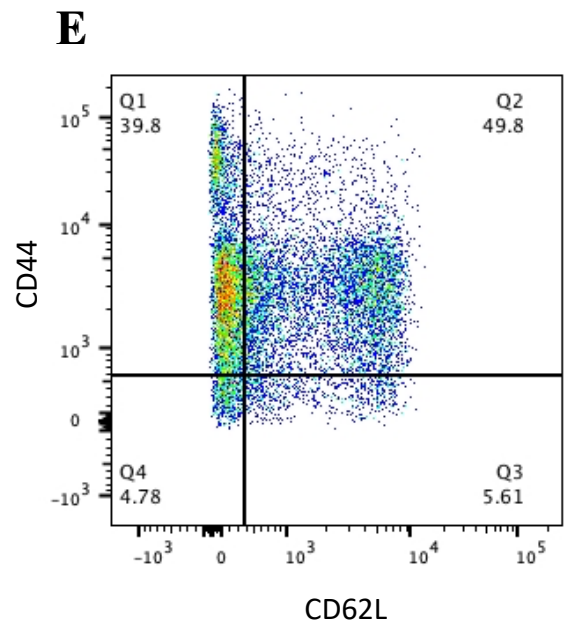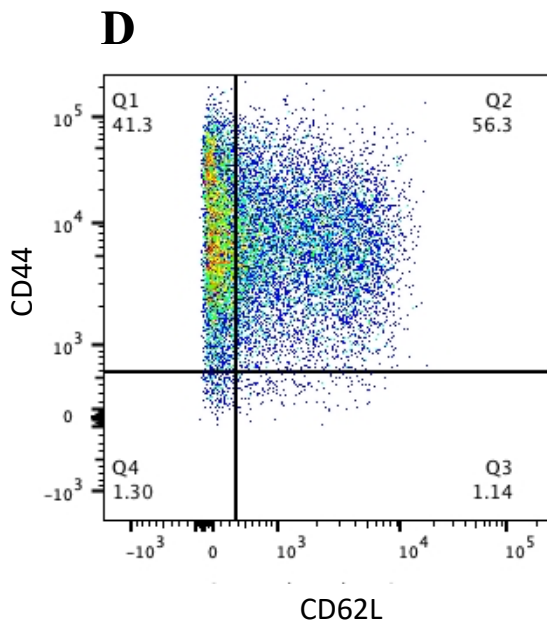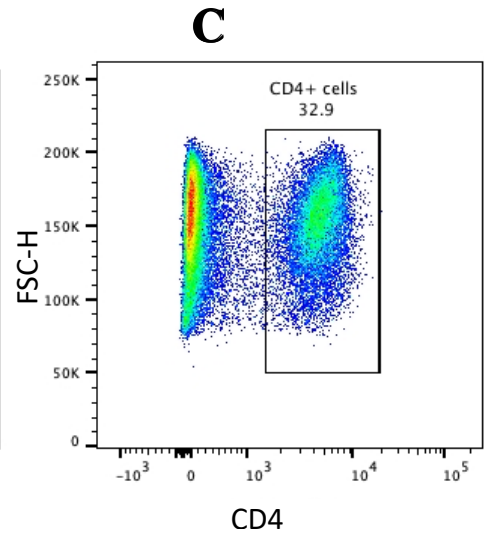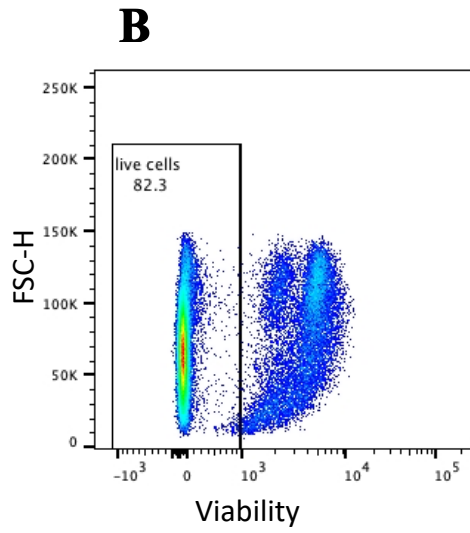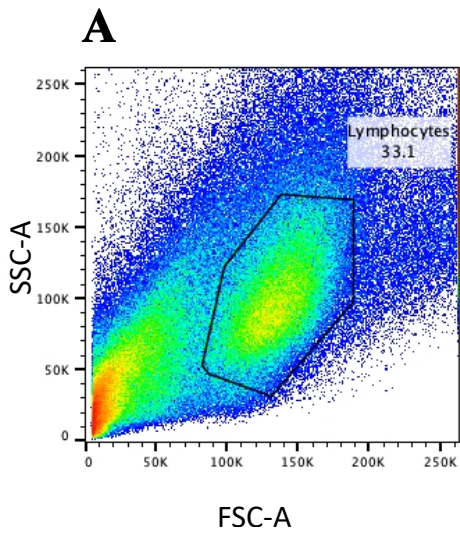
Figure 5-9 Flow cytometry plots of splenocyte phenotype following restimulation with sheep IgG in the nephrotoxic nephritis model
Representative flow cytometry plots of murine splenocytes from the nephrotoxic nephritis model stimulated with sheep IgG for 72 hrs to induce a recall response. A-C represents gating for live CD4+ cells. Representative plots showing frequency of CD44^{high} CD62L^{low} CD4+ splenocytes of an animal that received vehicle (D) and AZM198 (E) is shown. F) shows the fluorescence minus one (FMO) gating for CD44 and G) the FMO for CD62L.

Finally, the effect of AZM198 on antigen-specific T cell responses was tested, using adoptive transfer of DO11.10 lymphocytes into OVA immunised mice. The frequency of activated CD4 cells and activated OVA-specific T cells in draining lymph nodes were determined by staining for CD4, CD44 and the DO11.10 T cell receptor (Figure 5-10). Treatment with AZM198 did not result in higher frequency of activated total (CD4, CD44) or OVA-specific (CD44, KJ) T cells (CD44^{high}% on CD4+ cells: AZM198 12.6% (11.8-13.8) *vs* vehicle 19.35% (16.5-19.9) p=0.10, CD44^{high}KJ+% on CD4+ cells (AZM198 1.9(1.64-3.14) *vs* vehicle 4.1(3.9-5.0), p=0.05). These results suggest that pharmacological MPO inhibition, unlike genetic MPO-deficiency, does not augment antigen-specific T cell responses in the draining lymph nodes.

A

B
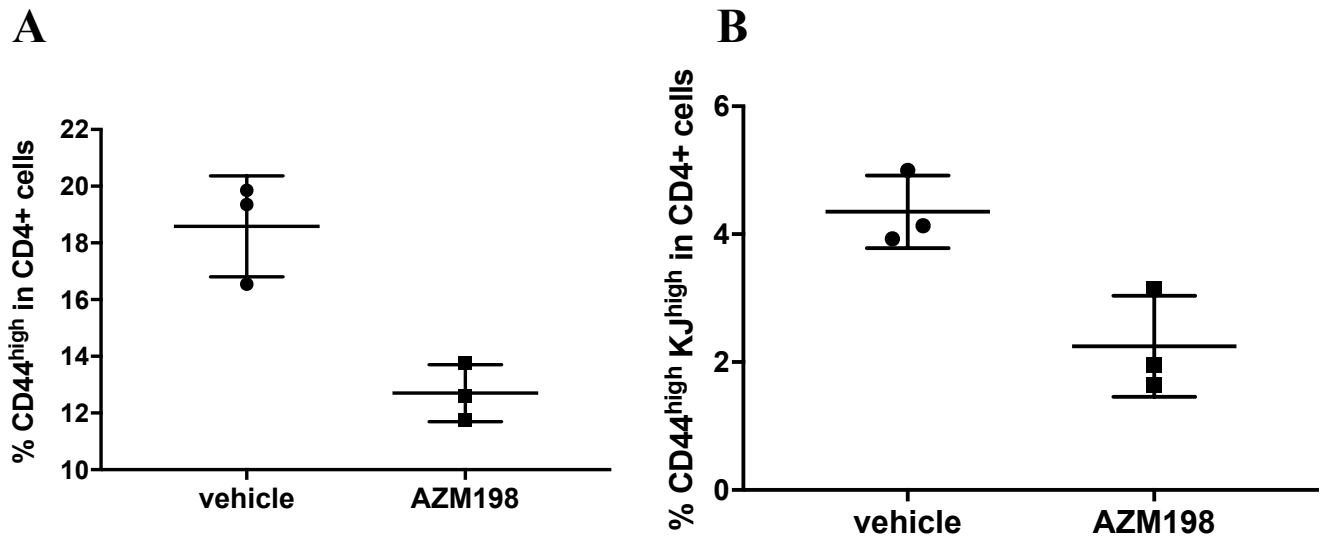
Figure 5-10 Effect of AZM198 on antigen-specific T cell responses

DO11.10 T cell adoptive transfer model: antigen-specific T cell responses using adoptive transfer of DO11.10 lymphocytes into OVA immunised mice, median (IQR) frequency of CD44^{high}CD4+ cells (A) and CD44^{high} KJ+ CD4+ cells(B). Mann-Whitney test, p=NS

5.4.5 Pharmacokinetic studies of AZM198

We collected the terminal plasma samples from the animals that received vehicle or AZM198 at two different doses in the nephrotoxic nephritis model and outsourced them to AstraZeneca, Gothenburg, for measurement of plasma AZM198. Mice in the nephrotoxic nephritis model were dosed every 12h with AZM198 and plasma concentration 19h after the final dose were measured (grey triangles represent the individual mice receiving 133 µmol/kg, and black squares 400 µmol/kg).

A satellite group of mice were dosed with 133 µmol/kg AZM198 and sampled at 2, 12 and 19h to measure the maximal (C_{max}) and trough (C_{min}) levels and to bridge the data to the terminal samples of the efficacy study, respectively (n=3/timepoint, white triangles represent mean values, grey area representing 95% confidence interval). The free plasma concentration of AZM198 corresponding to 80% inhibition of the activity of purified MPO is illustrated with a dashed line, and the concentration corresponding to 80% inhibition of peroxidase activity in zymosan-stimulated whole blood is illustrated with a dotted line.
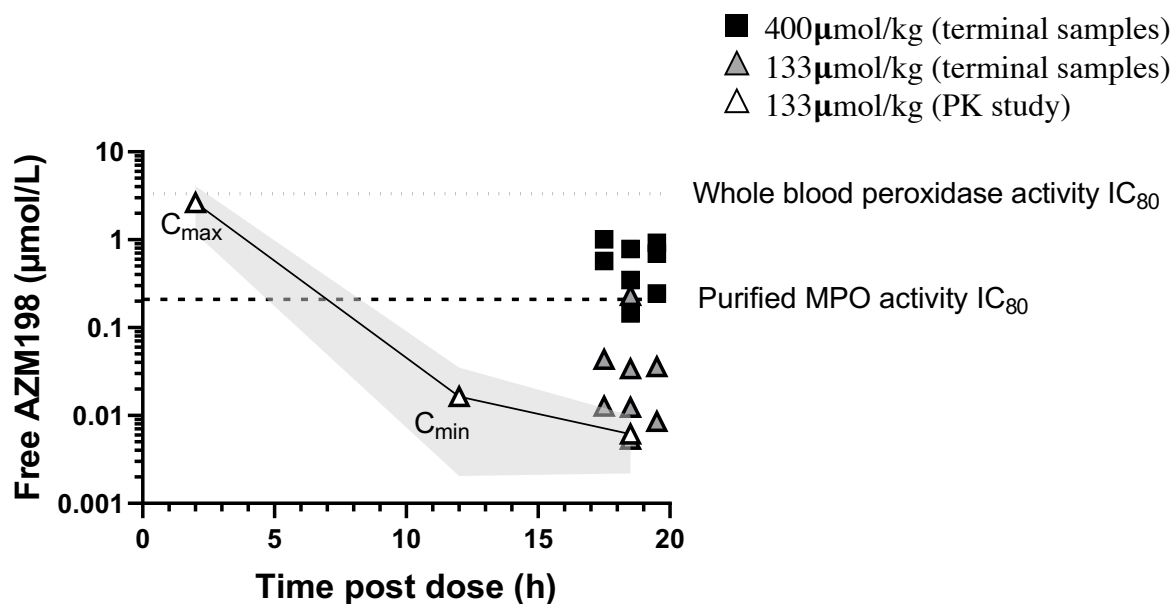
Figure 5-11 Pharmacokinetic studies of AZM198

5.5 Discussion

The experiments included in this chapter demonstrate that selective delayed MPO inhibition with AZM198 reduced glomerular inflammation in a neutrophil and T cell mediated model of crescentic GN, without augmentation of T cell responses.

The accelerated nephrotoxic nephritis model of CGN was used, which is dependent on adaptive and innate immunity and representative clinically of a rapidly progressive glomerulonephritis due to immune-complex disease. Despite the initiation of treatment one day after the glomerular neutrophil influx, AZM198 at two different doses attenuated glomerular inflammation clinically and histologically. When I assessed the effect of AZM198 on neutrophil influx I found no significant difference in neutrophil influx at an early time point. Acknowledging the small sample size of animals tested in this experiment (n=4 in each group), a biological effect on neutrophil recruitment may have been missed which has been shown in previous reports (Odobasic *et al.*, 2007). Alternatively, these results may be explained by an effect of the delayed MPO inhibition on neutrophil

activation/degranulation and inhibition of the biological effects of enzymatically active MPO, in addition to any effect on neutrophil recruitment.

Similarly, a significant protective biological effect of MPO inhibition on adaptive T cell responses might also have been missed in this set of experiments because of the small animal size used. In fact, retrospective power calculation of our adoptive transfer model of DO11.10 lymphocytes into OVA immunised mice revealed that for an effect size of 1.6, six animals were required instead of three to reach a significance level of 0.05 with 80% power.

AZM198 is a membrane-permeable compound that acts as a suicide-substrate for MPO and has been shown to inhibit enzymatically active extracellular MPO, while at higher concentrations it also inhibits intragranular MPO, together with NET formation (Tidén *et al.*, 2011; Halla Björnsdottir *et al.*, 2015). The rationale for the dose setting in the current experiments was to yield exposures that would mainly inhibit extracellular (133 µmol/kg) or extracellular, as well as intragranular MPO (400 µmol/kg). A satellite group of mice was dosed with 133 µmol/kg AZM198 and sampled at 2, 12 and 19 h to define the maximal (C_{max}) and trough (C_{min}) levels, and to bridge the data with the terminal samples of the efficacy study. The observed pharmacokinetic responses, which also shows the concentration of AZM198 predicted to inhibit 80% of extracellular MPO and 80% peroxidase activity in human whole blood (the latter corresponding to the intragranular MPO potency). The reported IC_{50} of AZM198 is 0.015 µM. Therapeutic AZM198 levels were achieved throughout the study. Our PK data suggest that the peak plasma concentrations our MPO inhibitor achieved in the current experiments were in the range found to inhibit intragranular MPO, even using the lower dose of AZM198. However, the limited benefit of 400 µmol/kg over 133 µmol/kg may argue that some beneficial effect of AZM198 on glomerular inflammation in this model might also be due to the inhibition of extracellular MPO activity.

The NTN model dissociates the effect of the AZM198 from the induction and perpetuation of autoreactivity. As there is no autoimmunity in this model and the treatment is delayed, we can reasonably assume that this is testing MPO inhibition

largely for its effects in the kidney and not on the induction or maintenance of immunity to sheep Ig. These data confirm and extend previous observations made by Zheng *et al.*(2015), which showed that prophylactic MPO inhibition attenuated disease in a mild, non-crescentic murine anti-GBM model and a model of lung vasculitis (Zheng *et al.*, 2015).

Importantly, the methodology used here differs in that we used an accelerated severe nephrotoxic nephritis model with features of glomerular thrombosis and administered delayed MPO inhibition, reflecting clinical presentations to a greater extent. Moreover, we demonstrate for the first time that there is no impact on adaptive T cell responses, a critical requirement for translation of such therapy to the clinic in the setting of autoimmune crescentic glomerulonephritidies.

6 Investigation of the role of nephritis on atheroma formation and future work

6.1   Introduction

In this chapter, the role of glomerular inflammation as a risk factor for the development of atheroma formation is explored.

Evidence that inflammation is important in the development of atherosclerosis is strongly supported by many studies showing that increased plasma concentrations of markers of inflammation, such as C-reactive protein (CRP), IL-6, IL-1 and serum amyloid A are independent predictors of coronary events (Hansson, Robertson and Söderberg-Nauclér, 2006). In addition, recent genetic polymorphism studies suggest that IL-6 receptor (IL-6R) signalling seems to have a causal effect on coronary artery disease while IL-6R blockade in patients with rheumatoid arthritis leads to improvement in endothelial function (Bacchiega *et al.*, 2017) . Furthermore, a clinical trial in patients with recent myocardial infarction showed that colchicine, a potent anti-inflammatory, led a to lower risk of cardiovascular complications than placebo (Tardif *et al.*, 2019).

Histopathologic analysis of atherosclerotic lesions suggests they are composed of immune cells as well as vascular endothelial, smooth muscle cells, lipids and debris. Atherosclerotic plaques form typically in the intima, the innermost layer of the artery and are preceded chronologically by so-called fatty streaks, early lesions of atherosclerosis that consist of subendothelial accumulations of lipid-laden immune cells (Hansson, Robertson and Söderberg-Nauclér, 2006). Lipid-laden macrophages also known as foam cells as they contain lipid droplets in their cytoplasm, dominate these fatty streaks, which also contain T cells, dendritic cells, and mast cells. Until recently, neutrophils classically have been neglected in the pathophysiology of atherosclerosis partly because of their short life span and partly because of their ability to undergo phenotypic changes displaying markers typically expressed on antigen-presenting cells (Yamashiro *et al.*, 2001).

However, over the past years, sensitive detection techniques and neutrophil markers such as Ly6G (in mice) and CD177 and CD66b (in humans) in conjunction with MPO have allowed the detection of neutrophils in murine and human atherosclerotic plaques. There are primarily two mouse strains that develop hypercholesterolemia and atherosclerosis. The apolipoprotein E (*ApoE*) homozygous knockout (−/−) mouse develops spontaneous atherosclerosis that culminates in myocardial infarction, stroke, and aneurysm, whereas the LDL receptor (*Ldlr*) −/− mouse responds to fat feeding by hypercholesterolemia and lesion development (Lee *et al.*, 2017). In early atherosclerotic lesions in ApoE-/- mice, neutrophils were identified in the intima and subendothelium while in more advanced lesions neutrophils localise within the plaque shoulder and the adventitia (Hansson, Robertson and Söderberg-Nauclér, 2006).

NETs and neutrophil granule proteins, including MPO, azurocidin, LL-37, and α-defensins, have also been identified in murine and human atherosclerotic lesions, further supporting that activated neutrophils may directly contribute to lesion development (Edfeldt *et al.*, 2006; Warnatsch *et al.*, 2015). In addition, serum levels of MPO have been shown to predict risks of subsequent major adverse cardiac events (nonfatal myocardial infarction, death, and need for revascularization) in patients presenting with acute coronary syndromes (Baldus *et al.*, 2003).

The impact of inflammation on atherosclerosis has been demonstrated by our collaborator using the ApoE deficient mouse fed a high fat diet (HFD) (Chen *et al.*, 2014). Studies on the effect of glomerular inflammation on atheroma formation are mainly focused on preclinical lupus nephritis, where there is increased plaque formation in combined models of ApoE deficient mice and SLE (Ma *et al.*, 2008).

We set out to investigate the effect of nephritis on the development of atheroma formation using the model of nephrotoxic nephritis (NTN). Early atherosclerotic lesions in the intima of the murine aorta of ApoE-/- animals develop after 8-10 weeks (Nakashima *et al.*, 1994). The NTN model we used in chapter 5 was adapted to create a model of chronic kidney disease secondary to chronic glomerular inflammation. As the NTN model is largely described as a model of

acute glomerulonephritis, the knowledge of the long-term pathogenesis in the non-accelerated murine NTN model is therefore limited, but histologically it has been characterised by mesangial expansion and glomerular thrombosis` (Ougaard *et al.*, 2018).

6.2   Aims

To investigate the role of glomerular inflammation in the development of atheroma formation

6.3   Experimental design

Six ApoE-/- mice (three females, three males) and 5 C57BL/6 mice (three females, two males) were immunised intravenously with sheep nephrotoxic serum/ LPS and 6 ApoE-/- mice (three females, three males) received intravenous 0.9% NaCl. The wild type C57BL/6 mice acted as a control group for the role of nephritis on atheroma formation in the absence of a pro-atherogenic phenotype. After immunisation all mice received the same pelleted high fat diet (AFE 45%FAT +0.15% Cholesterol, # 824063, Special Diets Services) for 10 weeks. Weekly weights were recorded, and mice were placed in metabolic cages for 16hr urine collection every two weeks for the duration of the study. At week 11, urine and blood were collected, and murine kidneys, hearts and aortas were harvested for measurement of proteinuria, plasma IL6 levels, renal histology and en-face microscopy of murine aortas. Plaque area of murine aortic lesions was quantified using Image J software. A diagram of the experimental protocol is shown in Figure 6-1.
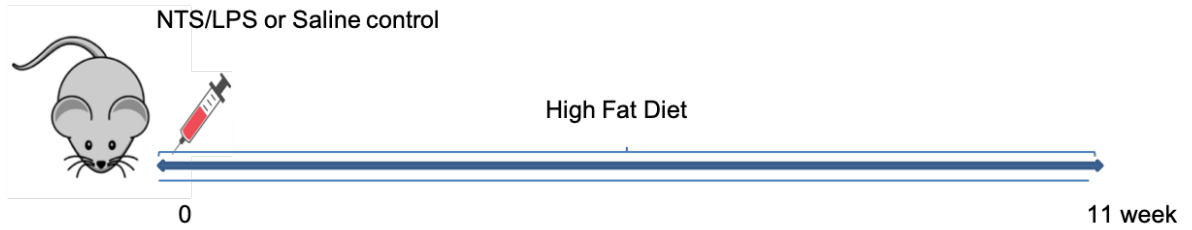
Figure 6-1 Study design of combined chronic nephritis and atheroma model

Study design on the 10-week combined non-accelerated nephrotoxic nephritis and atherosclerosis model

6.4 Results

6.4.1 Chronic glomerular inflammation accelerates atheroma formation

En-face microscopy examination revealed increased atheroma formation in ApoE-/- mice with non-accelerated nephrotoxic nephritis compared to ApoE-/- saline controls and WT mice with NTS (% aortic area occupied by plaque (SD): ApoE-/- NTN 13.8 (3.1)% vs ApoE-/- Saline 4.7(0.9)% and WT NTN 1.6 (1.9)%, all $p<0.0001$, Figure 6-2 and 6-3). The increment in weight over the 10-week period in all three groups is shown in Figure 6-4.
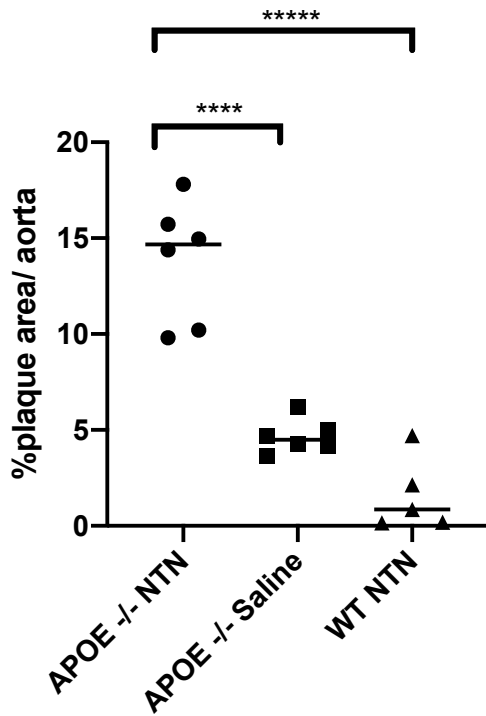
Figure 6-2 Quantification of aortic plaque area in the combined chronic nephritis and atheroma model

Quantification of aortic plaque areas of APOE -/- or C57BL/6 (WT) 12 week old mice fed a high fat for 10 weeks in the presence and absence of nephrotoxic nephritis (NTN), one-way ANOVA ****P<0.0001
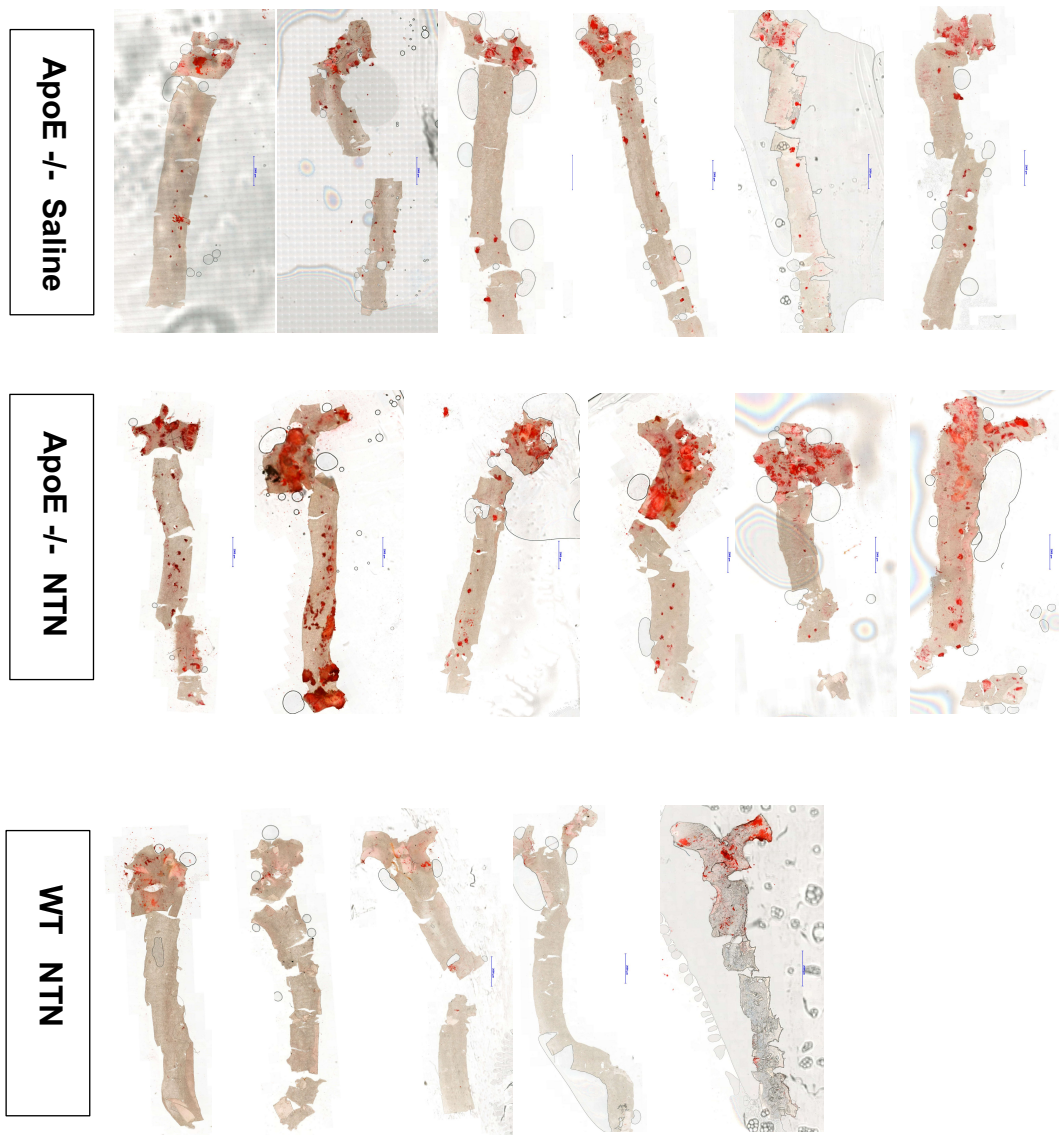
Figure 6-3 En-face micrographs from the combined chronic nephritis and atheroma model

En-face micrographs of mounted aortas stained with Oil Red O (red) of APOE -/- or C57BL/6 (WT) 12-week old mice fed a high fat for 10 weeks in the presence and absence of nephrotoxic nephritis (NTN)
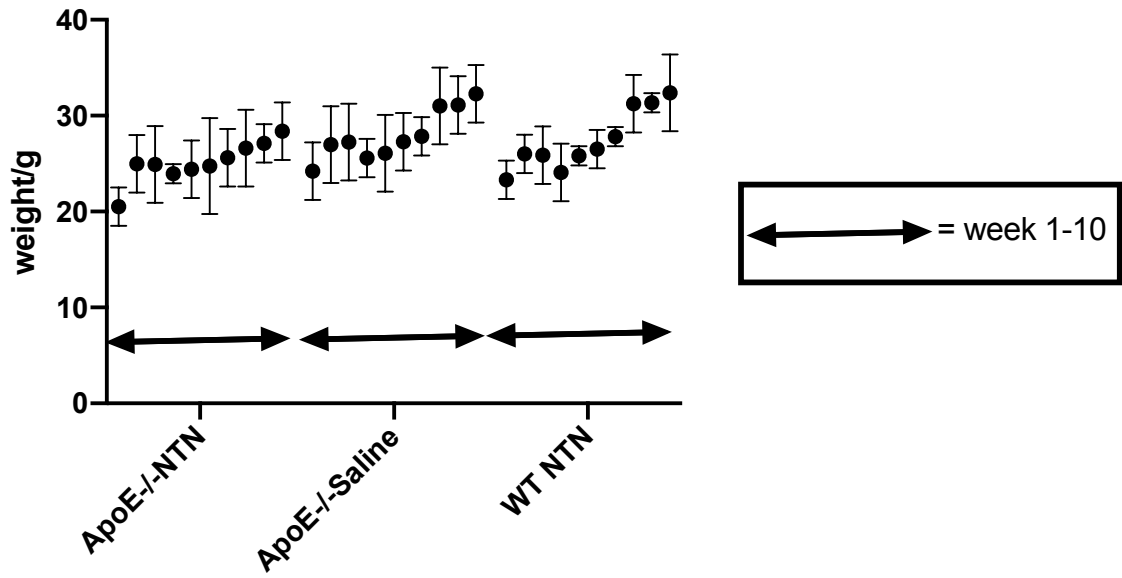
Figure 6-4 Weight gain during the 10-week study period

Plotted weekly mean weight gain of each group during the10 week study period where mice in all three groups were fed a high fat diet

6.4.2 Cytokine profile in the combined chronic nephritis and atheroma model

There was no significant difference in serum IL-6 and IL1β levels amongst the three groups although the most elevated IL6 levels were found in the ApoE -/- with nephrotoxic nephritis (Figure 6-5). (Serum IL6 (SD) ; ApoE-/- NTN 328.4(392.4)pg/mL vs ApoE-/- Saline 80.1(78) pg/mL (p= 0.22) and WT NTN 22.3(12.6)pg/mL (p=0.17) and serum IL1β ApoE -/- NTN 23(14.3) pg/mL vs ApoE -/- Saline 38.3(11.1)pg/mL (p=0.1) and WT NTN 20.7(8.8) pg/mL (p=0.8))
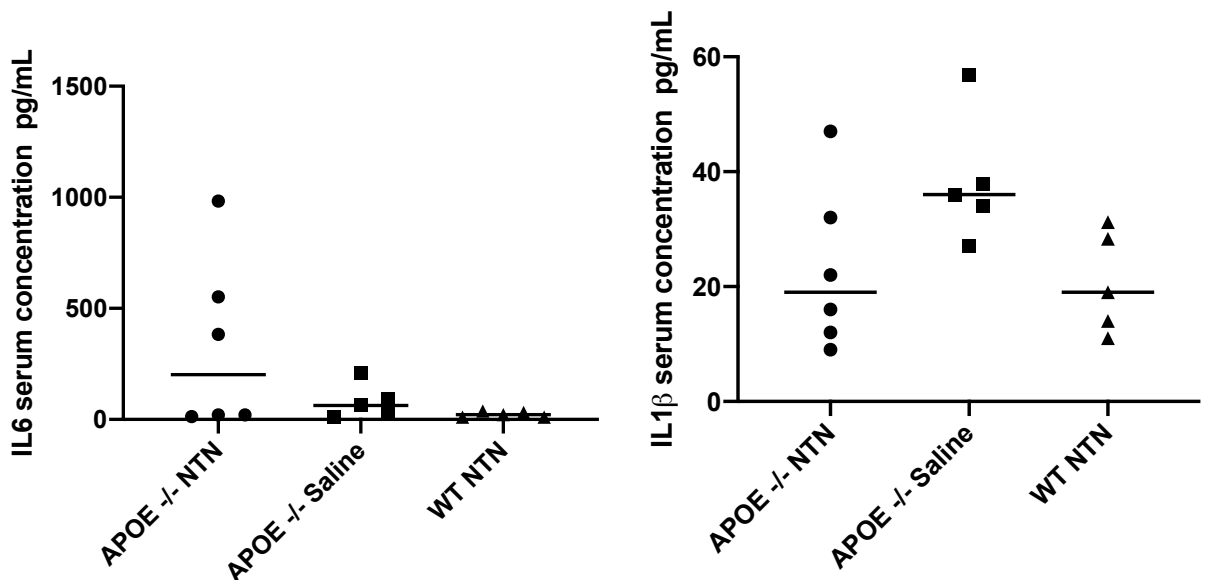
Figure 6-5 Serum pro-atherogenic cytokine profile in the combined chronic nephritis and atheroma model

Mean IL6 and IL1β levels of APOE -/- or C57BL/6 (WT) 12-week old mice fed a high fat for 10 weeks in the presence and absence of nephrotoxic nephritis (NTN). Cytokine profiles were assessed using commercial ELISA assays as per manufacturer's instructions (IL6 ELISA M6000B, R&D systems, IL1beta ELISA ab100704)

6.4.3 Renal profile in the combined chronic nephritis and atheroma model

The levels of proteinuria between the ApoE-/- and WT animals with nephrotoxic nephritis were comparable (proteinuria mg/16hours ApoE -/- NTN 2.7(1.8) mg vs WT NTN 4.2(2.5)mg, p=0.71 and ApoE Saline 0.7(0.5)mg,p=0.23) (Figure 6-6).
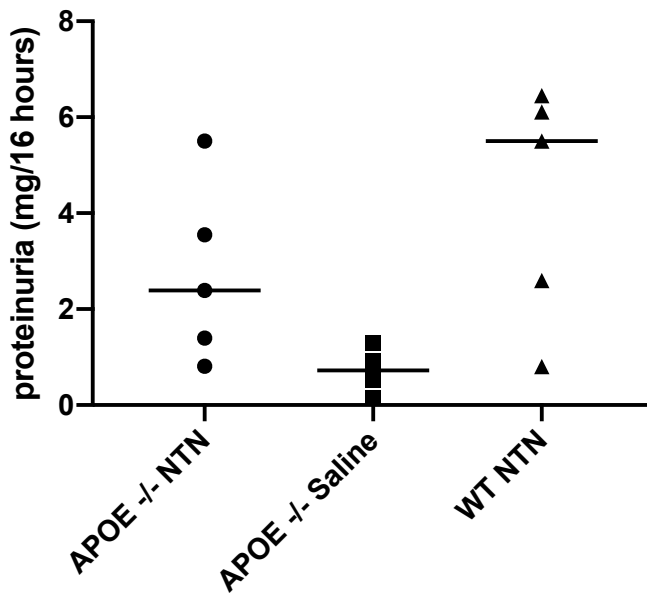
Figure 6-6 Proteinuria in the combined chronic nephritis and atheroma model.

Mean proteinuria values of APOE -/- or C57BL/6 (WT) 12-week old mice fed a high fat for 10 weeks in the presence and absence of nephrotoxic nephritis (NTN), one-way ANOVA.

However, ApoE-/- animals with nephritis had histologically mildly worse disease compared to the WT animals with nephritis (Figure 6-8) as defined by glomerular thrombosis and tubular cast score (glomerular thrombosis score ApoE-/- 2.3(0.5)AU vs WT NTN (1(1.4)AU p=0.049 and ApoE Saline 0 (0) p<0.001,

tubular cast score ApoE-/- NTN 1.4(0.6)AU vs WT NTN 0.7(0.6) p=0.049 and
ApoE-/- Saline 0 (0) p<0.001) (Figure 6-7and 6-8).
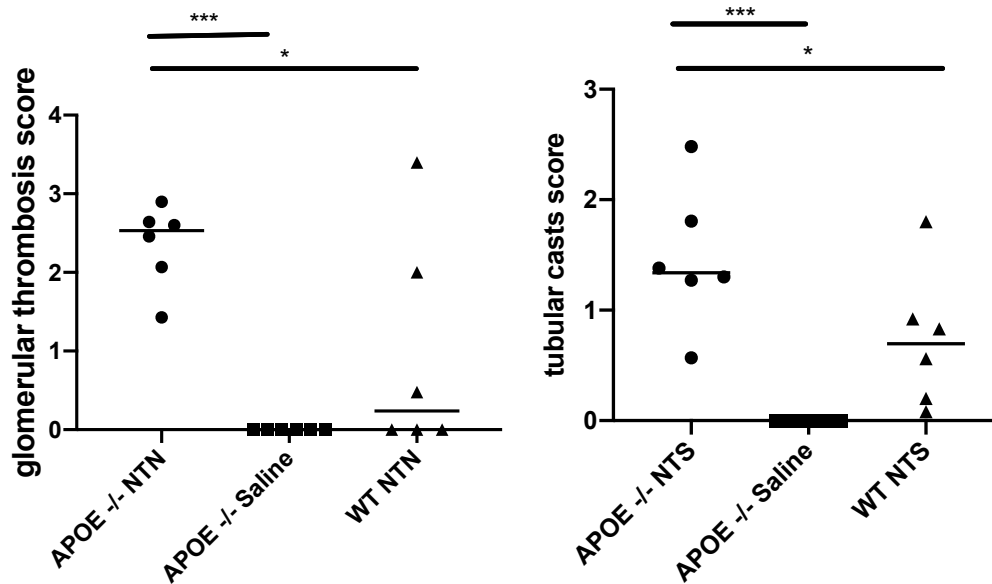
Figure 6-7 Renal histology in the combined chronic nephritis and atheroma model

Mean glomerular thrombosis and tubular cast score of APOE -/- or C57BL/6 (WT) 12-week old mice fed a high fat for 10 weeks in the presence and absence of nephrotoxic nephritis (NTN), one-way ANOVA, *P< 0.05, ***P< 0.001
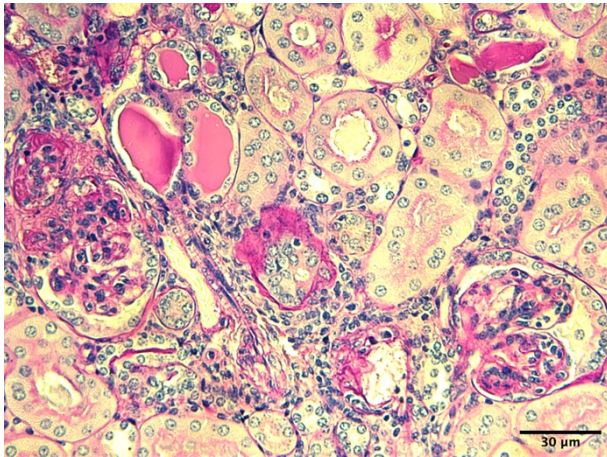
**ApoE-/- NTN**   **ApoE-/- Saline**   **WT NTN**
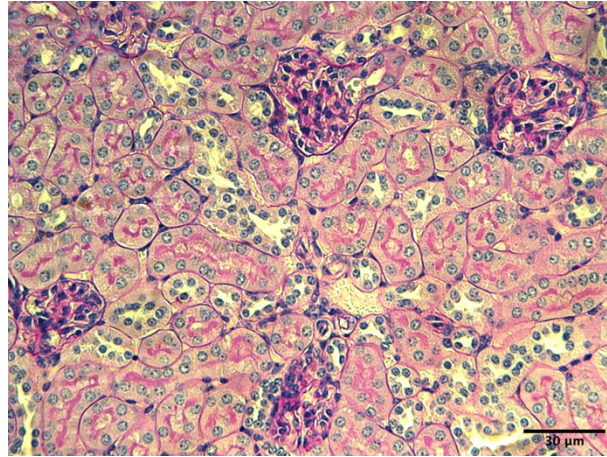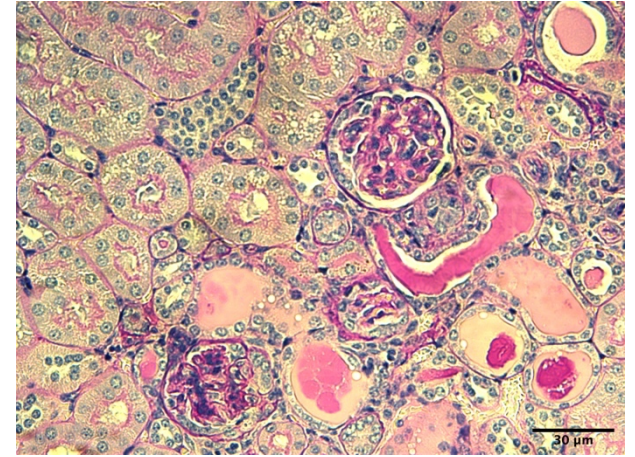
Figure 6-8 Representative micrographs of renal histology in the combined chronic nephritis and atheroma model

6.5 Discussion

In this chapter, the data derived using a combined murine model of chronic nephritis and atheroma demonstrate that glomerular inflammation enhances atheroma formation.

These findings are corroborated by other preclinical studies showing that renal inflammation secondary to glomerulonephritis is a risk factor for atheroma formation. In particular, in a chimeric mouse model that combined the Ldlr-/- phenotype and lupus susceptibility (LDLr.*Sle*), the LDLr.*Sle* chimeras had increased mortality and atherosclerotic lesions compared to control donors (Stanic *et al.*, 2006). In addition, amplification of complement activation by the alternative pathway, which is pivotal for driving inflammation in crescentic GN , in response to LPS or high fat diet was found to be pro-atherogenic in Ldlr -/- mice (Malik *et al.*, 2010). Although the serum IL6 levels were higher in the ApoE-/- animals with NTN there was no significant difference compared to ApoE-/- and WT controls. It is possible that the study was underpowered in animal numbers and a biological effect was missed. In fact, using updated power calculations based on the data obtained to date, for the effect size of 0.9 shown between the NTN and saline groups, 17 animals in each group would be required to show a significant statistical difference in IL6 serum concentration.

Interestingly, although levels of proteinuria were comparable between the ApoE-/- and WT mice with NTN, there were histological differences showing increased tubular casts and glomerular thrombosis in the ApoE-/- mice. One possible explanation is that ApoE-/- being genetically different from WT might be predisposed to developing worse renal disease. Another explanation is that the pro-atherogenic phenotype in combination with the western diet for 10 weeks had an independent effect on glomerular inflammation. In fact, although the ApoE-/- animals without nephritis did not have histological changes, they still had a mean value of 0.7mg proteinuria over 16 hours.

A study on double ApoE-/-Ldlr-/- knockout mice found that the animals developed perivascular inflammation and glomerular capillary aneurysms with thrombosis even in the absence of a high fat diet after 80 weeks (Langheinrich *et al.*, 2010). A separate study in mice deficient in both ApoE and endothelial nitric oxide synthase found a decreased kidney weight, increased plasma creatinine, and an increased number of glomeruli with lipid deposits in double knockout mice at the age of 4 months. A small number of glomeruli with lipid deposits were also described in control ApoE−/− mice, but the pathology in these mice was not fully addressed (Knowles *et al.*, 2000). A later study described in more detail the renal injury in ApoE deficient mice that is characterised by foam cell accumulation and intracapillary lipid deposits that resemble human lipoprotein glomerulopathy. These findings suggest that renal injury in our combined model of nephritis and atheroma formation is attributed to a combination of glomerular inflammation secondary to immune complex disease as well as hyperlipidaemia (Wen *et al.*, 2002).

Unfortunately, in view of the COVID19 pandemic and the unprecedented closure of laboratory facilities I was not able to measure cholesterol levels in the mouse sera. The model we used is severely hyperlipidaemic and correlation of aortic plaque area and serum cholesterol would be informative and it will form part of future work. Although the receptor by which cholesterol crystals might activate neutrophils has not been identified, recent literature has offered insights into how cholesterol can impact neutrophil function. In macrophages, cholesterol crystals activate the inflammasome through the receptor CD36 which mediates apoptosis in neutrophils and might be implicated in NETosis (DeLeon-Pennell, K. Y. *et al.* 2016). Cholesterol crystals have also been shown to induce NETs that prime macrophages for IL-1β and IL6 release, activating Th-17 cells that amplify immune cell recruitment in atherosclerotic plaques (Warnatsch *et al.*, 2015).

In our future work detailed in the next section, we aim to test the effect of MPO deficiency on atheroma formation in the presence of non-accelerated nephrotoxic nephritis. In order to achieve this, I have generated a double MPO-ApoE knockout murine line by crossing the two species. In addition, we aim to investigate the role

of MPO inhibition on chronic nephritis and associated atheroma formation and compare these end points with corticosteroid therapy, the current gold standard treatment for CGN.

7 Discussion

7.1 Summary of results

Chapter 3 explored the role of MPO as a marker of disease activity in diverse
forms of CGN. MPO is detected intra- and extracellularly in inflamed glomeruli, in
biopsies from patients with the most common form of CGN in adults, ANCA-
Associated Vasculitis, as well as in ANCA-negative disease, crescentic IgA
nephropathy and Lupus Nephritis. Total, neutrophil-associated and extracellular
MPO deposition in the whole kidney, and total glomerular MPO deposition,
correlated with clinical and histological disease severity in the initial renal biopsy.
Extracellular glomerular MPO deposition alone correlated with eGFR and crescent
formation, suggesting that extracellular MPO could be an important driver
mediating renal inflammation. Our data on the distribution of extracellular and
intracellular MPO within kidneys of AAV patients confirm and extend previous
observations (Brouwer *et al.*, 1994; Kessenbrock *et al.*, 2009; Arimura *et al.*, 2013;
O'Sullivan *et al.*, 2015). Additionally, circulating MPO levels are increased in AAV
patients with active disease compared with disease in remission, confirming it as a
modifiable marker of disease activity.

In Chapter 4, MPO inhibition inactivated enzymatically active MPO and reduced
neutrophil degranulation, ROS production and NET formation in cytokine- and
ANCA-stimulated neutrophils from patients and healthy controls. One of the
hallmarks of CGN is endothelial injury and rupture of the glomerular capillary loops
due to aberrant leucocyte activation. TNFα/PR3-ANCA-stimulated neutrophils led
to EC injury that was attenuated by enzymatic NET degradation using DNAse

(Gupta *et al.*, 2010; Schreiber *et al.*, 2017), as well as pharmacological inhibition of MPO.

In Chapter 5, the accelerated nephrotoxic nephritis model of CGN was used, which is dependent on adaptive and innate immunity and representative clinically of a rapidly progressive glomerulonephritis due to immune-complex disease. Despite the initiation of treatment one day after the glomerular neutrophil influx, AZM198 at two different doses attenuated glomerular inflammation clinically and histologically. When we assessed the effect of AZM198 on neutrophil influx we found no significant difference in neutrophil influx at an early time point. Acknowledging the small sample size of animals tested in this experiment (n=4 in each group), we may have missed a biological effect on neutrophil recruitment which has been shown in previous reports (Odobasic *et al.*, 2007). Alternatively, our results may be explained by an effect of the delayed MPO inhibition on neutrophil activation/degranulation and inhibition of the biological effects of enzymatically active MPO, in addition to any effect on neutrophil recruitment. The rationale for the dose setting in these experiments was to yield exposures that would mainly inhibit extracellular (133 µmol/kg) or extracellular, as well as intragranular MPO (400 µmol/kg). A satellite group of mice was dosed with 133 µmol/kg AZM198 and sampled at 2, 12 and 19 h to define the maximal (C_{max}) and trough (C_{min}) levels, and to bridge the data with the terminal samples of the efficacy study. Therapeutic AZM198 levels were achieved throughout the study. The PK data suggest that the peak plasma concentrations our MPOi achieved in the current experiments were in the range found to inhibit intragranular MPO, even using the lower dose of AZM198. However, the limited benefit of 400 µmol/kg over

133 µmol/kg may argue that some beneficial effect of AZM198 on glomerular inflammation in this model might also be due to the inhibition of extracellular MPO activity.

In Chapter 6, the role of glomerular inflammation on the development of atheroma formation was explored. Inflammation in the context of chronic immune complex nephritis enhanced atheroma formation. Disease severity on renal histology was greater in ApoE-/- animals with nephrotoxic nephritis compared to WT controls suggesting an additive role of hyperlipidemia to glomerular injury as well as the presence of the nephritis.

7.2 Thesis limitations

7.2.1 Off target effects of AZM198

AZM198 is a membrane-permeable compound that acts as a suicide-substrate for MPO and has been shown to inhibit enzymatically active extracellular MPO, while at higher concentrations it also inhibits intragranular MPO, together with NET formation (Halla Björnsdottir *et al.*, 2015). It is a selective inhibitor and crystallographic analysis has located its binding to MPO at the entrance of the narrow distal heme cavity (Tidén *et al.*, 2011). It has also been shown that is specific to MPO and does not react with other peroxidases such as lactoperoxidase and thyroid peroxidase (Tidén *et al.*, 2011). Based on this knowledge we assume the selectivity and specificity of AZM198. However, off-target effects of AZM198 have not been specifically excluded in the experiments included in this thesis.

7.2.2 Limitations of mouse models

7.2.2.1   Limitations of nephrotoxic nephritis

The model of nephrotoxic nephritis (NTN) is not a vasculitis model, but instead a model of immune-mediated glomerulonephritis characterised by macrophage and T cell infiltration and glomerular thrombosis. The model is primarily characterised by the presence of glomerular thrombosis rather than crescent formation which is in contrast to human disease in AAV.

In addition, the NTN model dissociates the effect of the AZM198 from the induction and perpetuation of autoreactivity. As there is no autoimmunity in this model and the treatment is delayed, we can reasonably assume that this is testing MPO inhibition largely for its effects in the kidney and not on the induction or maintenance of immunity to sheep Ig.

Furthermore, NTN is characterised by variation within the animal groups. Relatively large numbers of animals are needed to see an overall effect. This variation can partly be explained by several different steps required to induce disease (pre-immunisation and the injection of NTS may differ depending on operator). However, the mice were all housed under the same conditions, and injected with the same batch of sheep IgG, CFA and NTS which was prepared at the same time, by the same single operator but there still remains a difference in disease susceptibility within the same experimental group. Therefore, when possible, the groups were combined to investigate if there was an overall significant effect. This combination of animals and the resultant increase in animal numbers, allowed analysis of various disease parameters in chapter 5, which had previously been a trend when analysing smaller groups, to then became statistically significant but that was possibly not the case with the smaller group numbers in chapter 6.

7.2.2.2 Limitations of ApoE deficient mouse model

The advantage of the ApoE deficient mouse model is that if fed a high fat diet mice develop plaques more rapidly than other models such as the LDLr-/- mice, making the ApoE-/- model widely used in experimental atherosclerosis (Silvestre-Roig *et al.*, 2014). However, this model has some limitations. ApoE is a multifunctional protein that has an impact on inflammation that can influence plaque development in different ways. It is involved in oxidation, reverse cholesterol transport by macrophages, and smooth muscle proliferation and migration. These functions might affect atherosclerotic plaque development in ApoE$^{-/-}$ mice, independent of plasma lipid levels (Getz and Reardon, 2009). It is also well established that mice and humans differ in several aspects of lipoprotein metabolism (Getz and Reardon, 2012). When fed a chow diet, mice carry approximately two thirds of plasma cholesterol in HDL particles, whereas humans carry a similar proportion in LDL particles. Furthermore, the most abundant lipoprotein in ApoE-/-mice is VLDL, not LDL, which is characteristic of human atherosclerosis (Plump *et al.*, 1992) giving this model a 'non-human' like lipid profile, although lipid changes in renal failure and CKD are also not typically atherogenic, with elevated LDL.

7.2.2.3 Differences in neutrophil biology between mice and men

There are differences in neutrophil biology between humans and mice. Neutrophils represent the majority of white blood cells in humans (50–70%), but are less common in mice (10–30%) (Mestas and Hughes, 2004). In addition, the granule content in human neutrophils is very different than in mice, which might dramatically alter neutrophil effector functions in mice versus human. For instance, mouse neutrophils do not produce defensins, while human neutrophils do and human neutrophils contain about 5–10-fold higher levels of MPO than murine neutrophils (Rausch and Moore, 1975). Furthermore, the production of immunoregulatory cytokines such as IL-6 and IFN-γ also differs between the two species.

7.3 Future work

7.3.1 Role of myeloperoxidase deficiency in atheroma formation

In order to test the effect of MPO deficiency on atheroma formation in the context of inflammatory kidney disease, mimicking the accelerated cardiovascular disease in patients with lupus or vasculitis, we have developed a murine double knockout line that combines MPO deficiency and vulnerability to atheroma formation. The non-accelerated nephrotoxic nephritis model described in Chapter 6 will be used in double MPO-/-ApoE-/- animals that will subsequently be fed a HFD for 10 weeks. At the end of the study aortas will be assessed for atheroma plaque formation and renal parameters for disease severity. We hypothesize that in the absence of MPO that is involved in both glomerular inflammation and atheroma formation, MPO-/-ApoE-/- will have less atheroma than ApoE-/- controls with NTN. We also hypothesize that these animals will have less severe nephritis however a previous report has shown that MPO-/- mice have less glomerular inflammation in the early neutrophil-mediated stage of nephrotoxic nephritis but they later show increased adaptive T cell responses that contribute to renal injury (Odobasic *et al.*, 2007)

7.3.2 Comparison of the effect of late treatment with AZM198 and corticosteroids.

In our future work, we aim to perform a proof of concept study to test the effect of late treatment with AZM198 on glomerular inflammation and compare its efficacy and side effect profile to gold standard corticosteroid treatment that is associated with significant comorbidity (Mebrahtu *et al.*, 2019) and potentially greater rates of cardiovascular disease.

We will use the chronic model of CGN we have established that in ApoE-/- mice results in accelerated atheroma compared to WT mice. In order to better mimic the clinical setting, we wish to test the effect of late therapeutic intervention by inducing glomerulonephritis in ApoE-/- mice and allowing the disease to become established for two weeks before treating. During this time, all animals will receive

a high fat diet ad libitum. On week 3, the animals will be randomly allocated to three groups where they will receive high fat diet alone, or high fat diet mixed with either AZM198 (500µmol/kg) or corticosteroids (5mg/kg) for 8 weeks. An illustration of the experimental design is shown in Figure 7-1.

Weights will be recorded weekly, glucose monitoring and 16hr urine collection every two weeks until the end of the experiment to determine weight gain, proteinuria and development of glycosuria. Mice will be sacrificed at the end of week 10. Blood and urine will be collected, and hearts, aortas and kidneys will be harvested. Read outs will include atheroma plaque area per aorta, kidney histology, proteinuria, serum glucose, creatinine and urea, serum levels of IL1β, IL6, TNFα and oxidized LDL. Secondary endpoints will include hyperglycaemia, weight gain, mortality and any significant cutaneous infections.
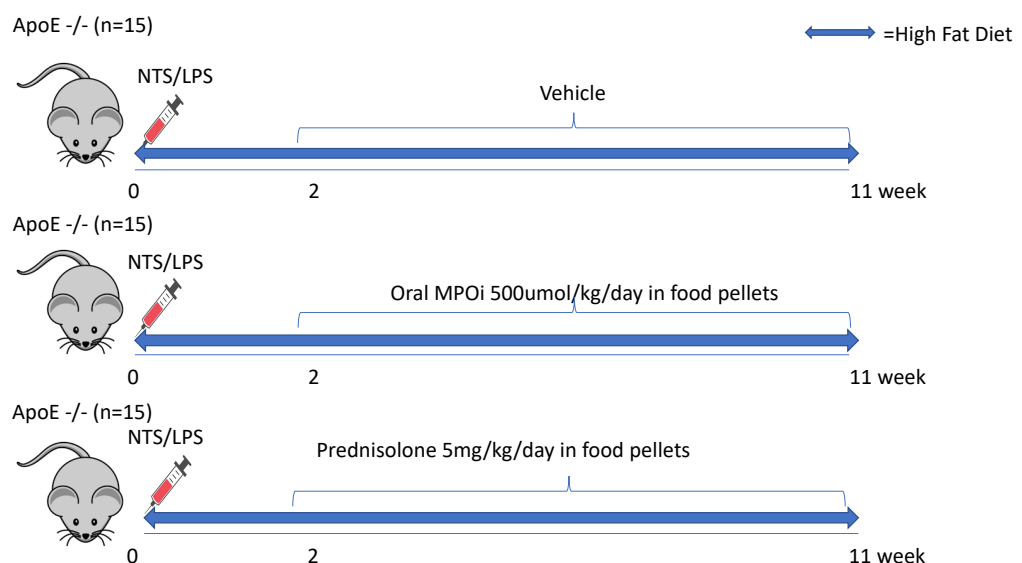
Figure 7-1 Experimental design of future work

Experimental design of the study to investigate the effect of late treatment with AZM198 or corticosteroids in the non-accelerated nephrotoxic nephritis model, on nephritis and atheroma formation.

7.3.3 Concluding remarks

The work in this thesis shows that selective MPO inhibition reduces degranulation and NET formation in neutrophils from patients with AAV, and attenuated kidney damage in preclinical models of CGN without augmenting adaptive immune responses, suggesting that MPO inhibition may be an effective adjunctive therapy in various forms of CGN. It also shows that inflammation secondary to nephritis can independently lead to increased atheroma formation.

There is still significant morbidity in vasculitis patients associated with current treatments, and there are also forms of CGN for which we have limited effective treatments. Glucocorticoid therapy is currently used to treat most conditions associated with CGN and it carries significant long-term morbidity. Therapeutic interventions to inhibit aberrant NETosis or the production of neutrophilic proteins linked to the pathogenesis of these conditions, may be the next step in providing targeted treatments with better side effect profiles.

References

Abou-Raya, A. and Abou-Raya, S. (2006) 'Inflammation: A pivotal link between autoimmune diseases and atherosclerosis', *Autoimmunity Reviews*, 5(5), pp. 331–337.

Agner, K. (1941) *Verdoperoxidase: a ferment isolated from leucocytes. Acta Physiologica Scandinavica.* 1941;2:1–62

Al Laham, F. *et al.* (2010) 'Inhibition of neutrophil-mediated production of reactive oxygen species (ROS) by endothelial cells is not impaired in anti-neutrophil cytoplasmic autoantibodies (ANCA)-associated vasculitis patients', *Clinical and Experimental Immunology*, 161(2), pp. 268–275.

Aldib, I. *et al.* (2016) 'Novel bis-arylalkylamines as myeloperoxidase inhibitors: Design, synthesis, and structure-activity relationship study', *European Journal of Medicinal Chemistry*, 123, pp. 746–762.

Ali, M. *et al.* (2016) 'Myeloperoxidase Inhibition Improves Ventricular Function and Remodeling After Experimental Myocardial Infarction', *JACC: Basic to Translational Science*, 1(7), pp. 633–643.

Amos, L. A. *et al.* (2018) 'ASK1 inhibitor treatment suppresses p38/JNK signalling with reduced kidney inflammation and fibrosis in rat crescentic glomerulonephritis', *Journal of Cellular and Molecular Medicine*, 22(9), pp. 4522–4533.

Aratani, Y. *et al.* (1999) 'Severe Impairment in Early Host Defense againstCandida albicans in Mice Deficient in Myeloperoxidase', *Infection and Immunity*, 67(4), pp. 1828–1836.

Aratani, Y. *et al.* (2000) 'Differential Host Susceptibility to Pulmonary Infections with Bacteria and Fungi in Mice Deficient in Myeloperoxidase', *The Journal of Infectious Diseases*, 182(4), pp. 1276–1279.

Arimura, Y. *et al.* (2013) 'The role of myeloperoxidase and myeloperoxidase–antineutrophil cytoplasmic antibodies (MPO-ANCAs) in the pathogenesis of human MPO-ANCA-associated glomerulonephritis', *Clinical and Experimental Nephrology*, 17(5), pp. 634–637.

Arrizabalaga, P. *et al.* (2008) 'Renal expression of adhesion molecules in anca-associated disease', *Journal of Clinical Immunology*, 28(5), pp. 411–419.

Askari, A. T. *et al.* (2003) 'Myeloperoxidase and plasminogen activator inhibitor 1 play a central role in ventricular remodeling after myocardial infarction', *The Journal of Experimental Medicine*, 197(5), pp. 615–624.

Bacchiega, B. C. *et al.* (2017) 'Interleukin 6 Inhibition and Coronary Artery Disease in a High-Risk Population: A Prospective Community-Based Clinical Study', *Journal of the American Heart Association: Cardiovascular and Cerebrovascular Disease*, 6(3).

Bainton, D. F. and Farquhar, M. G. (1970) 'Segregation and packaging of granule enzymes in eosinophilic leukocytes', *The Journal of Cell Biology*, 45(1), pp. 54–73.

Baldus, S. *et al.* (2003) 'Myeloperoxidase serum levels predict risk in patients with acute coronary syndromes', *Circulation*, 108(12), pp. 1440–1445.

Bardoel, B. W. *et al.* (2014) 'The balancing act of neutrophils', *Cell Host & Microbe*, 15(5), pp. 526–536.

Beauvillain, C. *et al.* (2007) 'Neutrophils efficiently cross-prime naive T cells in vivo', *Blood*, 110(8), pp. 2965–2973.

Behnen, M. *et al.* (2014) 'Immobilized immune complexes induce neutrophil extracellular trap release by human neutrophil granulocytes via FcγRIIIB and Mac-1', *Journal of Immunology (Baltimore, Md.: 1950)*, 193(4), pp. 1954–1965.

Björnsdottir, H. *et al.* (2015) 'Neutrophil NET formation is regulated from the inside by myeloperoxidase-processed reactive oxygen species.', *Free radical biology & medicine*, 89, pp. 1024–1035.

Borregaard, N. (2010) 'Neutrophils, from Marrow to Microbes', *Immunity*, 33(5), pp. 657–670.

Bos, A. J. *et al.* (1982) 'Characterization of hereditary partial myeloperoxidase deficiency', *The Journal of Laboratory and Clinical Medicine*, 99(4), pp. 589–600.

Bos, A., Wever, R. and Roos, D. (1978) 'Characterization and quantification of the peroxidase in human monocytes', *Biochimica et Biophysica Acta (BBA) - Enzymology*, 525(1), pp. 37–44.

Branzk, N. *et al.* (2014) 'Neutrophils sense microbe size and selectively release neutrophil extracellular traps in response to large pathogens', *Nature Immunology*, 15(11), pp. 1017–1025.

Brinkmann, V. *et al.* (2004) 'Neutrophil Extracellular Traps Kill Bacteria', *Science*, 303(5663), pp. 1532–1535.

Brouwer, E. *et al.* (1994) 'Neutrophil activation in vitro and in vivo in Wegener's granulomatosis', *Kidney International*, 45(4), pp. 1120–1131.

Carmona-Rivera, C. *et al.* (2015) 'Neutrophil extracellular traps induce endothelial dysfunction in systemic lupus erythematosus through the activation of matrix metalloproteinase-2', *Annals of the Rheumatic Diseases*, 74(7), pp. 1417–1424.

Chen, Y. *et al.* (2014) 'Inflammatory stress induces statin resistance by disrupting 3-hydroxy-3-methylglutaryl-CoA reductase feedback regulation', *Arteriosclerosis, Thrombosis, and Vascular Biology*, 34(2), pp. 365–376.

Cheng David *et al.* (2019) 'Inhibition of MPO (Myeloperoxidase) Attenuates Endothelial Dysfunction in Mouse Models of Vascular Inflammation and

Atherosclerosis', *Arteriosclerosis, Thrombosis, and Vascular Biology*, 39(7), pp. 1448–1457.

Cochrane, C. G., Unanue, E. R. and Dixon, F. J. (1965) 'A role of polymorphonuclear leukocytes and complement in nephrotoxic nephritis', *The Journal of Experimental Medicine*, 122(1), pp. 99–116.

Cramer, R. *et al.* (no date) 'Incidence of myeloperoxidase deficiency in an area of northern Italy: histochemical, biochemical and functional studies', *British Journal of Haematology*, 51(1), pp. 81–87.

Csernok, E. *et al.* (1994) 'Activated neutrophils express proteinase 3 on their plasma membrane in vitro and in vivo', *Clinical and Experimental Immunology*, 95(2), pp. 244–250.

Daugherty, A. *et al.* (1994) 'Myeloperoxidase, a catalyst for lipoprotein oxidation, is expressed in human atherosclerotic lesions.', *Journal of Clinical Investigation*, 94(1), pp. 437–444.

DeLeon-Pennell, K. Y. *et al.* (2016) CD36 is a matrix metalloproteinase-9 substrate that stimulates neutrophil apoptosis and removal during cardiac remodeling. *Circulation: Cardiovascular Genetics* **9**, 14–25.

Dinauer, M. C. (2014a) 'Disorders of Neutrophil Function: An Overview', in *Neutrophil Methods and Protocols*. Humana Press, Totowa, NJ (Methods in Molecular Biology), pp. 501–515.

Dinauer, M. C. (2014b) 'Disorders of neutrophil function: an overview', *Methods in Molecular Biology (Clifton, N.J.)*, 1124, pp. 501–515.

Dörner, T., Giesecke, C. and Lipsky, P. E. (2011) 'Mechanisms of B cell autoimmunity in SLE', *Arthritis Research & Therapy*, 13(5), p. 243.

Dwyer, M. *et al.* (2014) 'Cystic fibrosis sputum DNA has NETosis characteristics and neutrophil extracellular trap release is regulated by macrophage migration-inhibitory factor', *Journal of Innate Immunity*, 6(6), pp. 765–779.

Edfeldt, K. *et al.* (2006) 'Involvement of the antimicrobial peptide LL-37 in human atherosclerosis', *Arteriosclerosis, Thrombosis, and Vascular Biology*, 26(7), pp. 1551–1557.

Esdaile, J. M. *et al.* (2001) 'Traditional Framingham risk factors fail to fully account for accelerated atherosclerosis in systemic lupus erythematosus', *Arthritis and Rheumatism*, 44(10), pp. 2331–2337.

Falk, R. J. *et al.* (1990) 'Anti-neutrophil cytoplasmic autoantibodies induce neutrophils to degranulate and produce oxygen radicals in vitro', *Proceedings of the National Academy of Sciences of the United States of America*, 87(11), pp. 4115–4119.

Fazio, J. *et al.* (2014) 'Inhibition of human γδ T cell proliferation and effector functions by neutrophil serine proteases', *Scandinavian Journal of Immunology*, 80(6), pp. 381–389.

Fiedler, T. J., Davey, C. A. and Fenna, R. E. (2000) 'X-ray Crystal Structure and Characterization of Halide-binding Sites of Human Myeloperoxidase at 1.8 Å Resolution', *Journal of Biological Chemistry*, 275(16), pp. 11964–11971.

Frangou, E. *et al.* (2019) 'An emerging role of neutrophils and NETosis in chronic inflammation and fibrosis in systemic lupus erythematosus (SLE) and ANCA-associated vasculitides (AAV): Implications for the pathogenesis and treatment', *Autoimmunity Reviews*, 18(8), pp. 751–760.

Fuchs, T. A. *et al.* (2007) 'Novel cell death program leads to neutrophil extracellular traps', *The Journal of Cell Biology*, 176(2), pp. 231–241.

Fuchs, T. A. *et al.* (2010) 'Extracellular DNA traps promote thrombosis', *Proceedings of the National Academy of Sciences*, 107(36), pp. 15880–15885.

Gehrke, N. *et al.* (2013) 'Oxidative damage of DNA confers resistance to cytosolic nuclease TREX1 degradation and potentiates STING-dependent immune sensing', *Immunity*, 39(3), pp. 482–495.

Getz, G. S. and Reardon, C. A. (2009) 'Apoprotein E as a lipid transport and signaling protein in the blood, liver, and artery wall', *Journal of Lipid Research*, 50(Suppl), pp. S156–S161.

Getz GS, Reardon C. A. Animal models of atherosclerosis. (2012) Arteriosclerosis Thrombosis and Vascular Biology. *32*:1104–1115.

Grayson, P. C. *et al.* (2015) 'Neutrophil-Related Gene Expression and Low-Density Granulocytes Associated With Disease Activity and Response to Treatment in Antineutrophil Cytoplasmic Antibody-Associated Vasculitis', *Arthritis & Rheumatology*, 67(7), pp. 1922–1932.

Grishkovskaya, I. *et al.* (2017) 'Structure of human promyeloperoxidase (proMPO) and the role of the propeptide in processing and maturation', *The Journal of Biological Chemistry*, 292(20), pp. 8244–8261.

Gupta, A. K. *et al.* (2010) 'Activated endothelial cells induce neutrophil extracellular traps and are susceptible to NETosis-mediated cell death', *FEBS letters*, 584(14), pp. 3193–3197.

Gupta, S. and Kaplan, M. J. (2016) 'The role of neutrophils and NETosis in autoimmune and renal diseases', *Nature reviews. Nephrology*, 12(7), pp. 402–413. d

Hakkim, A. *et al.* (2010a) 'Impairment of neutrophil extracellular trap degradation is associated with lupus nephritis', *Proceedings of the National Academy of Sciences of the United States of America*, 107(21), pp. 9813–9818.

Halbwachs, L. and Lesavre, P. (2012) 'Endothelium-neutrophil interactions in ANCA-associated diseases', *Journal of the American Society of Nephrology: JASN*, 23(9), pp. 1449–1461.

Han, W. *et al.* (2013) 'NADPH oxidase limits lipopolysaccharide-induced lung inflammation and injury in mice through reduction-oxidation regulation of NF-κB activity', *Journal of Immunology (Baltimore, Md.: 1950)*, 190(9), pp. 4786–4794.

Hansson, G. K., Robertson, A.-K. L. and Söderberg-Nauclér, C. (2006) 'Inflammation and Atherosclerosis', *Annual Review of Pathology: Mechanisms of Disease*, 1(1), pp. 297–329.

Hansson, M., Olsson, I. and Nauseef, W. M. (2006) 'Biosynthesis, processing, and sorting of human myeloperoxidase', *Archives of Biochemistry and Biophysics*, 445(2), pp. 214–224.

Hazell, L. J., Baernthaler, G. and Stocker, R. (2001) 'Correlation between intima-to-media ratio, apolipoprotein B-100, myeloperoxidase, and hypochlorite-oxidized proteins in human atherosclerosis', *Free Radical Biology & Medicine*, 31(10), pp. 1254–1262.

Hazen, S. L. and Heinecke, J. W. (1997) '3-Chlorotyrosine, a specific marker of myeloperoxidase-catalyzed oxidation, is markedly elevated in low density lipoprotein isolated from human atherosclerotic intima', *The Journal of Clinical Investigation*, 99(9), pp. 2075–2081.

Herías, V. *et al.* (2015) 'Leukocyte cathepsin C deficiency attenuates atherosclerotic lesion progression by selective tuning of innate and adaptive immune responses', *Arteriosclerosis, Thrombosis, and Vascular Biology*, 35(1), pp. 79–86.

Hong, Y. *et al.* (2012) 'Anti-Neutrophil Cytoplasmic Antibodies Stimulate Release of Neutrophil Microparticles', *Journal of the American Society of Nephrology*, 23(1), pp. 49–62.

Hooke, D. H., Gee, D. C. and Atkins, R. C. (1987) 'Leukocyte analysis using monoclonal antibodies in human glomerulonephritis', *Kidney International*, 31(4), pp. 964–972.

Huugen, D. *et al.* (2005) 'Aggravation of Anti-Myeloperoxidase Antibody-Induced Glomerulonephritis by Bacterial Lipopolysaccharide', *The American Journal of Pathology*, 167(1), pp. 47–58.

Ibarrola, I. *et al.* (1997) 'Influence of tyrosine phosphorylation on protein interaction with FcγRIIa', *Biochimica et Biophysica Acta (BBA) - Molecular Cell Research*, 1357(3), pp. 348–358.

Inazawa, J. *et al.* (1989) 'Assignment of the human myeloperoxidase gene (MPO) to bands q21.3----q23 of chromosome 17', *Cytogenetics and Cell Genetics*, 50(2–3), pp. 135–136.

Jayne, D. R. W. *et al.* (2017) 'Randomized Trial of C5a Receptor Inhibitor Avacopan in ANCA-Associated Vasculitis', *Journal of the American Society of Nephrology*, 28(9), pp. 2756–2767.

Jerke, U. *et al.* (2019) '196. Characterization of cathepsin c as a treatment target in ANCA-associated vasculitis', *Rheumatology*, 58(Supplement_2).

Jiménez-Alcázar, M. *et al.* (2015) 'Impaired DNase1-mediated degradation of neutrophil extracellular traps is associated with acute thrombotic microangiopathies', *Journal of thrombosis and haemostasis: JTH*, 13(5), pp. 732–742.

Johnston, R. B. and Baehner, R. L. (1970) 'Improvement of leukocyte bactericidal activity in chronic granulomatous disease', *Blood*, 35(3), pp. 350–355.

Kameoka, Y., Persad, A. S. and Suzuki, K. (2004) 'Genomic variations in myeloperoxidase gene in the Japanese population', *Japanese Journal of Infectious Diseases*, 57(5), pp. S12-13.

Kang, A. *et al.* (2018) 'High Incidence of Arterial and Venous Thrombosis in Antineutrophil Cytoplasmic Antibody–associated Vasculitis', *The Journal of Rheumatology*, 46 (3), 285-293

Karmakar, M. *et al.* (2012) 'Cutting Edge: IL-1β Processing during Pseudomonas aeruginosa Infection Is Mediated by Neutrophil Serine Proteases and Is Independent of NLRC4 and Caspase-1', *The Journal of Immunology*, 189(9), pp. 4231–4235.

Karsten, C. M. and Köhl, J. (2012) 'The immunoglobulin, IgG Fc receptor and complement triangle in autoimmune diseases', *Immunobiology*, 217(11), pp. 1067–1079.

Kawashima, S. *et al.* (2013) 'Immunopathologic co-localization of MPO, IgG, and C3 in glomeruli in human MPO-ANCA-associated glomerulonephritis', *Clinical Nephrology*, 79(4), pp. 292–301.

Keshari, R. S. *et al.* (2012) 'Cytokines Induced Neutrophil Extracellular Traps Formation: Implication for the Inflammatory Disease Condition', *PLOS ONE*, 7(10), p. e48111.

Kessenbrock, K. *et al.* (2009) 'Netting neutrophils in autoimmune small-vessel vasculitis', *Nature Medicine*, 15(6), pp. 623–625.

Kettle, A. J. *et al.* (2004) 'Myeloperoxidase and protein oxidation in the airways of young children with cystic fibrosis', *American Journal of Respiratory and Critical Care Medicine*, 170(12), pp. 1317–1323.

Kettritz, R. *et al.* (2001) 'Role of Mitogen-Activated Protein Kinases in Activation of Human Neutrophils by Antineutrophil Cytoplasmic Antibodies', *Journal of the American Society of Nephrology*, 12(1), pp. 37–46.

Kettritz, R. (2012) 'How anti-neutrophil cytoplasmic autoantibodies activate neutrophils', *Clinical and Experimental Immunology*, 169(3), pp. 220–228.

Kettritz, R. (2016) 'Neutral serine proteases of neutrophils', *Immunological Reviews,* 273(1):232-248 ·

Khan, A. A., Alsahli, M. A. and Rahmani, A. H. (2018) 'Myeloperoxidase as an Active Disease Biomarker: Recent Biochemical and Pathological Perspectives', *Medical Sciences*, 6(2).

Khandpur, R. *et al.* (2013) 'NETs Are a Source of Citrullinated Autoantigens and Stimulate Inflammatory Responses in Rheumatoid Arthritis', *Science Translational Medicine*, 5(178), pp. 178ra40-178ra40.

Kindzelskii, A. L. *et al.* (2006) 'Myeloperoxidase accumulates at the neutrophil surface and enhances cell metabolism and oxidant release during pregnancy', *European Journal of Immunology*, 36(6), pp. 1619–1628.

Kitahara, M. *et al.* (1981) 'Hereditary myeloperoxidase deficiency', *Blood*, 57(5), pp. 888–893.

Klebanoff, S. J. (1968) 'Myeloperoxidase-halide-hydrogen peroxide antibacterial system', *Journal of Bacteriology*, 95(6), pp. 2131–2138.

Klebanoff, S. J. (1970) 'Myeloperoxidase: contribution to the microbicidal activity of intact leukocytes', *Science (New York, N.Y.)*, 169(3950), pp. 1095–1097.

Klebanoff, S. J. (1999) 'Myeloperoxidase', *Proceedings of the Association of American Physicians*, 111(5), pp. 383–389.

Klebanoff, S. J. (2005) 'Myeloperoxidase: friend and foe', *Journal of Leukocyte Biology*, 77(5), pp. 598–625.

Klinke, A. *et al.* (2018) 'Myeloperoxidase aggravates pulmonary arterial hypertension by activation of vascular Rho-kinase', *JCI insight*, 3(11).

Knight, J. S. *et al.* (2014) 'Peptidylarginine deiminase inhibition reduces vascular damage and modulates innate immune responses in murine models of atherosclerosis', *Circulation Research*, 114(6), pp. 947–956.

Knight, J. S. *et al.* (2015) 'Peptidylarginine deiminase inhibition disrupts NET formation and protects against kidney, skin and vascular disease in lupus-prone MRL/lpr mice', *Annals of the Rheumatic Diseases*, 74(12), pp. 2199–2206.

Knowles, J. W. *et al.* (2000) 'Enhanced atherosclerosis and kidney dysfunction in eNOS–/–Apoe–/– mice are ameliorated by enalapril treatment', *Journal of Clinical Investigation*, 105(4), pp. 451–458.

Korkmaz, B. *et al.* (2018) 'Therapeutic targeting of cathepsin C: from pathophysiology to treatment', *Pharmacology & Therapeutics*, 190, pp. 202–236.

Kumar, S. V. R. *et al.* (2015) 'Neutrophil Extracellular Trap-Related Extracellular Histones Cause Vascular Necrosis in Severe GN', *Journal of the American Society of Nephrology*, 26(10), pp. 2399–2413.

Kutter, D. *et al.* (2000) 'Consequences of total and subtotal myeloperoxidase deficiency: risk or benefit ?', *Acta Haematologica*, 104(1), pp. 10–15.

Langheinrich, A. C. *et al.* (2010) 'Atherosclerosis, inflammation and lipoprotein glomerulopathy in kidneys of apoE-/-/LDL-/- double knockout mice', *BMC Nephrology*, 11, p. 18.

Lawrence, S. M., Corriden, R. and Nizet, V. (2017) 'Age-Appropriate Functions and Dysfunctions of the Neonatal Neutrophil', *Frontiers in Pediatrics*, 5 (23)

Lee, T. D. *et al.* (2003) 'CAP37, a neutrophil-derived inflammatory mediator, augments leukocyte adhesion to endothelial monolayers', *Microvascular Research*, 66(1), pp. 38–48.

Lee, Y. T. *et al.* (2017) 'Mouse models of atherosclerosis: a historical perspective and recent advances', *Lipids in Health and Disease*, 16 (12).

Lood, C. *et al.* (2016) 'Neutrophil extracellular traps enriched in oxidized mitochondrial DNA are interferogenic and contribute to lupus-like disease', *Nature Medicine*, 22(2), pp. 146–153.

Lu, X. *et al.* (2006) 'Mediation of endothelial cell damage by serine proteases, but not superoxide, released from antineutrophil cytoplasmic antibody-stimulated neutrophils', *Arthritis and Rheumatism*, 54(5), pp. 1619–1628.

Ma, Z. *et al.* (2008) 'Accelerated atherosclerosis in ApoE deficient lupus mouse models', *Clinical Immunology (Orlando, Fla.)*, 127(2), pp. 168–175.

Malik, T. H. *et al.* (2010) 'The Alternative Pathway is critical for Pathogenic Complement Activation in Endotoxin- and Diet-induced Atherosclerosis in Low-Density Lipoprotein Receptor-Deficient Mice', *Circulation*, 122(19), pp. 1948–1956.

Martinod, K. *et al.* (2013) 'Neutrophil histone modification by peptidylarginine deiminase 4 is critical for deep vein thrombosis in mice', *Proceedings of the National Academy of Sciences*, 110(21), pp. 8674–8679.

Mayadas, T. N., Cullere, X. and Lowell, C. A. (2014) 'The Multifaceted Functions of Neutrophils', *Annual review of pathology*, 9, pp. 181–218.

McAdoo, S. P. *et al.* (2014) 'SyK inhibition in experimental autoimmune vasculitis and its glomerular expression in ANCA-associated vasculitis', *The Lancet*, 383, p. S72.

McAdoo, S. P. *et al.* (2020) 'Spleen tyrosine kinase inhibition is an effective treatment for established vasculitis in a pre-clinical model.', *Kidney International*, 0(0). In press

McAdoo, S. and Tam, F. W. K. (2018) 'Role of the Spleen Tyrosine Kinase Pathway in Driving Inflammation in IgA Nephropathy', *Seminars in Nephrology*, 38(5), pp. 496–503.

Mebrahtu, T. F. *et al.* (2019) 'Dose Dependency of Iatrogenic Glucocorticoid Excess and Adrenal Insufficiency and Mortality: A Cohort Study in England', *The Journal of Clinical Endocrinology and Metabolism*, 104(9), pp. 3757–3767.

Megens, R. T. A. *et al.* (2012) 'Presence of luminal neutrophil extracellular traps in atherosclerosis', *Thrombosis and Haemostasis*, 107(3), pp. 597–598.

Mestas, J. and Hughes, C. C. W. (2004) 'Of mice and not men: differences between mouse and human immunology', *Journal of Immunology (Baltimore, Md.: 1950)*, 172(5), pp. 2731–2738.

Metzler, K. D. *et al.* (2011) 'Myeloperoxidase is required for neutrophil extracellular trap formation: implications for innate immunity', *Blood*, 117(3), pp. 953–959.

Metzler, K. D. *et al.* (2014) 'A Myeloperoxidase-Containing Complex Regulates Neutrophil Elastase Release and Actin Dynamics during NETosis', *Cell Reports*, 8(3), pp. 883–896.

Morgan, M. D. *et al.* (2009) 'Increased incidence of cardiovascular events in patients with antineutrophil cytoplasmic antibody–associated vasculitides: A matched-pair cohort study', *Arthritis & Rheumatism*, 60(11), pp. 3493–3500.

Mor-Vaknin, N. *et al.* (2017) 'DEK-targeting DNA aptamers as therapeutics for inflammatory arthritis', *Nature Communications*, 8.

Naish, P. F. *et al.* (1975) 'The role of polymorphonuclear leucocytes in the autologous phase of nephrotoxic nephritis.', *Clinical and Experimental Immunology*, 22(1), pp. 102–111.

Nakashima, Y. *et al.* (1994) 'ApoE-deficient mice develop lesions of all phases of atherosclerosis throughout the arterial tree', *Arteriosclerosis and Thrombosis: A Journal of Vascular Biology*, 14(1), pp. 133–140.

Nakazawa, D. *et al.* (2012) 'Abnormal conformation and impaired degradation of propylthiouracil-induced neutrophil extracellular traps: Implications of disordered neutrophil extracellular traps in a rat model of myeloperoxidase antineutrophil cytoplasmic antibody–associated vasculitis', *Arthritis & Rheumatism*, 64(11), pp. 3779–3787.

Nakazawa, D. *et al.* (2014) 'Enhanced Formation and Disordered Regulation of NETs in Myeloperoxidase-ANCA–Associated Microscopic Polyangiitis', J Am Soc Nephrol, 25 (5), 990-7

Nauseef WM, McCormick S, 'Roles of heme insertion and the mannose-6-phosphate receptor in processing of the human myeloid lysosomal enzyme, myeloperoxidase', Blood 80 (10), 2622-33

Nunoi, H. *et al.* (no date) 'Prevalence of Inherited Myeloperoxidase Deficiency in Japan', *Microbiology and Immunology*, 47(7), pp. 527–531.

Odobasic, D. *et al.* (2007) 'Endogenous Myeloperoxidase Promotes Neutrophil-Mediated Renal Injury, but Attenuates T Cell Immunity Inducing Crescentic Glomerulonephritis', *Journal of the American Society of Nephrology*, 18(3), pp. 760–770.

Ohlsson, S. M. *et al.* (2014) 'Neutrophils from vasculitis patients exhibit an increased propensity for activation by anti-neutrophil cytoplasmic antibodies', *Clinical and Experimental Immunology*, 176(3), pp. 363–372.

Olsen, R. L. and Little, C. (1984) 'Studies on the subunits of human myeloperoxidase', *The Biochemical Journal*, 222(3), pp. 701–709.

O'Sullivan, K. M. *et al.* (2015) 'Renal participation of myeloperoxidase in antineutrophil cytoplasmic antibody (ANCA)-associated glomerulonephritis', *Kidney International*, 88(5), pp. 1030–1046.

O'Sullivan, K. M. *et al.* (2019) '209. Inhibition of peptidylarginine deiminase 4 limits neutrophil extracellular trap formation and inflammation in experimental anti MPO-ANCA glomerulonephritis', *Rheumatology*, 58(Supplement_2).

Ougaard, M. K. E. *et al.* (2018) 'Murine Nephrotoxic Nephritis as a Model of Chronic Kidney Disease', *International Journal of Nephrology*, 2018.

Panda, R. *et al.* (2017) 'Neutrophil Extracellular Traps Contain Selected Antigens of Anti-Neutrophil Cytoplasmic Antibodies', *Frontiers in Immunology*, 8, p. 439.

Papayannopoulos, V. *et al.* (2010) 'Neutrophil elastase and myeloperoxidase regulate the formation of neutrophil extracellular traps', *The Journal of Cell Biology*, 191(3), pp. 677–691.

Papayannopoulos, V. (2018) 'Neutrophil extracellular traps in immunity and disease', *Nature Reviews Immunology*, 18(2), pp. 134–147.

Parker, H. *et al.* (no date) 'Myeloperoxidase associated with neutrophil extracellular traps is active and mediates bacterial killing in the presence of hydrogen peroxide', *Journal of Leukocyte Biology*, 91(3), pp. 369–376.

Pereira, H. A., Moore, P. and Grammas, P. (1996) 'CAP37, a neutrophil granule-derived protein stimulates protein kinase C activity in endothelial cells', *Journal of Leukocyte Biology*, 60(3), pp. 415–422.

Pepper R. J *et al.* (2013) Leukocyte and Serum S100A8/S100A9 Expression Reflects Disease Activity in ANCA-associated Vasculitis and Glomerulonephritis, *Kidney International,* 83(6):1150-8.

Pham, C. T. N. *et al.* (2004) 'Papillon-Lefèvre syndrome: correlating the molecular, cellular, and clinical consequences of cathepsin C/dipeptidyl peptidase I deficiency

in humans', *Journal of Immunology (Baltimore, Md.: 1950)*, 173(12), pp. 7277–7281.

Plump, A. S. *et al.* (1992) 'Severe hypercholesterolemia and atherosclerosis in apolipoprotein E-deficient mice created by homologous recombination in ES cells', *Cell*, 71(2), pp. 343–353.

Popat, R. J. and Robson, M. G. (2019) 'Neutrophils are not consistently activated by antineutrophil cytoplasmic antibodies in vitro', *Annals of the Rheumatic Diseases*, 78(5), pp. 709–711.

Rausch, P. G. and Moore, T. G. (1975) 'Granule enzymes of polymorphonuclear neutrophils: A phylogenetic comparison', *Blood*, 46(6), pp. 913–919.

Roth, A. J. *et al.* (2013) 'Epitope specificity determines pathogenicity and detectability in ANCA-associated vasculitis', *The Journal of Clinical Investigation*, 123(4), pp. 1773–1783.

Sangaletti, S. *et al.* (2012) 'Neutrophil extracellular traps mediate transfer of cytoplasmic neutrophil antigens to myeloid dendritic cells toward ANCA induction and associated autoimmunity', *Blood*, 120(15), pp. 3007–3018.

Schreiber, A. *et al.* (2009) 'C5a receptor mediates neutrophil activation and ANCA-induced glomerulonephritis', *Journal of the American Society of Nephrology: JASN*, 20(2), pp. 289–298.

Schreiber, A. *et al.* (2012) 'Neutrophil Serine Proteases Promote IL-1β Generation and Injury in Necrotizing Crescentic Glomerulonephritis', *Journal of the American Society of Nephrology*, 23(3), pp. 470–482.

Schreiber, A. *et al.* (2017) 'Necroptosis controls NET generation and mediates complement activation, endothelial damage, and autoimmune vasculitis', *Proceedings of the National Academy of Sciences*, 114(45)

Schuster, S., Hurrell, B. and Tacchini-Cottier, F. (2013) 'Crosstalk between neutrophils and dendritic cells: a context-dependent process', *Journal of Leukocyte Biology*, 94(4), pp. 671–675.

Sengeløv, H., Kjeldsen, L. and Borregaard, N. (1993) 'Control of exocytosis in early neutrophil activation', *Journal of Immunology (Baltimore, Md.: 1950)*, 150(4), pp. 1535–1543.

Silvestre-Roig, C. *et al.* (2014) 'Atherosclerotic plaque destabilization: mechanisms, models, and therapeutic strategies', *Circulation Research*, 114(1), pp. 214–226.

Smith, C. K. *et al.* (2014) 'Neutrophil Extracellular Trap–Derived Enzymes Oxidize High-Density Lipoprotein: An Additional Proatherogenic Mechanism in Systemic Lupus Erythematosus', *Arthritis & Rheumatology*, 66(9), pp. 2532–2544.

Söderberg, D. *et al.* (2015) 'Increased levels of neutrophil extracellular trap remnants in the circulation of patients with small vessel vasculitis, but an inverse correlation to anti-neutrophil cytoplasmic antibodies during remission', *Rheumatology (Oxford, England)*, 54(11), pp. 2085–2094.

Söderberg, D. and Segelmark, M. (2016) 'Neutrophil Extracellular Traps in ANCA-Associated Vasculitis', *Frontiers in Immunology*, 7.

Soehnlein Oliver (2012) 'Multiple Roles for Neutrophils in Atherosclerosis', *Circulation Research*, 110(6), pp. 875–888.

Sokolove, J. *et al.* (2013) 'Citrullination within the atherosclerotic plaque: A potential target for the anti-citrullinated protein antibody response in rheumatoid arthritis', *Arthritis and rheumatism*, 65(7), pp. 1719–1724.

Stambe, C. *et al.* (2003) 'Blockade of p38α MAPK Ameliorates Acute Inflammatory Renal Injury in Rat Anti-GBM Glomerulonephritis', *Journal of the American Society of Nephrology*, 14(2), pp. 338–351.

Stamp, L. K. *et al.* (2012) 'Myeloperoxidase and oxidative stress in rheumatoid arthritis', *Rheumatology (Oxford, England)*, 51(10), pp. 1796–1803.

Stanic, A. K. *et al.* (2006) 'Immune dysregulation accelerates atherosclerosis and modulates plaque composition in systemic lupus erythematosus', *Proceedings of the National Academy of Sciences*, 103(18), pp. 7018–7023.

Stone, J. H. *et al.* (2010) 'Rituximab versus Cyclophosphamide for ANCA-Associated Vasculitis', *New England Journal of Medicine*, 363(3), pp. 221–232.

Strömberg, K., Persson, A. M. and Olsson, I. (1986) 'The processing and intracellular transport of myeloperoxidase. Modulation by lysosomotropic agents and monensin.', *European journal of cell biology*, 39(2), pp. 424–431.

Sugiyama, S. *et al.* (2001) 'Macrophage myeloperoxidase regulation by granulocyte macrophage colony-stimulating factor in human atherosclerosis and implications in acute coronary syndromes', *The American Journal of Pathology*, 158(3), pp. 879–891.

Sugiyama, S. *et al.* (2004) 'Hypochlorous acid, a macrophage product, induces endothelial apoptosis and tissue factor expression: involvement of myeloperoxidase-mediated oxidant in plaque erosion and thrombogenesis', *Arteriosclerosis, Thrombosis, and Vascular Biology*, 24(7), pp. 1309–1314.

Sullivan, D. P. and Muller, W. A. (2014) 'Neutrophil and Monocyte Leukocyte recruitment by PECAM, CD99 and other molecules via the LBRC', *Seminars in immunopathology*, 36(2), pp. 193–209.

Suzuki, K. *et al.* (1983) 'Assay method for myeloperoxidase in human polymorphonuclear leukocytes', *Analytical Biochemistry*, 132(2), pp. 345–352.

Suzuki, S. *et al.* (1998) 'Effects of a novel elastase inhibitor, ONO-5046, on nephrotoxic serum nephritis in rats', *Kidney International*, 53(5), pp. 1201–1208.

Taekema-Roelvink, M. E. *et al.* (2001) 'Proteinase 3 enhances endothelial monocyte chemoattractant protein-1 production and induces increased adhesion of neutrophils to endothelial cells by upregulating intercellular cell adhesion molecule-1', *Journal of the American Society of Nephrology: JASN*, 12(5), pp. 932–940.

Tardif, J.-C. *et al.* (2019) 'Efficacy and Safety of Low-Dose Colchicine after Myocardial Infarction', *New England Journal of Medicine*, 381(26), pp. 2497–2505.

Tarzi, R. M. and Pusey, C. D. (2014) 'Current and future prospects in the management of granulomatosis with polyangiitis (Wegener's granulomatosis)', *Therapeutics and Clinical Risk Management*, 10, pp. 279–293.

Tidén, A.-K. *et al.* (2011) '2-thioxanthines are mechanism-based inactivators of myeloperoxidase that block oxidative stress during inflammation', *The Journal of Biological Chemistry*, 286(43), pp. 37578–37589.

Tipping, P. G. and Holdsworth, S. R. (2006) 'T Cells in Crescentic Glomerulonephritis', *Journal of the American Society of Nephrology*, 17(5), pp. 1253–1263.

Tsuboi, N. *et al.* (2008) 'Human neutrophil Fcgamma receptors initiate and play specialized nonredundant roles in antibody-mediated inflammatory diseases', *Immunity*, 28(6), pp. 833–846.

Ui Mhaonaigh, A. *et al.* (2019) 'Low Density Granulocytes in ANCA Vasculitis Are Heterogenous and Hypo-Responsive to Anti-Myeloperoxidase Antibodies', *Frontiers in Immunology*, 10.

van der Veen, B. S., de Winther, M. P. J. and Heeringa, P. (2009) 'Myeloperoxidase: Molecular Mechanisms of Action and Their Relevance to Human Health and Disease', *Antioxidants & Redox Signaling*, 11(11), pp. 2899–2937.

Villanueva, E. *et al.* (2011) 'Netting neutrophils induce endothelial damage, infiltrate tissues, and expose immunostimulatory molecules in systemic lupus erythematosus', *Journal of Immunology (Baltimore, Md.: 1950)*, 187(1), pp. 538–552.

Warnatsch, A. *et al.* (2015) 'Neutrophil extracellular traps license macrophages and Th17 cells for cytokine production in atherosclerosis', *Science (New York, N.Y.)*, 349(6245), pp. 316–320.

Wen, M. *et al.* (2002) 'Renal Injury in Apolipoprotein E–Deficient Mice', *Laboratory Investigation*, 82(8), pp. 999–1006.

Wiesner, O. *et al.* (2004) 'Antineutrophil cytoplasmic antibodies reacting with human neutrophil elastase as a diagnostic marker for cocaine-induced midline

destructive lesions but not autoimmune vasculitis', *Arthritis and Rheumatism*, 50(9), pp. 2954–2965.

Winterbourn, C. C. (2002) 'Biological reactivity and biomarkers of the neutrophil oxidant, hypochlorous acid', *Toxicology*, 181–182, pp. 223–227.

Witko-Sarsat, V. *et al.* (1999) 'Presence of proteinase 3 in secretory vesicles: evidence of a novel, highly mobilizable intracellular pool distinct from azurophil granules', *Blood*, 94(7), pp. 2487–2496.

Woodfin, A. *et al.* (2009) 'Endothelial cell activation leads to neutrophil transmigration as supported by the sequential roles of ICAM-2, JAM-A, and PECAM-1', *Blood*, 113(24), pp. 6246–6257.

Woodfin, A., Voisin, M.-B. and Nourshargh, S. (2010) 'Recent developments and complexities in neutrophil transmigration', *Current Opinion in Hematology*, 17(1), pp. 9–17.

Yamashiro, S. *et al.* (2001) 'Phenotypic and functional change of cytokine-activated neutrophils: inflammatory neutrophils are heterogeneous and enhance adaptive immune responses', *Journal of Leukocyte Biology*, 69(5), pp. 698–704.

Yang, J. J. *et al.* (1996) 'Apoptosis of endothelial cells induced by the neutrophil serine proteases proteinase 3 and elastase.', *The American Journal of Pathology*, 149(5), pp. 1617–1626.

Yu, Y. and Su, K. (2013) 'Neutrophil Extracellular Traps and Systemic Lupus Erythematosus', *Journal of Clinical & Cellular Immunology*, 4.

Zheng, W. *et al.* (2015) 'PF-1355, a mechanism-based myeloperoxidase inhibitor, prevents immune complex vasculitis and anti-glomerular basement membrane glomerulonephritis', *The Journal of Pharmacology and Experimental Therapeutics*, 353(2), pp. 288–298.